Ministry of Higher Education and Scientific Research

Hassiba BENBOUALI University of Chlef
Faculty of Technology

Department of Mechanical Engineering

THESIS

Presented to obtain diploma of

DOCTORATE

Field : Mechanical Engineering

Speciality : Energetics

By

BENCHAMMA Sofiane

Theme :

Design, optimization and energy performance of hybrid Photovoltaic-Thermal solar-assisted heat pump systems for buildings applications in Algeria.

Presented on April 11th, 2026 in front of the jury composed of :

Mr. KHELIL Ali	Professor	UHB-Chlef	President
Mr. CHETTI Boualem	Professor	UBD-Khemis-Miliana	Examiner
Mr. KAMLA Youcef	MCA	UHB-Chlef	Examiner
Mr. BELALIA Azeddine	MCA	UHB-Chlef	Examiner
Mr. MISSOUM Mohammed	MCA	U-Tipaza	Supervisor
Miss. BELKACEM Nefissa	MCB	UHB-Chlef	Co-Supervisor


بسم الله الرحمن الرحيم

Abstract

The demand for solar-assisted heat pumps is increasing over time to meet human needs for home comfort, such as heating and domestic hot water, while maintaining lower costs. This trend aligns with the commitment of governments around the world, including Algeria, to provide clean renewable energy and move away from polluting fossil fuels that contribute to gas emissions. The energy source for operating a heat pump system can be single, such as solar energy alone or air energy alone or can be dual or multiple sources in same time, meaning the heat pump system operates using more than one source of energy, like solar energy and air. Solar heat pump systems are divided into two types. One is referred as the direct-expansion system, abbreviated as DX-SAHP, where the solar collector acts as the evaporator at the same time and the other type is referred as the indirect-expansion system, abbreviated as IX-SAHP, where the solar collector and the evaporator are separated from each other. The contribution of this study is to design and optimize a new dual solar-air heat pump system that can operate in direct-expansion mode (DSM), or in indirect-expansion mode (ISM) and it can also operate in a third mode Direct/indirect-expansion (D/ISM). The objective is to investigate and compare the performance of the new system when operating in the three modes. First, a mathematical model for DX-SAHP system based on the fundamentals of thermodynamics and heat transfer is developed, validated and implemented in MATLAB. Then, a TRNSYS model simulating IX-DSHP system type is developed. In the third step, the two models are integrated to obtain the new DX/IX-DSHP system. Results show that when the system operates in D/ISM mode, it achieves better performances. The coefficient of performance is 2.89, the seasonal performance factor is 9.19 and the solar fraction is 63%. Whereas, they are 2.63, 6.23 and 51% in ISM and are 2.41, 3.76 and 29% in DSM. Parametric study indicates that the area of the solar collector, whether conventional thermal collector or photovoltaic thermal collector, has a direct effect on performance, while the set-point temperature of the tanks has a minimal impact. Economically, the D/ISM shows a shorter payback period compared to the other two modes if global energy prices are considered. The PBP is 7, whereas it is 8 and 9 in the ISM and DSM respectively.

keywords: dual source solar-assisted heat pump; hot water production; space heating; coefficient of performance; solar fraction; seasonal performance factor; water source heat pump; air source heat pump.

تصميم وتحسين وأداء الطاقة لأنظمة المضخات الحرارية المدعومة بالطاقة الشمسية الهجينة الفوتوفولتية-الحرارية لتطبيقات المباني في الجزائر

ملخص

يشهد الطلب على المضخات الحرارية بمساعدة الطاقة الشمسية تزايدا مع الوقت وهذا لتلبية حاجيات الناس إلى الرفاهية المنزلية من تدفئة ومياه منزلية دافئة بما يتماشى مع كلفة أقل. يساير هذا التوجه، التزام السياسات الحكومية عبر العالم، بما فيها الجزائر، لتوفير الطاقات المتجددة النظيفة والابتعاد عن الطاقات الأحفورية الملوثة والمساعدة على إنبعاث الغازات.

مصدر الطاقة لتشغيل المضخة الحرارية يمكن أن يكون أحادي مثلا الطاقة الشمسية أو طاقة الهواء. ويمكن أن يكون مصدر الطاقة متعدد، كأن تعمل منظومة المضخة الحرارية بمصدرين للطاقة الحرارية مثلا الطاقة الشمسية والهواء. أثبتت الدراسات أن تعدد مصادر الطاقة المغذية لمنظومة المضخة الحرارية يعطي أداء أفضل لها.

تقسم منظومات المضخات الحرارية الشمسية إلى صنفين. الصنف الأول يدعى المنظومة ذات التمدد المباشر، يرمز لها DX-SAHP، حيث يلعب فيها اللاقط الشمسي دور المبخر في نفس الوقت. الصنف الثاني يدعى المنظومة ذات التمدد غير المباشر ويرمز لها IX-SAHP حيث يكون اللاقط الشمسي والمبخر منفصلين عن بعضهما.

في هذه الدراسة، أجري بحث على أداء منظومة مضخة حرارية جديدة تعمل بمصدرين للطاقة الحرارية وهما الطاقة الشمسية وحرارة الهواء، يمكن أن تعمل بالتمدد المباشر، يرمز لها DX-DSHP أو التمدد غير المباشر، يرمز لها IX-DSHP ويمكن أن تعمل بتصنيف ثالث في آن واحد، حيث سمي التصنيف الثالث-DX/IX-DSHP.

للبحث في أداء التصنيفات الثلاثة ومقارنتها، تم تطوير نموذج رياضي باستخدام برنامج Matlab طبق على منظومة DX-SAHP. باستخدام برنامج TRNSYS تم تطوير برنامج يحاكي منظومة حرارية من صنف IX-DSHP كمرحلة ثانية. في المرحلة الثالثة، تم دمج النموذجين معا لدراسة المنظومة الحرارية الجديدة DX/ID-DSHP. أصبحت هذه المنظومة الجديدة قابلة للتشغيل على أنماط ثلاثة، تم تسميتها DSM، ISM و D/ISM.

أظهرت النتائج أن المنظومة الحرارية حين تعمل بنمط D/ISM يكون لها أداء أفضل. معامل الأداء هو (COP=2.89)، معامل الأداء الموسمي هو(SPF=9.19) والمعامل الشمسي هو (SF=63%) بينما المعاملات هي 2.63، 6.23 و 51% على الترتيب في نمط ISM .وفي نمط DSM كانت 2.41، 3.76و 41% على الترتيب. تبين من خلال الدراسة المعاملاتية أن مساحة اللاقط الشمسي، سواء اللاقط الشمي الحراري أو الحراري الضوئي، لها تأثير مباشر على الأداء أما درجة حرارة الصهريج فلها تأثير قليل. من الناحية الاقتصادية، أظهر صنف D/ISM فترة عودة أقل من الصنفين الآخرين إذا تم إعتماد أسعار الطاقة العالمية.

الكلمات المفتاحية: مضخة حرارية ثنائية المصدر شمسي-هوائي، إنتاج المياه الحارة المنزلية، تدفئة البنايات، معامل الأداء، عامل الأداء الموسمي، المعامل الشمسي، مضخة حرارية مائية المصدر، مضخة حرارية هوائية المصدر.

Résumé

La demande de pompes à chaleur solaire augmente au fil du temps pour répondre aux besoins de confort thermique en chauffage et en eau chaude sanitaire, tout en maintenant des coûts réduits. Cette demande s'aligne avec l'engagement des gouvernements du monde entier, dont l'Algérie, à fournir une énergie propre et renouvelable en conservant leur sécurité énergétique et en abandonnant les combustibles fossiles polluants qui contribuent aux émissions de gaz à effet de serre. Un système de pompe à chaleur peut fonctionner par une source thermique unique, comme l'énergie solaire seule ou l'aérothermique seule, ou par deux ou plusieurs sources en même temps, comme la dualité solaire-aérothermique. Les systèmes de pompes à chaleur solaire se catégorisent en deux types. Le premier est appelé système à détente directe, ou DX-SAHP, dans lequel le capteur solaire joue le rôle d'évaporateur. Le second est appelé système à détente indirecte, ou IX-SAHP, dans lequel le capteur solaire et l'évaporateur sont séparés. La contribution de la présente étude est de développer et optimiser un nouveau système de pompe à chaleur à dualité de source d'énergie solaire-air, pouvant fonctionner en mode détente directe (DSM) ou détente indirecte (ISM), ainsi qu'en mode détente directe/indirecte (D/ISM). L'objectif est d'étudier et de comparer les performances du nouveau système dans ces trois modes. Un modèle mathématique a d'abord été développé à l'aide du logiciel Matlab pour le système DX-SAHP. Ensuite, un modèle TRNSYS a été développé pour simuler le système IX-DSHP. Dans une troisième étape, les deux modèles ont été intégré pour créer le nouveau modèle du système DX/IX-DSHP. Les résultats montrent que le système fonctionnant en mode D/ISM atteint de meilleures performances. Le coefficient de performance est de 2,89, le facteur de performance saisonnier est de 9,19 et la contribution de l'énergie solaire est de 63 %. Alors qu'ils sont de 2,63; 6,23 et 51% dans l'ISM, et de 2,41; 3,76 et 29 % dans le DSM. L'étude paramétrique indique que la surface des capteurs solaires, qu'ils soient thermiques ou photovoltaïques thermiques, a un impact direct sur les performances, tandis que la température de consigne du réservoir a un effet minimal. D'un point de vue économique, le D/ISM présente un délai d'amortissement (PBP) plus court que les deux autres modes, compte tenu des prix mondiaux de l'énergie. Le PBP est de 7, alors qu'il est de 8 et 9 dans le ISM et le DSM respectivement.

Les mots clés: pompe à chaleur à double source solaire-air; production d'eau chaude sanitaire; chauffage bâtiment; coefficient de performance ; fraction solaire; facteur de performance saisonnier ; pompe à chaleur à eau; pompe à chaleur à air.

Acknowledgements

I would like to express my heartfelt gratitude to my dedicated and supportive thesis supervisor, Dr. Mohammed Missoum, without Him, this work would never have seen the light, and to my co-supervisor, Dr. Nefissa Belkacem for her guidance, feedback, and constructive encouragement. Their unwavering commitment, extensive knowledge, and continuous guidance have been invaluable. Their encouragement have significantly contributed to the successful completion of this work.

I would also like to extend my thanks to CFD (Doctoral Training Committee) members at the Faculty of Technology for being always side by side. Your shared insights, discussions, and collective efforts have enriched the research experience and made it a memorable one.

I am grateful to the esteemed jury members for their time, consideration, and expertise in reviewing my doctoral work. Your constructive feedback are deeply valued and greatly contribute to the integrity of this work.

I thank my colleagues and fellow group for their support and camaraderie.

Especially,

I am also deeply and profoundly grateful to my dead parents, whose unwavering support, love, and encouragement have been my pillar of strength throughout my life.

I would like to thank my wife for her unlimited support all the way.

.

DEDICATION

I would like to award this success I have achieved to my beloved parents, whose unwavering love and guidance continue to light my path even in their absence. This work is dedicated to their memory with deepest gratitude and eternal love. Though you are no longer here, but your dreams and prayers are carried with me.

To my beloved wife, sons and daughter.

To my brothers and sisters.

Contents

List of Figures

List of Tables

Abbreviations

AE	**A**ir **E**vaporator
AM	**A**ir **M**ode
ASHP	**A**ir **S**ource **H**eat **P**ump
COP	**C**oefficient **O**f **P**erformance
CS	**C**ost **S**aving
DHW	**D**omestic **H**ot **W**ater
D/ISM	**D**irect/ **I**ndirect **S**olar **M**ode
DSM	**D**irect **S**olar **M**ode
DSHP	**D**ual **S**ource **H**eat **P**ump
DX-DSHP	**D**irect **E**xpansion **D**ual **S**ource **H**eat **P**ump
DX/IX-DSHP	**D**irect/**I**ndirect **E**xpansion **D**ual **S**ource **H**eat **P**ump
DX-SAHP	**D**irect **E**xpansion **S**olar **A**ssisted **H**eat **P**ump
EH	**E**lectrical **H**eater
GB	**G**as **B**oiler
HCA	**H**eat **C**ollection **A**rea
HP	**H**eat **P**ump
HX	**H**eat **E**xchanger
IC	**I**nvestment **C**ost
IX-DSHP	**I**ndirect **D**ual **S**ource **H**eat **P**ump
ISM	**I**ndirect **S**olar **M**ode
IX-SAHP	**I**ndirect **E**xpansion **S**olar **A**ssisted **H**eat **P**ump
OC	**O**perating **C**ost
PBP	**P**ay **b**ack **P**eriod
PEC	**P**rimary **E**nergy **C**onsumption
PES	**P**rimary **E**nergy **S**aving
PVT	**P**hoto **V**oltaic **T**hermal
SAHP	**S**olar **A**ssisted **H**eat **P**ump
SCE	**S**olar **C**ollector **E**vaporator
SH	**S**pace **H**eating
SF	**S**olar **F**raction
SPF	**S**easonal **P**erformance **F**actor
TK	**T**ank
WE	**W**ater **E**vaporator
WSHP	**W**ater **S**ource **H**eat **P**ump

List of Symbols

A_c	Solar collector-evaporator area	m^2
d	External diameter of the pipe	m
E	Electrical Energy	kW h
F	Efficiency of fins	—
F'	Collector efficiency factor	—
$h_{in,SCE}$	Inlet enthalpy of solar collector evaporator	$J\,kg^{-1}$
$h_{out,SCE}$	Outlet enthalpy of solar collector evaporator	$J\,kg^{-1}$
I	Solar radiation intensity	$W\,m^{-2}$
IT	Solar radiation	$kW\,m^{-2}$
k	Thermal conductivity	$W\,m^{-1}\,^{\circ}C$
$\dot{m}_r$	Refrigerant mass flow rate	$kg\,s^{-1}$
q_0	Difference between emissive power from a black body at the ambient air temperature and the emissive power from the sky	—
q_∞	Sky radiation	—
Q	Heat rate	W
Q_{coll}	Useful heat gain of solar collector/evaporator	W
Q_r	Refrigerant heat gain at the solar collector	W
S	Symbol	—
T	Temperature	°C
T_a	Ambient temperature	°C
T_{rm}	Average temperature of the refrigerant at the solar collector-evaporator	°C
U_b	Dimensionless number	—
U_L	Overall heat loss coefficient	$W\,m^{-2}\,^{\circ}C^{-1}$
w	Distance between the pipes	m
a_1, a_3	Model parameters	—
A_{pvt}	Area of the PVT collector	m^2
$Cap_{heating}$	Heat pump heating capacity	W
C_p	Specific heat of the circulating water	$J\,kg^{-1}\,^{\circ}C$
C_w	Specific heat of water	$J\,kg^{-1}\,^{\circ}C$
d	External diameter of the pipe	m
$F_{R,r}$	Heat removal efficiency factor	—

G_t	Incident solar radiation on the PVT collector	$\mathrm{W\,m^{-2}}$
h_3, h_4	Specific enthalpies	$\mathrm{J\,kg^{-1}}$
$h_{in,cond}$	Enthalpy at the inlet of the condenser	$\mathrm{J\,kg^{-1}}$
$h_{out,cond}$	Enthalpy at the outlet of the condenser	$\mathrm{J\,kg^{-1}}$
k	Polytropic index of the refrigerant fluid	—
$\dot{m}_{PVT}$	Circulating water flow rate through the PVT collector	$\mathrm{kg\,s^{-1}}$
MW	Mass of water	kg
N	Compressor rotational speed	
P_{dis}	Discharge pressure of the compressor	Pa
$P_{heating}$	Heat pump power consumption	W
P_{suc}	Suction pressure of the compressor	Pa
t	Heating time	s
$T_{in,cond}$	Water temperature at the inlet of condenser	°C
T_w	Water temperature	°C
$U_{L,r}$	Overall heat loss coefficient	$\mathrm{W\,m^{-2}\,{}^\circ C^{-1}}$
V_d	Displacement volume rate of the compressor	$\mathrm{m^3\,s^{-1}}$
V_{suc}	Specific volume of the refrigerant at the inlet	$\mathrm{m^3\,kg^{-1}}$

Greek symbols

α	Convective heat transfer coefficient	$\mathrm{W\,m^{-2}\,{}^\circ C}$
δ	Thickness of the collector plate	m
ϵ	Emissivity of the collector plate	—
σ	Stefan–Boltzmann constant	$\mathrm{W/m^2K^4}$
θ	Absorptivity of the collector plate	—
η	Efficiency	—
η_{com}	Total efficiency of the compressor	—
ϕ	Volumetric efficiency of the compressor	—
$(\tau\alpha)_{PV}$	Product of transmittance and absorptance of the PV cell	—

Subscripts

amb	Ambient
in	Inlet
out	Outlet
pv	Photovoltaic
th	Thermal

General Introduction

All aspects of life improvement, industry, transportation, buildings and technological facilities are entwined with energy. In a world facing environmental challenges, where the need for sustainable energy sources is increasing to meet daily human needs, clean energy has emerged as one of the most important solution for a more sustainable future. Clean energy, or renewable energy, is derived from inexhaustible natural sources and is characterized by being environmentally friendly, achieving sustainable development, improving public health, ensuring self-sufficiency, and not contributing to harmful greenhouse gas emissions. The importance of clean energy lies in its being the optimal alternative to fossil fuel sources, such as oil and coal, which are among the main causes of environmental pollution and climate change. Scientific research and technological development are working to reduce the costs of producing clean energy, making it more commercially competitive. This aligns with governments policies directions around the world, including Algeria, which supports energy security and advocates the transition to clean energy, contributing to the acceleration of its adoption.

The human need for home comfort means such as heating and hot water drives more efforts to find the optimal means to provide them. Heat pumps were developed as an alternative to air conditioning and traditional heating methods that operate on electricity or natural gas combustion. The specificity of heat pumps is that they use renewable energy sources to absorb low heat, like in air and water, converting them within their components: evaporator, compressor, condenser, and valve into useful heat that can be used for heating homes and domestic water.

Previous studies and research have shown that using a single energy source, such as solar energy alone, reduces the efficiency and performance of heat pumps due to weather fluctuations, geographical differences, and the day-night cycle. Therefore, the trend now is towards using multiple sources of thermal energy to operate heat pump.

Additionally, a heat pump is assisted by solar thermal energy via solar collectors, which may be solar thermal collectors, photovoltaic collectors or photovoltaic/thermal collectors. The evaporator present in a heat pump system can be the thermal collector itself, and in this case, the system is classified as a direct-expansion solar assisted heat pump system, referred to as

DX-SAHP, or the evaporator can be separated of the thermal collector, in which case the system is classified as an indirect-expansion solar assisted heat pump system, denoted by IX-SAHP.

Technological development and research are working to achieve the highest efficiency and performance rates for these systems by improving their components with minimal cost and required space. However, we found through the literature review that all works have been conducted based on the two independent classifications mentioned in the previous paragraph.

The current study aims to investigate the performance of the novel designed system able to operate under the two classifications either simultaneously or seperately. We denote the new solar system with the symbol DX/IX-DSHP to compare the obtained results between the three working modes of the system: Direct solar mode (DSM), Indirect solar mode (ISM) and Direct/Indirect solar mode (D/ISM).

The methodology adopted in this work starts with the development of a mathematical model using Matlab to obtain the results provided by a solar assisted heat pump system that uses solar thermal energy as a single energy source, classified as direct-expansion system, denoted by DX-SAHP.
Secondly, TRNSYS dynamic simulating program is used to develop a model that allows the investigation of the performance of an indirect-expansion dual solar-air heat pump system, referred to as IX-DSHP.
In the third stage, the two models related to DX-SAHP and IX-DSHP were integrated into one TRNSYS environment to create a model for the new heat pump system developed in this study, which we referred to as DX/IX-DSHP. The results show an improvement in performance indicators of the new hybrid heat pump system by optimally utilizing the thermal energy available from the two dual solar-air energy sources.

Thesis structure

The thesis is divided into three chapters. In the first chapter, we present and define the background of the literature relevant to the research work. The results of previous studies related to the current study are outlined, followed by an explanation of the contribution and the novelty of the topic with the efforts made aiming the optimal performance of heat pump systems.

In the second chapter, we review the methodology employed to investigate the performance of the newly developed thermal system. After detailing the building under study and the climatic conditions surrounding the area where the building is located, we ensure that the proposed model under the TRNSYS program operates efficiently, guaranteeing the necessary energy for space heating as well as hot water for domestic use at the required temperatures. We then explain in detail the procedure of mathematical modelling using Matlab and then integrated with the TRNSYS program, and we review all related mathematical equations.

Chapter three deals with the presentation of obtained results. We begin by presenting the daily results and then the total results throughout the entire heating period, which corresponds to the months of the year when there is demand for space heating and domestic hot water. Additionally, we present a parametric study relevent to the impact of system components effect on its performance. The chapter concludes with an economic analysis to the proposed system.

The presentation of the thesis ends with a general conclusion, presenting the idea of the research, the contributions made, the results derived, and recommendations for future work.

Chapter 1

Literature Review

1.1 Introduction

Worldwide energy consumption still increases in response to human needs for thermal comfort, urbanism and technology development. Most people spend 90% of their daily lives indoors and relying on heating and air conditioning, thus leading to buildings becoming a large energy consumer [1]. Statistics show that the residential sector is the third total energy worldwide consumer after industrial and transportation sectors [2]. This increase in energy consumption is associated with steady growth in fossil fuels consumption leading to gases emissions, pollution and greenhouse effect that influence the environment and nature. For instance, the EU revealed that the building residential sector in the continent consumes 40% of total energy end-use, generating 36% of greenhouse gas emissions [3]. This demand is divided into three main consumption categories: Space Heating (SH) (53%), as the largest segment; and Domestic Hot Water (DHW) supply (9%). The remaining is used for other heating and cooling purposes [4], [5] and [6]. In last decades, the world big concern has become to shift to renewable energies in attempts to cope with human needs and climate impacts.

In case of Algeria, a promising renewable energy program has been launched to increase the renewable energy share in the country energy production [7]. The national energy mix program is to attain the objective of 65% solar renewable energy by 2050 [8].

Heat pumps are attended to play a crucial role in switching from fossil energies reliance to renewable energies benefits. They have been a popular technology for last decades attracting the attention of researchers to enhance their performances and governments to expand their widespread use. Heat pumps are highly efficient devices that transfer heat from a lower-temperature location to another higher temperature using a small amount

of energy. The performance of heat pumps strongly depends on the source temperature. Therefore, the studies are carried out depending on the source nature and weather conditions. The heat pump system components and arrangements constitute large contributions of studies in an objective to continuously rise its performance.

This chapter is divided into three parts. The first part presents the key vocabulary used in this thesis in the form of definitions and basic principles. The second part presents a literature review relevant to this study, with a particular focus on recent researches. The final section summarizes the research problem and presents the research's contribution.

1.2 Part One: Definitions

1.2.1 Heat pump systems

Heat pump systems are energy efficient systems in which a heat pump allows the heat transfer from a colder environment to a warmer environment contrary to natural flow of thermal energy which is from a higher temperature medium to a lower temperature one. The big interest from using heat pumps is that they use a small amount of thermal energy [9], they offer economical and efficient alternative of recovering heat from different heat sources [10] and they produce heating with a quality [11]. Environmentally, they are characterized by low gases emission due to low consumption of primary fossil energy sources and they can be supported by renewable energies such as solar energy [12].
The functioning of a heat pump system is achieved through a basic heat pump connected to an environment of different energy source from one side and the application or the desired energy output on the other side.

1.2.2 Basic cycle of a heat pump

The basic cycle of a heat pump consists of four important components, namely an evaporator, a compressor, a condenser and an expansion valve as shown in Figure 1.1. The circulating fluid, or energy-carrying medium or refrigerant, when passes through the evaporator, is heated by absorbing heat from the surrounding. It is at vapour state with low pressure and high temperature at exit 1 shown on the figure. This is then driven to a compressor to produce high pressure and high temperature at exit 2 that can be delivered to a heat exchanger (condenser). The high-pressure and high temperature

fluid when enters the condenser cools to its saturation temperature by exchanging heat with a cooling medium and turns into liquid at exit 3. At expansion valve level, the fluid undergoes an isenthalpic process, becoming a two-phase mixture of the refrigerant at exit 4 with low pressure and temperature. The two-phase re-enters the evaporator to be fully vapour so the heat pump cycle is repeated.

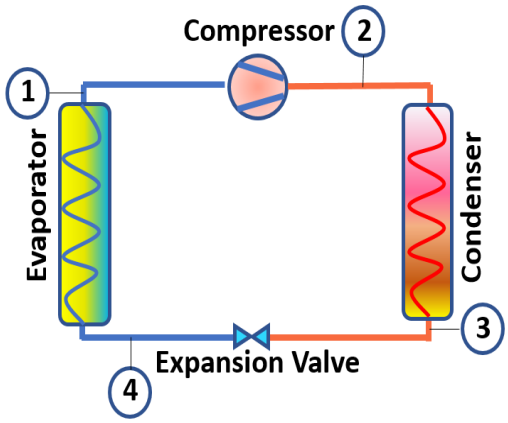

FIGURE 1.1: Schematic illustration of a heat pump cycle.

1.2.3 Air source heat pump

An air source heat pump used for space heating or for water heating absorbs heat from the outside air and uses electricity from the grid to turn the compressor. The work principle is the same of a heat pump cycle. It transfers the heat energy, by utilizing ducts, to water or indoors by evaporating coolant liquid fluid which is compressed to a higher pressure and temperature. This coolant fluid is then condenses in the condenser allowing the heat from the environment to be transferred to the home heating system [13].

ASHPs are known by their convenience to install and are less susceptible to frosting in high-altitude plateau areas due to the relatively low humidity [14]. They are suitable for climate regions where temperatures in winter is above -10°C and summer temperatures are moderate [15]. These weather conditions are typically similar to the conditions of the city of Djelfa under case study.

Nowadays air-source heat pumps are efficient heating devices compared to conventional heating systems like gas boiler systems due to their positive ratio between what they consume and what they release as energy [16]. The drawback is that these systems become less efficient in very low ambient temperatures due to high electricity consumption [17].

ASHPs come in two varieties air-to-air and air-to-water heat pumps [18] [19]. A schematic of both types is illustrated in Figure 1.2.

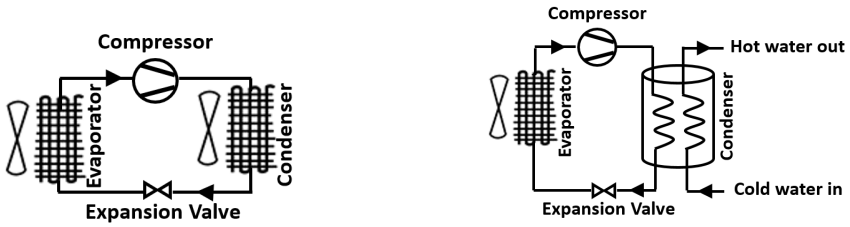

(a) Air-to-air HP (b) Air-to-water HP

FIGURE 1.2: Types of air-source HPs, inspired from [20].

Air-to-air heat pump

Air-to-air system directly heats the air of a room which is circulated by fans using a slim wall-mounted box with two units connected via ducts, one indoor unit located in a room that requires heating and the second located outdoor. Both units operates with a single compressor. Most air-to-air heat pumps are actually reversible air conditioning units, as they perform both heating and cooling. The drawback is that air-to-air load is only for space heating application. [21]

Air-to-water heat pump

In air-to-water heat pump system, the heat is transferred to a water-based central heating system consisting of pipes and wall radiators to provide indoor space heating and hot water. To transmit heat from the refrigerant, the system needs a heat exchanger in hot water tank. Air-to-water heat pumps have a factory sealed refrigerant loop, and can be installed by regular plumbers and heating engineers [18].
Air-to-water heat pumps surpass air-to-air heat pumps by the both supply of hot water and space heating. However, for space heating reasons alone, air-to-air HP has bigger heating capacity than air-to-water [22]

Figure 1.3 illustrates the two different indoor units of ASHP. On the left, air-to-air HP indoor unit and on the right, a radiator of air-to-water HP.

1.2.4 Water source heat pump

Water-source heat pump uses heat in the tank as a heat source for the HP. In this type, solar energy is collected by the solar collector to heat the water.

FIGURE 1.3: ASHP ouput units [22].

The evaporator draws energy from solar heated water and sends the working fluid to the compressor. After compression phase, the working fluid goes into the condenser. Thereby the working fluid releases heat application medium [23].

Depending on the application water heating or space heating, WSHP may be water-to-water heat pump or water-to-air heat pump as illustrated in the schematic of Figure 1.4.

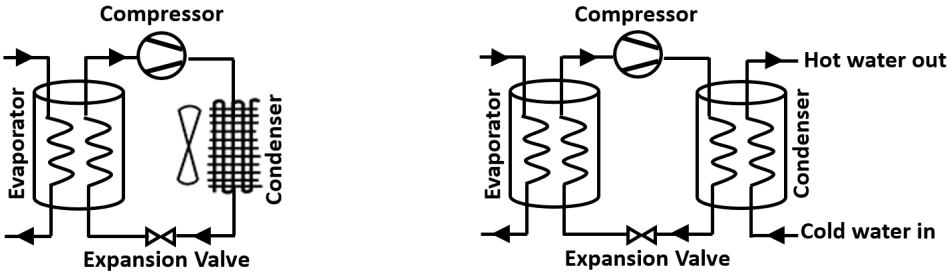

(a) Water-to-air HP (b) Water-to-water HP

FIGURE 1.4: Types of water-source HPs, inspired from [20].

.

Water-to-air heat pump

A water-to-air heat pump extracts thermal energy from a water source and transfers it to air circulated in ducts inside a building. This kind of heat pumps is suitable for space heating and cooling. Circulation pumps are controlled to operate when heat gain from the heating water source and a storage capacity for heat are available [24].

Water-to-water heat pump

A water-to-water heat pump transfers thermal energy between two water loops. It absorbs heat from a source water loop and releases it to a load water loop. Efficient for space heating, cooling, and domestic hot water production, water-to-water HP surpasses water-to-air HP by the production of hot water for domestic needs [25].

After this overview of heat pumps, we would like to point out that the type used in the present work is a heat pump that operates with double sources, air and water, to become air-to-water source and water-to-water source heat pump. Obviously, the switch between the two sources obeys to a control. This is due to the requirements of supplying hot domestic water and space heating.

1.2.5 Heat pump components

The refrigerant

The refrigerant of the heat pump is a key element of evaluating the performance of the heat pump. The refrigerants have unique properties which undergo phase transition from liquid to gas and vice versa. This phase change allows a latent heat storage between the condenser and evaporator [6]. The gas phase takes place after evaporation at low pressure (evaporating pressure) and the liquid phase takes place after the condenser at high pressure (condensing pressure). The performance of a heat pump relies strongly the circulating refrigerant and its evaporating temperature [26].
R134a or HFC-134a or (1.1.1.2-Tetrafluoroethane CH_2FCF_3) is a common Freon-based refrigerant [27]. It still widely used in household facilities, this is attributed to its zero Ozone depletion and its safety and non-flammability [28]. Its physical properties are shown in Appendix A.
R134a is the refrigerant selected for this study as discussed in the second chapter.

The evaporator

As its name indicates, an evaporator evaporates the heat coming into the low-pressure liquid refrigerant after being absorbed from the surroundings. Common configurations of evaporators are direct-expansion coil evaporator, finned-tube evaporator and shell-and-tube evaporator.

- **Direct-expansion coil evaporator**:
  Embedded refrigerant tubes installed in a metal plate, usually in copper on aluminium, and directly exposed to heat source (sun or air), see photo in Figure 1.5 (a).

- **Finned tube evaporator**:
  It consists of tubes with extended metal surfaces, named fins, to increase its surface area hence increasing the heat transfer with air, see photo in Figure 1.5 (b). It is commonly used in air-source HP type.

- **Roll-bond evaporator**:
  Roll-bond evaporator consists of tubes where the circulating fluid flows connected to an absorber plate. This design increases the heat transfer area between the fluid and the plate as seen in Figure 1.5 (c). [29].

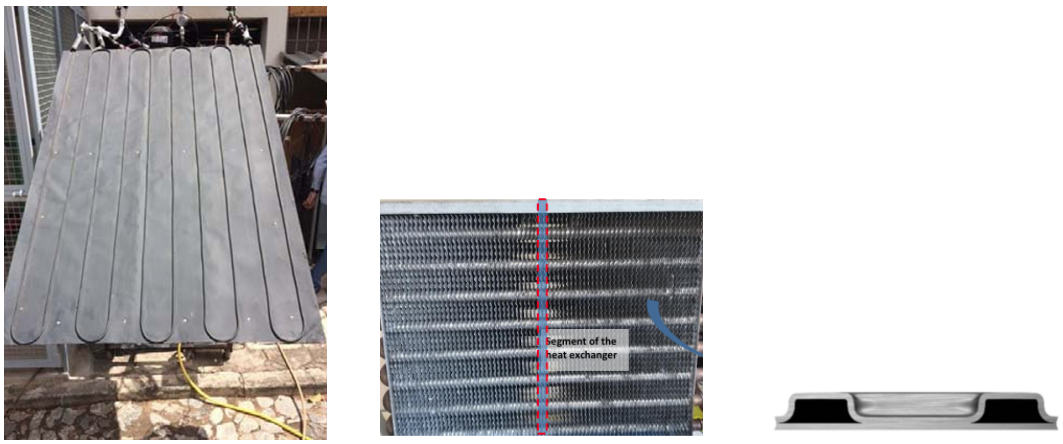

(a) Coil [30] (b) Finned tubes (c) Roll-bond [29]

FIGURE 1.5: Common types of evaporators

The compressor

A compressor is a mechanical device that drives the vapour refrigerant through the heat pump cycle by increasing its pressure and temperature, enabling heat transfer in the condenser.
Common types of compressors are rotary, scroll, reciprocating, screw and centrifugal compressors as shown in Figure 1.6.

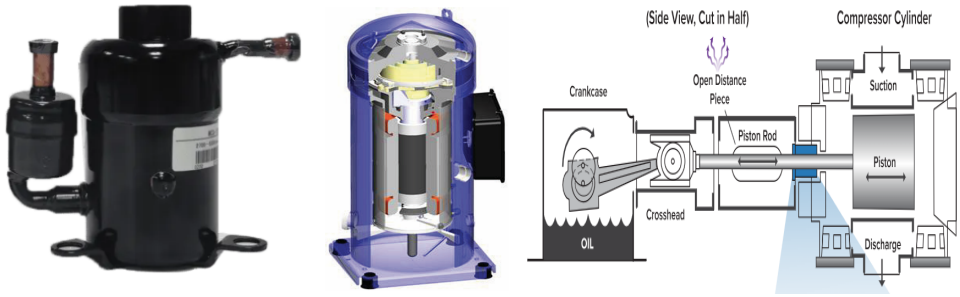

(a) rotary [31] (b) scroll [32] (c) reciprocating [33]

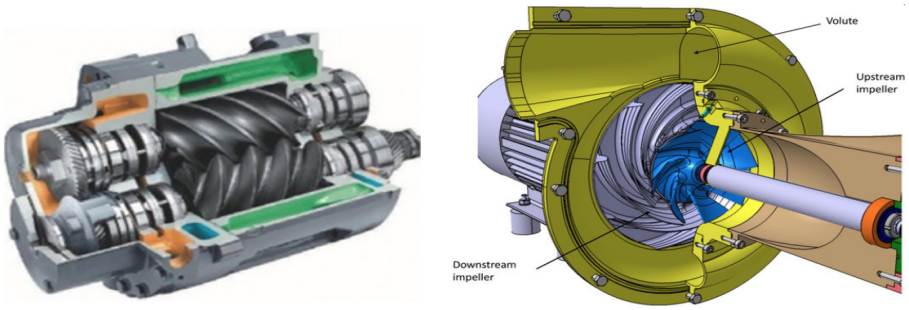

(d) screw [34] (e) schematic of centrifugal [35]

FIGURE 1.6: Common types of compressors

The working principle differs from one type to other. A rotary compressor uses two helical rotors to compress the gas. A scroll compressor is formed by two identical spiral-shaped metallic pieces (scrolls) with eccentric motor shaft arranged within a hermetic shell . One of the scrolls is stationary and the other moves in an orbital motion [32]. A reciprocating compressor is considered as high piston velocity machines. It uses pistons driven by a crankshaft in a reciprocating motion [36]. A screw compressor consists of two rotors in a common housing. Both rotors have helical lobes and rotate relative to each other. As they rotate, the lobes and housing create compression chambers [37]. The centrifugal compressor is a high-volume machine. The pressure of the air is increased as it is pushed by centrifugal force utilizing the blades of a centrifugal pump [38].

Indeed, compressors are classified according to their heating capacity as shown in Figure 1.7. Rotary-type compressors are low-noise machines and suitable for household heating [39].

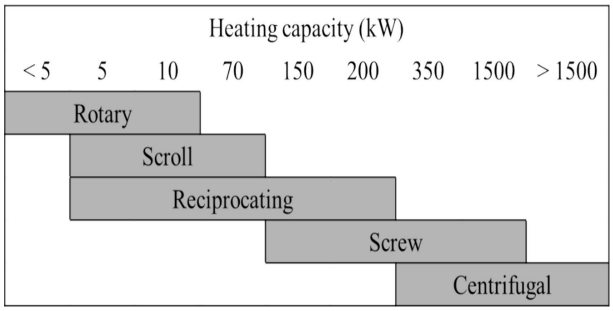

FIGURE 1.7: Heating capacity of compressors [40].

The condenser

A condenser is generally a copper tube. Its role is to release heat from the refrigerant to the surroundings (air or water), causing the refrigerant to condense from vapour to liquid. Condenser design underwent two stages style with annular flow and U style pipe [41]. When considering COP as the function of mean water temperature, the performance of U style pipe system is better than that of annular condenser system. System COP and the rate of heat production increase with the loop number increases [41] [42]. Figure 1.8 (a) represents a photography of an immersed condenser of the R134a in a DX-SAHP and Figure 1.8 (b) represents a schematic of an annular condenser.

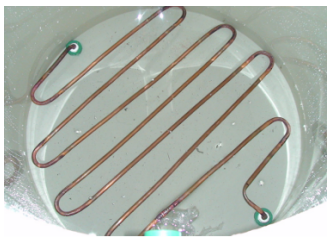

(a) U-stile pipes [43]

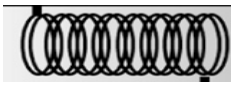

(b) Annular [44]

FIGURE 1.8: Common types of condensers

The expansion valve

The role of an expansion valve is to decrease the pressure of the liquid refrigerant before it enters the evaporator. It controls the flow rate and pressure drop of the refrigerant for optimal evaporation conditions in the evaporator. Common expansion valve types are Thermostatic Expansion Valve (TXV), electronic expansion valve (EEV) and capillary tube expansion valve. Figure 1.9 represents, for indication purposes only, some available on-line models of expansion valves.

(a) TXV [45] (b) EEV [46] (c) Capillary tube [47]

FIGURE 1.9: Common types of expansion valves

1.2.6 Solar thermal collector

Of all renewable energy sources, solar energy emerges as one of the most promising alternatives to fossil fuels [48]. Solar thermal collectors are panels which convert the incident solar radiation into thermal energy and transmit it to a working fluid flowing through the collectors. The solar irradiation heats up an absorber plate attached to the heat carrier tubes. The absorbed energy is then transferred to the working fluid in these tubes and conveyed for subsequent use for domestic hot water or space heating or be stored in a thermal storage tank for later uses.

Depending on their temperature outputs, solar thermal collectors may be categorised as stationery, sun tracking and concentrating collectors.

The range of temperature outputs of sun tracking and concentrating solar collectors is in between 60 °C and 2000 °C [49]. It is obvious that these are not the suitable collector types that can be employed in single-family house where the required heat source is less than 100 °C either for domestic hot water or for space heating. The structures and design of these panels are well discussed in literature for further readership.

The stationary collectors consist of flat-panel collectors (FPC), evacuated tube collectors (ETC), and compound parabolic collector where their temperature output is usually in between 30 °C and 240 °C [50].

The output temperature of a flat plate collector is generally between 30 °C and 80 °C, hence they are the most suitable collector types and commonly used in residential building applications for domestic hot water production

[49] [51].

Flat plate collectors come in two varieties, glazed FPC or unglazed, as discussed in the two next sub-paragraphs.

Glazed collector

In solar thermal collectors, glazing refers to the transparent cover usually made of glass or plastic that sits above the absorber plate. Its role is for both energy capture and heat retention via the greenhouse effect in addition to the protection of internal components from weather, debris, and mechanical damage. Also, the glazing may be single or double-glazed which offers thermal insulation and helps reduce heat loss.

A typical glazed FPC consists of following components shown in Figure 1.10:

- Glazing (single or double): the glazing is a transparent layer used to reduce the convection and radiation losses,
- Header tube: used to charge and discharge the working fluid,
- Liquid transport tubes or passages: used to transfer or direct the flowing fluid from the inlet to the outlet,
- Absorber plate: used to absorb the incident solar irradiation and to hold the tubes or passages,
- Insulation: used to reduce the collector heat losses (back and sides),
- Casing: used as a box to hold the above components in place and protect them from dust and moisture.

Unglazed collector

Unglazed collector means that the collector does not include glazing layer as shown in Figure 1.11. With this kind of solar collector, solar heat collection is improved with reduced solar radiation reflection which improves consequently the system performance [53]. it prevents heat loss so that heat is completely absorbed by the plate and transmitted to refrigerant. Unglazed FPC is the most widely used and investigated one among other types of solar thermal collectors [54].

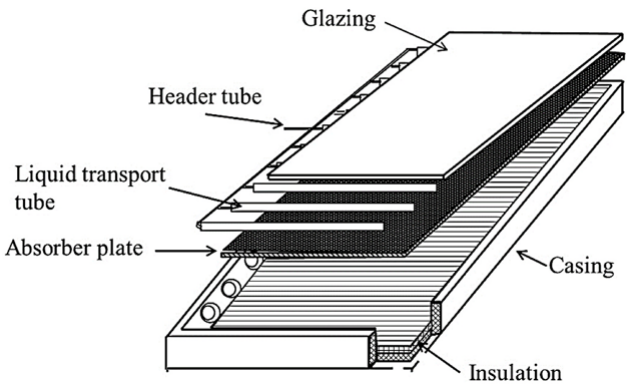

FIGURE 1.10: Schematic of a glazed flat-plate collector [52].

An unglazed flat-plate solar collector is usually used as evaporator in DX-SAHP system [53] and it is more efficient for temperatures below ambient [55].

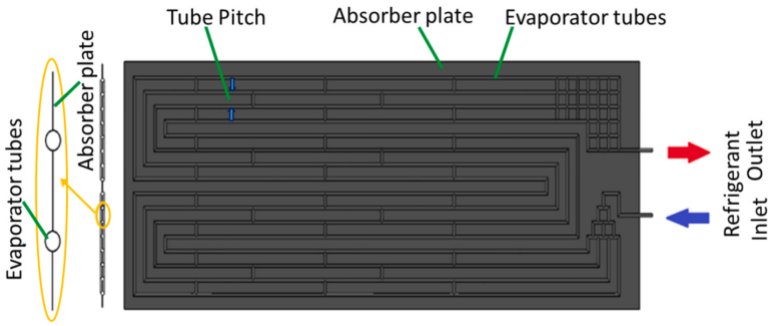

FIGURE 1.11: Schematic of unglazed flat-plate collector [56].

1.2.7 Photovoltaic thermal collector

With PVT notation, the terms "photo" and "voltaic" denote light and electricity, respectively. A photovoltaic cell, also known as a solar cell, is a device that converts sunlight into direct electricity without the interference of engines. When the cell is exposed to light, an electrical field is created between its two layers, causing a potential difference that can be connected to a circuit to generate electricity [57] [58].
A panel photovoltaic thermal (PVT) can simultaneously produce solar thermal energy (thermal part) and solar electricity (PV module) from a single integrated system with the principle illustrated in Figure 1.12. A simulation study found that 1 m² of unglazed PVT for DHW preheating per person can deliver 230 kWh thermal and 150 kWh electrical energy annually, outperforming standalone PV modules by 4% [59].

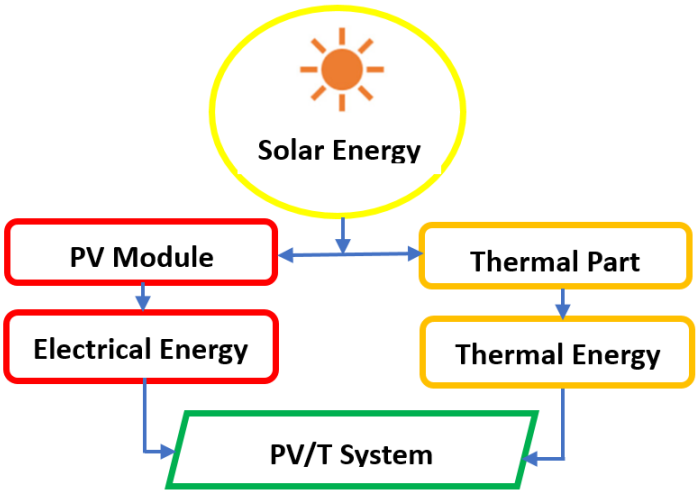

FIGURE 1.12: Schematic illustration of a PVT system operations.

The addition to a STC is that the absorber is covered by a PV layer [60]. The absorbed thermal energy is transferred to a transmitter fluid instead of dissipating it to the environment [61] [62]. The thermal energy is then carried via fluid flow tubes and channels under insulation to the rest of the HP system. The design of a PVT collector is shown in Figure 1.13.

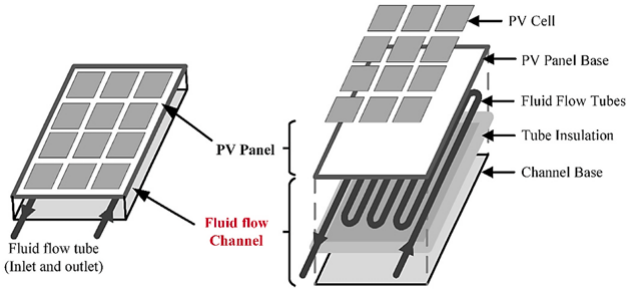

FIGURE 1.13: Schematic of a PVT collector [52].

Compared to a conventional solar thermal collector, a PVT collector possesses two distinct opposing qualities. It allows electricity production which is not involved in a STC, but it decreases the heat collection capacity [63].

It is worth to remember that two ways existing to combine the photovoltaic and the heat pumps. We are discussing in the present work the photovoltaic thermal (PVT), which uses the solar heat in the water as heat source. The system often abbreviated as (PVT-SAHP). The other way, which is not relevant to the present work, is the use of photovoltaic (PV-SAHP), which employs the solar heat on the PV as the heat source [64] and [65].

After this overview of solar collectors, we would like to mention that both types of collectors, unglazed bare plate solar thermal and photovoltaic/thermal collectors are used in the heat pump system under consideration.

1.2.8 Solar-assisted heat pump systems

SAHP system is a system that uses solar collectors, which may be either solar thermal, PVT or hybrid collectors, providing heat to the evaporator of the heat pump. Solar collectors provide thermal energy that can be utilized for space heating, water heating, steam generating, or stored in thermal storage to be subsequently used in periods of reduced solar radiation or during night-time. The solar energy that is gathered acts as the main heat source for a heat pump [66]. Due to higher evaporating temperatures, their coefficients of performance (COPs) are much higher than those of traditional heat pumps [67].

This makes SAHP a practical solution at low ambient temperatures and the reason of many researches in last decades [53].

There are two main types of SAHP systems, namely direct-expansion solar-assisted heat pump (DX-SAHP) systems and indirect-expansion solar-assisted heat pump (IX-SAHP) systems.

Direct-expansion solar-assisted heat pump system

In DX-SAHP, the thermal collector plays the role of evaporator, where the refrigerant circulates and absorbs heat directly from solar energy and ambient air[68], [69] and [70]. The solar collector in the DX-SAHP system is usually a flat plate type without any back insulation so that heat can also be extracted from the ambient air using the solar collector [20]. Thus, both processes, namely collecting solar energy and vaporizing the refrigerant, are realized in one unit only. This leads to several advantages:

- This design enables solar radiation to directly serve as a heat source for the evaporator, avoiding the necessity for any intermediate fluid and eliminates the need for a heat exchanger, making the system simpler and more efficient with low cost,
- The direct vaporization of the refrigerant in the solar collector–evaporator leads to higher heat transfer coefficients,
- The use of one unit solar collector-evaporator with no additional evaporator unit reduces overall system cost,

- The working fluid in the collector is refrigerant instead of water, which can prevent the freezing problem of solar collectors in cold nights [71] and eliminates corrosion, leading to longer system life [72].

DX-SAHP systems are primarily intended for the generation of domestic hot water (DHW) [66].

Figure 1.14 represents a schematic illustration of a DX-SAHP.

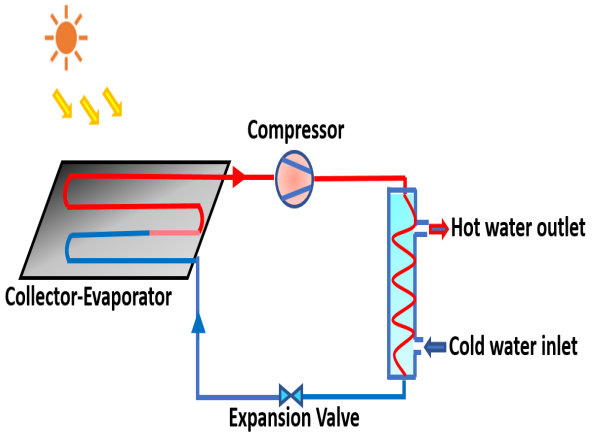

FIGURE 1.14: Schematic illustration of a DX-SAHP.

Indirect-expansion solar-assisted heat pump system

In IX-SAHP, the collector and the evaporator are separated by a heat exchanger [67] and [66]. Both the heat pump and the solar thermal collector (STC) supply the heating demand together but with two separated cycle with the aim of heating with different arrangements. The role of the STC is to extract heat from the heat source via working fluid, like water, glycol or air, and transfers it to the evaporator via a heat exchanger. The thermal energy is used for heating space directly or serving as heat source for heat pump [53]. Thus, advantages that can be drawn from IX-SAHP systems are:

- Both DHW provision and space heating can be supplied efficiently.
- They provide space heating directly, unlike DX-SAHP systems, by-passing the heat pump in high solar irradiations, which results in low energy consumption by circulation pump.
- The influence of unstable weather conditions is reduced owing to the presence of a heat exchanger between the solar heat transmitter loop and the refrigerant fluid loop and to the use of water storage tank

- A heat storage system is always integrated into the system to control the energy production and demand.

The configuration of a IX-SAHP is more complex system since it uses thermal storage materials. Figure 1.15 is a schematic representation of IX-SAHP.

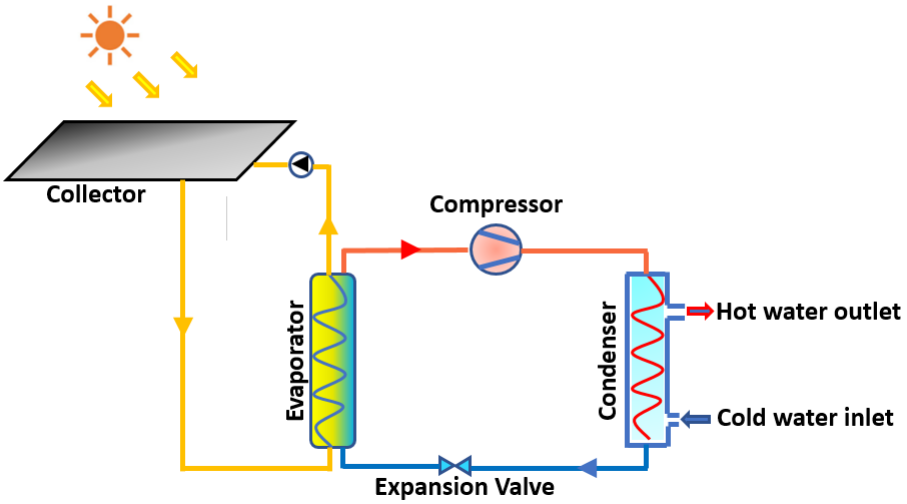

FIGURE 1.15: Schematic illustration of IX-SAHP.

1.2.9 Dual source SAHP system

As its name indicates, a single source SAHP system indicates that the HP absorbs thermal energy from a unique source. For example, air alone or solar alone. Given solar energy is the single thermal source of a SAHP system, its thermal performance declines under worse weathering conditions, particularly in low solar radiation availability [74], [73], [21] and [75].

As discussed above, a single source HP system presents a number of limitations that reduce its efficiency and performance due to its dependency on unstable weather conditions. For this reason, dual source heat pump (DSHP) system is proposed as a real solution to face these limitations.

The use of air ambient as a second heat source allows the heat pump working continuously and in stable conditions. A dual source solar-air heat pump (DSHP) system possesses two evaporators; one is used to absorb solar thermal energy and the other to absorb thermal energy from air environment [76].

DX-DSHP is usually investigated for DHW production, but the performance of this latter is rarely evaluated for space heating. Figure 1.16 highlights a schematic representation of a DSHP system.

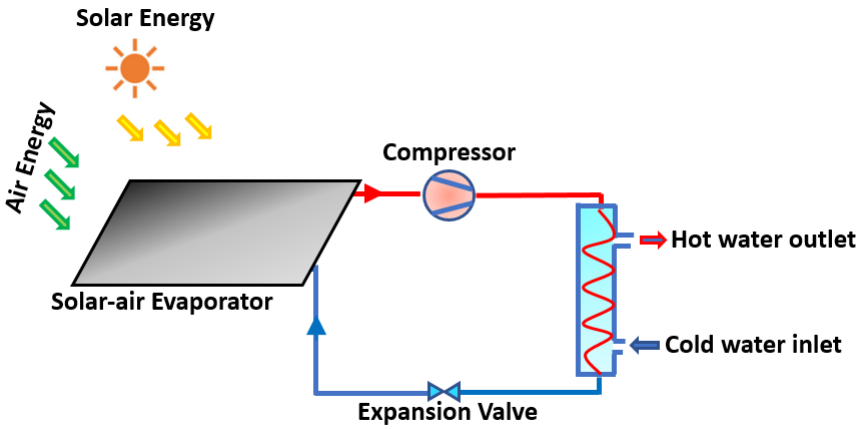

FIGURE 1.16: Schematic illustration of a DSHP system.

There are different possibilities for connection of the heat pump and the solar heating system. The solar collector of the system and the air evaporator of the heat pump (ASHP in this case) can be arranged in series or in parallel.

1.2.10 Series arrangement

In this arrangement, see Figure 1.17, solar collectors and heat pump are connected in series, directly or through a storage tank. The heat pump uses solar energy as a heat source, from a solar collector loop directly or through a storage tank [77]. In series scheme, the refrigerant takes heat from SCE and AE sequentially. In such configuration, heat transfer inconsistency between the two evaporators is to be taken into consideration.

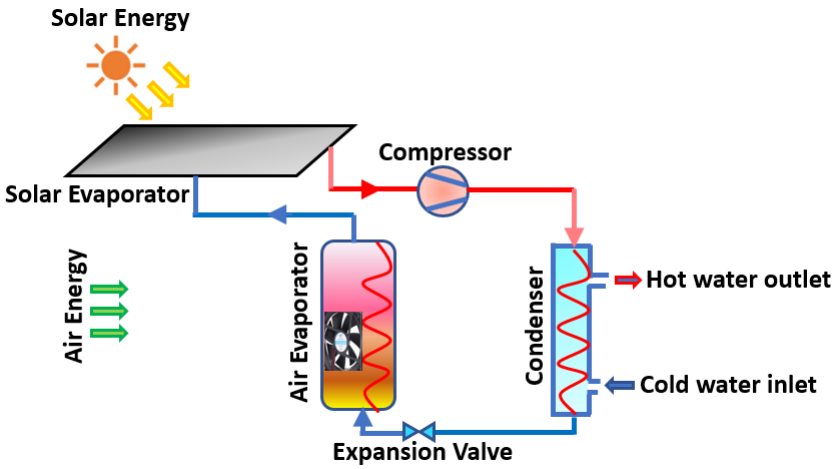

FIGURE 1.17: Schematic illustration of DSHP in series arrangement.

1.2.11 Parallel arrangement

In a parallel SAHP system, solar collectors and heat pump are independent units (subsystems) and simultaneously support the system heating load, see Figure 1.18.

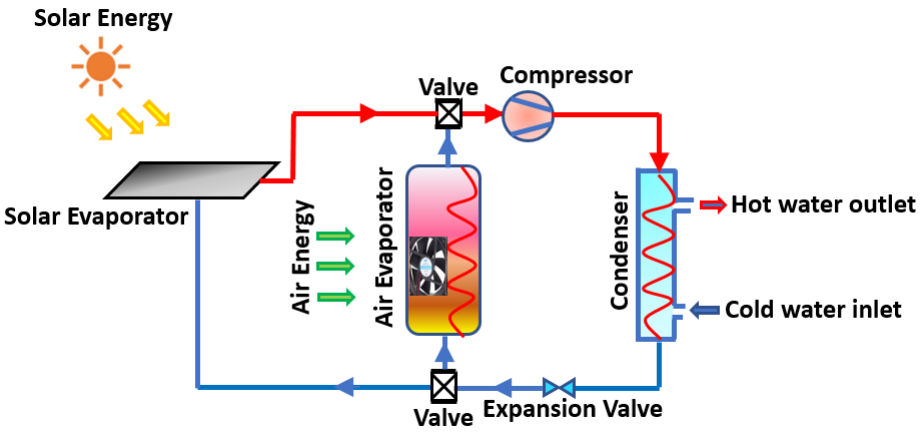

FIGURE 1.18: Schematic illustration of DSHP in parallel arrangement.

Solar energy can be used directly from a solar collector loop or from a storage tank. The heat pump is separated from the solar subsystem where it uses a heat source other than solar energy like air or ground [78].

An automatic control decides which subsystem should be used at a given time, i.e., which subsystem has better thermal performance at that time [77]. The great advantage of the parallel system is that the heat pump could stop operating when the heat output of the solar collector meets the system heating demand [78]. This gives a better performance under the condition of abundant solar radiation and ambient temperature. The parallel system is the most applicable system that accounts for 61% of the market [79].

1.2.12 Performance indicators

Coefficient of performance (COP)

Heat pump efficiency is determined by comparing the amount of heat energy delivered by the heat pump to the amount of energy it consumes. Referred as the Coefficient of Performance (COP) in heat pumps studies, it expresses the ratio of the amount of thermal energy in kilowatts provided by a heat pump to the kilowatts of power it consumes [13].

The COP of the heat pump is dimensionless (unitless) parameters using Equation 1.1:

$$COP = \frac{Q_{HP}}{E_{HP}} \tag{1.1}$$

Where Q_{HP} is the total thermal energy provided by the heat pump, defined by Equation 1.2 as:

$$Q_{HP} = Q_{DXHP} + Q_{ASHP} + Q_{WSHP} \tag{1.2}$$

Where Q_{DXHP}, Q_{ASHP} and Q_{WSHP} are the heat provided in DXHP mode, in ASHP mode and in WSHP mode respectively.
E_{HP} is the total electrical energy consumed by the heat pump, defined by Equation 1.3 as:

$$E_{HP} = E_{DXHP} + E_{ASHP} + E_{WSHP} \tag{1.3}$$

Where, E_{DXHP}, E_{ASHP} and E_{WSHP} are the electricity consumed in DXHP mode, in ASHP mode and in WSHP mode respectively.

Seasonal performance factor (SPF)

The seasonal performance factor of a heat pump takes into account how well the whole heating system performs throughout a period of time. It is a weighed average of the COP over a full heating season (i.e., the efficiency of the heat pump at standard operating conditions weighted by the number of days at which these occur) at a specified boundary of the heating system. This allows a meaningful energy label to be defined for eco-design [13].

The seasonal performance factor is a dimensionless (unitless) parameter calculated using Equation 1.4:

$$SPF = \frac{Q_{SH} + Q_{DHW}}{E_{HP} + E_{Pumps} - E_{PVT}} \tag{1.4}$$

Where Q_{SH} is the heat supplied for space heating, Q_{DHW} is the heat supplied for hot water, E_{HP} is the electricity consumption, E_{Pumps} is the electricity consumed by the pumps of the system, E_{PVT} is the electricity produced by the PVT panels.

It is worth to remember that both seasonal performance factor (SPF) and coefficient of performance (COP) differ from each other. SPF represents the mean season performance in a specific location, based on the mean outdoor temperatures over a heating period. Indeed, The SPFsys simulation studies vary widely depending on system configurations, sizing, loads and weather conditions [80] and [81].

Whereas, the COP is a steady-state metric. That say the COP of a HP is the same for different cities, whereas its SPF is different when the weather conditions differ. Another difference between COP and SPF is that the COP only is evaluated for heat production and electricity consumption by the heat

pump itself. The SPF estimation comprises production and consumption by auxiliary heaters (Q_{aux} and E_{aux}), electricity used to circulate the coolant loop or outdoor air (E_{fan}) and to defrost ASHP systems (E_{frost}).

Solar fraction (SF)

The solar fraction is a performance metric that indicates how much of the energy demand is supplied by the solar heating system. It is typically expressed in term of percent of total load met and varies between 0% (no Solar contribution) and 100% (all energy is supplied by the solar system). That is to say, on winter days or days with inclement weather, the solar heating system may meet none of the daily hot water demands, whereas on sunny days, the system may save more energy than is required to satisfy 100% of the heating needs [82].

The solar fraction of the system is calculated using Equation 1.5:

$$SF = 1 - \frac{E_{HP} + E_{Pumps} - E_{PVT}}{Q_{SH} + Q_{DHW}} \tag{1.5}$$

In case of IX-DSHP system, $Q_{DXHP} = 0$ and $E_{DXHP} = 0$.
In case of DX-DSHP system, $Q_{WSHP} = 0$ and $E_{WSHP} = 0$.

1.3 Part Two: Literature survey

The areas of building environment and energy consumption are important research topics aimed at offering the best end products based on quality and efficiency. Numerous numerical simulations, theoretical, and experimental analyses are conducted on DX-SAHP and IX-SAHP systems separately to optimize their efficiency.
This section presents a literature review on developments and advances of solar assisted heat pump technology reported in past two decades with particular attention to the works with relevance to the current study in term of the duality of energy sources, the categorizing of SAHP systems and solar collectors.

1.3.1 Glance in history

Solar assisted heat pump (SAHP) systems have been a popular research topic and evolved in the last two decades because this technology has proven its performance in the area of building and energy consumption. The aim of the

efforts and research works in the field is to contribute in the determination of the appropriate type of SAHP systems in terms of performance, environment, structure and cost.

The idea of SAHP was first introduced in 1955 [21], and its significance grew was in the 1970s driven by world energy crisis and interest in renewable technologies [66].
In United States, adoption of the strategy remained limited due to low electricity prices, high and lack of supports. The UK has seen gradual uptake of SAHPs in coming years. Later, Europe countries have been leaders in SAHP research and deployment, especially in countries like Finland, Sweden, Italy [5]. Chinese scholars began to carry out experimental studies on the SAHP manufactured by Hitachi in 1985 and then gradually conducted theoretical research on SAHP [67]. China is now a global leader in SAHP innovation, with remarkable efforts and research works in the field.

Indeed, investigations on SAHP systems gained a new era due to growing global interest in renewable energy and carbon reduction in earlier 2000s affected by international agreements and treaties on climate. In 1987, the Montreal protocol on substances depleting the Ozone layer such as chlorofluorocarbons (CFCs) based refrigerants banned the use of R-12 refrigerant. Montreal protocol is considered as the first environmental treaty, which led to other initiatives like the Kyoto protocol which was adopted in 1997 and become operational in 2005; and Paris agreement which was signed in 2016. The final commitment approved at the COP21, took place in Paris in 2015, was to hold the global warming increase below 2°C with an equivalent CO_2 concentration of 450 ppm in the atmosphere by 2050.

1.3.2 A heat pump components

A heat pump cycle contains four main components in addition to the heat transmitter fluid. As a summary, a number of papers is available in literature investigating a heat pump system performance from the point of view heat pump components to evaluate their performances.
With regard to evaporator, it is found that the coiled tubes embedded with a specific refrigerant, installed on flat plate made of aluminium is the most investigated type. When the plate is uncovered, this leads to the best choice [83] and [54].
Concerning the compressor, the investigations were carried out on how the

efficiency and speed of a compressor may affect refrigerant pressure and heating temperature rise. Kuang et al. [84] found that the possibility to vary speed compressor enhances COP of a HP. The conducted experimental study on a DX-SAHP where the found that COP increases from 2.6 to 3.3. In term of compressor life cycle and heat pump performance, Xu et al. [85] concluded that a compressor should be set at low speed which results in higher performance with low energy consumption mainly when both the solar radiation and ambient temperature are high. In newly developed system, they found that as the compressor speed decreases from 5000 r/min to 1500 r/min, the COP increases in two different weather conditions. It increases from 5.89 to 7.36 in Nanjing (China) and from 5.59 to 7.09 in Hong Kong. These findings are confirmed later by Huang et al. [86]. They found that the COP decreases from 2.82 to 1.86 as the compressor speed varies between 20 and 80Hz.
As for the condenser, it is widely mentioned in literature that U-tube form of a copper tube is the best installation in DWH applications as seen a previous paragraph in this chapter. The studies on condenser design and performance are based on water temperature, outdoor temperature, insulation of tank and heat transfer. In addition, the efficiency of a compressor plays an important role in heat gain by the condenser as pointed out by Chow et al. [62]. In an experimental study on a DX-SAHP, the condenser heating capacity was found to vary between 2.0 to 3.6 kW [87].

Two common used expansion valves in SAHP systems are thermostatic type and electronic type. The former is used because of its simplicity and the latter is recommended in case of weather conditions and ambient temperature fluctuations.
The use of refrigerants is restricted by international climate considerations and protocols. The selection of refrigerants affects evaporation temperature, which influence the coefficient of performance of a SAHP. Very few studies comparing the performance of DX-SAHP using different refrigerants were found in literature. Researchers test refrigerants under various conditions to optimize heat transfer, mass flow rate, and energy consumption. A study conducted by Chata et al. [88] investigated new refrigerants which were commercially available at early 2000s as the main working fluid and refrigerant for SAHP systems. The analysed refrigerants were: R-134a. R-404a, R-410a, and R-407c to identify the best suited refrigerant for SAHP application in comparison to R-12 and R-22, which are banned refrigerants. Results showed that SAHPs using R-134a had the best performance among the new refrigerant. A comparison of refrigerants for a DX-SAHP system carried out on some refrigerants in term of thermal performance and environmental impact by Durate et al. [89] showed that the COP of R134a is the highest.

1.3.3 Air source heat pump

ASHPs began gaining traction in residential use around the 1970s and have become increasingly popular due to their energy efficiency and eco-friendliness. Their appearance is very similar to traditional air conditioning outdoor units. They are effective heating systems when compared to traditional heating methods, such as gas boilers, due to their favourable ratio of energy consumption to energy output [16]. An air-source heat pump is flexible to install with low initial investment. Air-to-water heat pumps are widely used for domestic hot water production and heating buildings [90]. They show better performance than direct solar heat supply at low solar irradiance levels [91]. However, the drawback is that these systems become less efficient in very low ambient temperatures due to high electricity consumption [92] [93]. The majority of installed HPs providing space heating or DHW are air-to-water HPs due to relatively low investment costs and simple installation for residential buildings [94], [95]. Karmann et al. [96] conducted a summary of previous works on the difference in thermal comfort between radiator heating and full-air heating systems and concluded that radiator heating provides better thermal comfort than full-air heating systems. Xiao et al. [22] arrived at the same conclusion that the temperature and velocity distribution of indoor air with air-to-water HP is more uniform and the thermal comfort is better.
Advances in ASHP systems studies are to compensate the lack of efficiency in low-temperature climates and to reduce electricity consumption. For example, Wang et al. [97] make comparisons between three configurations of ASHP systems. The findings are: photovoltaic-assisted-ASHP system has the best techno-economic performance, with COP of around 3.75, but with moderate cost and payback time. Solar-thermal-assisted ASHP system and PVT-ASHP system have lower performance with mean COP of 2.90 and 3.03, respectively. Moreover, PVT-ASHP system has the highest cost and longest payback time, while solar-thermal-ASHP system has the lowest ones.

1.3.4 Water source heat pump

A WSHP integrates a HP with water as a source of heat. It can be multifunctional used for DHW, space cooling and heating. The studies on SAHP systems using WSHP are mainly due to compensate the lack encountered with ASHP. The advantage is that it is characterized by the use of heat stored in water in insufficient sunshine which results in energy saving [98]. Known that water temperature in summer is lower than the ambient temperature

and vice versa in winter, the efficiency of the heat pumps can be further improved [99].

In addition, the heat pump works with higher performance because of high temperature heat source with reduced heat loss [100]. Compared to ASHPs, ambient temperature and weather conditions do not significantly influence the performances of WSHPs, the temperature of the water in the tank fluctuates less than that of air [19] and the COP of a WSHP is higher than that of an ASHP [98]. For example, Wang et al. [101], under experimental conditions, have found that the COPs of PVT-WSHP heating mode and PVT-water-air-source heat pump system heating mode are 3.18 and 2.53, which are much higher than the COP of ASHP heating mode with 2.23.
The water-to-water HP technology is relatively economical, enables to use the energy potential of water from different intakes and domestic water networks to generate renewable heat. The advantage is water networks are large and widely available. [102].

1.3.5 SAHP systems

To address the limitation of ASHP systems and improve the overall performances of heat pump systems, solar-assisted heat pumps (SAHP) systems emerges as a promising solution that combines the advantages of the conventional heat pump with the use of solar energy to improve its efficiency and reduce its dependence on electricity [103]. SAHP systems are characterized by high evaporating temperature resulting in enhanced coefficients of performance. This makes SAHP a practical solution at low ambient temperatures and the reason of many researches in last decades [104].

The SAHP is based on the transformation of the heat exchanger of the traditional heat pump by utilizing solar energy as the heat source, or combined with other energy sources, to improve the coefficient of performance of the heat pump [67].

With the use of SAHP, advantages can be addressed as the enhancement of the performance of the technology and the improvement of solar radiation use, thereby increasing its adoption in residential settings [66].

SAHP systems classification

According to the coupling mode of the solar collector and evaporator, the SAHP system can be classified as direct-expansion solar-assisted heat pump (DX-SAHP) system or indirect-expansion solar-assisted heat pump (IX-SAHP)

[66].

In direct systems, the thermal collector plays the role of evaporator, where the refrigerant circulates and absorbs heat directly from solar energy [68], [69] and [70]. Wide spreading trend was observed in the SAHP research of early 2000s on the increasing interest in DX-SAHP systems. [16] .

In indirect systems, the collector and the evaporator are separated by a heat exchanger [67]. Indirect expansion systems are more complex than direct expansion systems and this limits their preferability. [53].

Dual-source heat pump systems

Given solar energy is the single thermal source of a SAHP system, its thermal performance declines under worse weathering conditions, particularly in low solar radiation availability [21], [73], [74] and [75]. The use of air ambient as a second heat source allows the heat pump working continuously and in stable conditions. In such system, the heat necessary to evaporate the refrigerant fluid is collected from solar energy in high solar radiation availability. In case of low or absence solar radiation, heat is absorbed from ambient air [105] and [106].

Zhang et al. [107] found that the coefficient of performance (COP) in the becoming solar-air heat pump mode can be increased by 50% compared to the air source heat pump mode. Consequently, dual source solar-air heat pump (DSHP) systems have emerged, featuring two evaporators; one is designed to capture solar thermal energy, while the other is utilized to collect thermal energy from the surrounding air [76].

In literature, different configurations and settings of solar-air DSHP systems, including solar collectors, refrigerants, solar radiation and ambient conditions effects have been studied. However, the studies were conducted on the basis that the solar-air DSHP systems are categorized as, either direct-expansion DSHP systems, or indirect-expansion DSHP systems.

In recent decades, the use of thermal and photovoltaic thermal solar collectors with heat pumps has been widely employed for simultaneous coverage with heating, domestic hot water, and power generation in residential buildings [108].

Direct-expansion dual-source heat pump (DX-DSHP) systems

Almost all studies using DX-SAHP systems, investigated their energetic performance for domestic hot water production purposes.

The solar collector/evaporator (SCE) in DX-DSHP system plays an important role in determining its performance. This latter is usually used as bare without back insulation, which allows the refrigerant to be evaporated by absorbing thermal energy from solar irradiation and air ambient simultaneously. With this kind of solar collector, solar heat collection is improved due the absence of glazing which reduces solar radiation reflection and improves consequently the system performance [53]. In addition, it prevents heat loss so that heat is completely absorbed by the plate and transmitted to the refrigerant [54].
Tagliafico et al. [109] compared the thermodynamic performance of a DX-SAHP system with three solar collector configurations to satisfy domestic hot water requirements. The annual primary energy savings achieved by the system were 49.5%, 48.5% and 48% for unglazed, glazed and double-glazed panels, respectively. The unglazed collector, the cheapest one, was the best choice for the DX-SAHP.

Additionally, SAHP systems are designed in different configurations with respect to the arrangement of solar thermal collectors and the evaporator of the heat pump in a way that the solar collector is in series or in parallel with the evaporator of the HP. It was found that series configuration yields higher outlet temperatures, making it suitable for applications needing elevated heat levels. However, parallel configuration offers better performance with better flow distribution and lower pressure drops, which can improve system stability and reduce pump energy. Cai et al. [110] investigated a DX-DSHP system with a finned tube evaporator in series with a bare solar collector. A COP of 2.71 is obtained under solar radiation of 100W/m^2 and ambient temperature of 10°C. In parallel arrangement, the system works in solar mode, air mode and solar-air mode. In solar mode, the evaporating process undergoes in the SCE when the solar radiation is strong. In absence of solar radiation, the system operates as a conventional ASHP. When the solar radiation is low and the heat produced by the SCE is not enough to evaporate the refrigerant, the AE completes the required heat and the system works in solar-air mode. In another work, Cai et al. [111] compared three

types of DSHP systems for DHW production, solar-air series heat pump (solar before air type evaporator), solar-air parallel heat pump and air-solar series (air before solar type evaporator) heat pump. They have shown that the first configuration is preferable in low solar irradiation, the second gives optimal performance at high ambient temperature or high solar irradiation and the third is suitable in low ambient temperature and high solar irradiation. In term of thermal performance under the same comparing weather data, the COP of solar-air parallel source heat pump was the highest (4.50-4.58).

The meteorological conditions such as solar radiation and ambient temperature are key parameters that affects a SAHP system performance. Kong et al. [112] have found that when the solar radiation increases from 300 to 900W/m2, the COP rises from 4.1 to 6.0. Zheng et al. [113] studied the effect of varying solar irradiance on a solar-air SAHP system designed for hot water supply. They proposed a dynamic operation method of control to enhance the solar collector heat collection. The thermal efficiency of the solar collector was improved by 11.8% and the system COP by 8.3%. In an experimental study performed on a DX-SAHP with a bare plate evaporator, Ji et al. [114] found that the COP increases by 6.6 % when the ambient temperature rises from 5 to 15°C.
Taking similar studies to the present work, that say with unglazed flat plate collector and R134a refrigerant in DX-SAHP systems, the COPs were found varying depending essentially on climatic conditions and collector area.
Hawlader et al. [115] found COPs ranging between 4 and 9 in Singapore to attain 55°C of water temperature using 250 L tank with 3m² collector area. Chyng et al. [116] found COPs ranging between 1.7 and 2.5 in Taiwan to hot water up to 56°C water when using a collector area of 1.9m² . Moreno-Rodriguez et al. [117] found COPs ranging between 1.7 and 2.9 in Madrid necessary to hot water up to 51°C water using 300 L tank and 5.6 m² of collector area. All these findings were simulated and experimentally agreed.
For large scale DX-SAHP of 12m² collector area and 1500L, Chow et al. [62] found in a theoretical work COPs ranging between 6.5 and 10 in Hong Kong to reach 50°C of DHW. Huang et al. [71] carried out laboratory experimental investigation on the performance of a DX-SAHP using bare plate unglazed and uninsulated collector-evaporator for space heating. When taking solar irradiation 300 W/m² and indoor temperature 20°C, they found that COPs vary from 2.12 to 2.26 as ambient temperature increses from 5°C to 15°C. When they consider ambient temperature 15°C and indoor temperature 20°C and they varied solar irradiation from 0 W/m2 to 500 W/m², they found that COPs of the DX-SAHP changes from 2.07 to 2.36.

To verify the effect of collector area on COP, Kong et al. conducted two separate experiments in the same city of Qingdao, on the east coast of China. Both systems included tanks of similar capacity (200 L). Both achieved a maximum water temperature of 60°C. However, COPs ranged from 2.8 to 4.3 with a collector area of 1.56 m² [118] and ranged from 3.6 to 5.6 with a collector area of 2.1 m² [119].

The integration of photovoltaic thermal (PVT) collectors in DX-SAHP systems is for electricity production, although they reduce heat collection capacity [63]. The PVT collector acts as the HP evaporator where the cooling fluid circulates. This setup increases the energy output from the condenser leading to an increase in the HP COP [120].
Simulated results of a PVT-HP system developed by Xu et al. [85] show that it can efficiently generate electricity and thermal energy to heat 150 L water up to 50° C simultaneously in Nanjing and Hong Kong cities all-year-round. COPs varied from 3.4 to 5.2. The system performance is enhanced in Hong Kong because of the higher solar radiation and higher ambient air temperature over the year.
Li et al. [121] investigated a DX-DSHP system with PVT solar collectors and air cooled evaporator. The COP under low weather conditions (0°C and 100 W/m²) was 4.76, which is 29.7% higher than that obtained by a single source heat pump.

Indirect-expansion dual-source heat pump (IX-DSHP) systems

In IX-DSHP system, the heat produced by solar collector can be used for water heating directly or serving as heat source for heat pump. Direct solar heating (DSH) is the most effective way to exploit solar radiation. It does not require any electrical energy consumption and reduces installation and operating cost. Unfortunately, in cold and harsh climates, solar energy by itself cannot guarantee a steady supply of heating.

The additional air evaporator is connected in parallel with water source evaporator to exploit thermal energy of air ambient when solar radiation is low and thus better performance is achieved. The main advantage of IX-DSHP lies on its ability to work efficiently over all the year and under different weather conditions.

Within the IX-DSHP system classification, many efforts have been undertaken on solar collector types to improve systems performances. For example, Ma et al. [122] proposed an IX-DSHP domestic hot water supply system with solar thermal collectors. The results show that the COP of ASHP is between 2.62 and 3.93 where the COP of solar-air dual source ASHP system is between 2.76 and 6.26 and the solar fraction is between 8.83% and 45.51% depending considerably on seasons. Li et al. [123] developed an IX-DSHP system to supply space heating working in three modes, namely, direct solar water heating, ASHP and HP taking heat from water heated by DSH. The system showed better performance when working as WSHP with average COP in heating season of 3.5. Whereas the average COP of ASHP is 3.0. A solar fraction of 40.2% is obtained with energy saving rate of 66.4% and investment pay-back period of 6.5 years.

Indeed, there are three different configurations for IX-SAHP which are parallel, dual and series. The arrangement of system components depends on the application either space heating or DHW provision [124]. In space heating application, the heat pump can be air-to-air or water-to-air heat pump but, in DHW application, the heat pump can be air-to-water or water-to-water heat pump.

In indirect parallel SAHP system, the ambient air is the heat source for heat pump and solar energy is the heat source for an indirect solar system which both work to meet the thermal energy demand separately. The configuration of this type depends on the application.[54]. A verified theoretical model for a parallel IX-SAHP system for DHW production in Athens, Greece, was designed and tested in two studies by Panaras et al. [125] [126]. The COP found is 2.34 and the results confirm that 70% of energy savings could be obtained by IX-SAHP compared to a conventional solar hot water system combined with electrical resistance or a direct-fired heater.
According to the study of Yerdesh et al. [127], it was shown that parallel arrangement system performance requires minimum solar irradiation for the transmitter fluid temperature to ensure heating space permanently. They conducted numerical simulations for severe climate conditions below - 30°C and maximum solar radiation value of 500 W/m^2. They concluded that the system cannot operate and the thermal storage tank holds the system operation out until reaching to adequate temperature.

In indirect series SAHP system, the solar loop, heat pump, and application are connected in series. In this case, the heat pump uses only solar energy as a heat source where the evaporator is connected, and the condenser is connected to the application. The configuration of this type also depends on the end-use.
Similarly, Tzivanidis et al. [128] performed a simulated comparison in term of system performance between parallel and series IX-SAHP systems applied in Athen, Greece. Between 2 and 9°C ambient temperature range and maximum solar irradiation of 600 W/m², COP of parallel and series IX-SAHP was 3.94 and 4.06 respectively.

In indirect dual SAHP system, a dual-source HP includes two evaporators. One connected to the solar source and the other connected to an ambient air source which permits the HP to absorb heat from either source. Hence, the weakness of the solar source is intended to be compensated by the air source [129].
In a study carried out by Huan et al. [130] on a combined SAHP system that can operate in serial or parallel modes, under spring conditions of Xi'an in China, it was shown that parallel arrangement is more sensitive to solar radiation availability. COPs of parallel IX-SAHP increased from 3.86 to 8.84 with solar irradiation increasing from 580 W/m² to 840 W/ m². However, COPs of series IX-SAHP little increase from 3.94 to 4.06.

Tank temperature settings interact with weather conditions and solar radiation intensity to influence overall system performance. Tank set temperature increases water heating time and energy consumption since it requires that the heat pump work longer, increasing thus compressor energy consumption. Yang et al. [131] investigated the hot water set temperature influence on electricity consumption and system performance of an IX-DSHP system for three cities in UK. The system is designed to supply hot water and space heating. A percentage of 19.1% reduction was obtained in electricity consumption and the same percentage was obtained seasonal performance augmentation when temperature decreases from 55°C to 40°C.
Wang et al. [132] introduced ice tank to IX-DSHP system in addition to PVT module, air heat exchanger and heat/cold storage tank. In winter, the latent heat from water condensation in the tank is used as low-temperature heat source supplying the heat pump. The ambient air was used as the auxiliary thermal energy source. The energy supply system has maintained high performance for long period under bad weather conditions in winter and summer. The seasonal performance factor of the system in winter and summer

was 2.93 and 2.6, respectively.

With reference to studies on performance regarding ambient conditions, Ji et al. [133] performed experimental study in laboratory on a series IX-SAHP applicated for space heating along with a flat-plate collector supplies heating in sufficient solar radiation and the HP evaporator supplies heating in insufficient irradiations. Taking indoor temperature and outdoor temperature at 20°C and 7°C respectively, it was found that as solar radiations vary from 0 to 500W/m², COPs vary 2.35 to 2.55.

Another innovative method for assisting IX-DSHP systems is the use of PVT collectors, which combine heat and electricity production using PV cells [134]. An intermediate heat exchanger already exists between the PVT collector and the HP, which can be used as heat storage [120]. The use of PVT collectors instead of thermal collectors improves the system performance by reducing the dependency on electricity network.
Water-based PVT systems are favourable since the large thermal mass of water tends to cool the PV modules and hence improve the efficiency of the collector [135]. Wang et al. [98] developed a solar PVT dual heat source composite heat pump system for hot water supply. The experimental setup is based on a finned tube evaporator and a flat plate PVT collector combined with the DSHP. The study achieved a COP of the DSHP greater than that of the single heat source-operating mode. Aste et al. [136] have numerically studied the performance of a dual source PVT-SAHP system designed to meet the building space heating and cooling and DHW production needs. In one-year simulation, the obtained monthly average COP ranges between 3 and 4.8. Simonetti et al. [137] investigated numerically and experimentally an integrated dual-source evaporator connected to PVT modules for DHW production and space heating. The parametric simulation indicates that the COP reaches 5.1 and it is 14% better than that of conventional ASHP. Besagni et al. [138] have experimentally investigated a multifunctional and reversible heat pump. The monthly average COP was between 2.97 and 3.08. Leonforte et al. [139] explored experimentally the performance of a multifunctional IX-DSHP system for different periods of the year in Milan, Italy. The system includes a PVT collector connected to the DSHP. An increase in COP of 28.4% was achieved in the dual-source mode compared to the simple air-source mode. The thermal energy needed by the DHW storage tank has been 11.7% provided by the PVT panels in the heating mode with set-point 40°C in the period from 10/01/2020 to 26/02/2020. The PVT electricity production contribution rose to 83.1% in summer days.

1.3.6 Conclusion of the survey

After this tour of works in connection with the present study and after surveying the published researches in this direction, we come out with an observation that a research gap is identified in the literature. It consists of all the works investigated the performance of a SAHP system as it is DX-SAHP or IX-SAHP system separately. No work investigated a SAHP system as it may wok in direct-expansion, in indirect-expansion and hybrid direct/indirect-expansion modes, which this thesis aims to fill.

A recent comparative study performed on solar assisted heat pump systems by Sezen and Gungor [53] may flows in this direction when comparing separate systems performance working separately but not as one system. It was concluded that the ASHP is preferred as the solar radiation is under 100m², a DX-SAHP system is more efficient for solar radiation below 400W/m² and an IX-DSHP system can perform better for solar radiation ranging between 400 and 800 W/m². This is because DX-SAHP is known by its ability to absorb heat from solar energy and air simultaneously below 400W/m². Above this limit, the temperature of the SCE exceeds that of air ambient and thus heat loss begins to occur. With IX-DSHP, the glazed solar collector minimises heat loss to ambient air. Above 800 W/m², a glazed solar collector is able to supply sufficient heat demand directly.

Exception can be made to the work of Dai et al. [140] where an activation of a hybrid mode of SAHP using both parallel IX-SAHP and DX-SAHP was performed. The study concluded that, in winter conditions with solar irradiation of 350 W/m² and ambient temperature of 5 °C, a parallel IX-SAHP can fulfil the requirement for heating process. However, in spring conditions with solar irradiation of 600 W/m² and ambient temperature of 15 °C, a parallel IX-SAHP solar collector is able to rise the temperature of the refrigerant to 32 °C, which is not sufficient for heating. So, a DX-SAHP was activated which raised water temperature up to 50°C to fill the need.

Thus, the aim of this work is to investigate and compare the performances of a DSHP system operating compositely or differently in direct, indirect and direct/indirect modes to remedy the shortcoming identified in literature to thoroughly explore the improvement of SAHP systems. The energy performance of the new system is investigated using mathematical modelling and simulation under TRNSYS environment.

The new system configuration is developed by inserting a solar thermal collector-evaporator in parallel with a water-source evaporator of an IX-DSHP system. The system takes advantages and benefits from DX-DSHP system and IX-DSHP system and it is expected to improve significantly the exploitation of solar energy, increasing consequently its energy performance. From the perspective of system size, the new system includes one condenser and one air evaporator, rather than two condensers and two air evaporators needed when using two separate systems. Therefore, it occupies less space. Obviously, this combination requires an appropriate control strategy to supply necessary space heating and DHW energies continuously over all heating period.

1.3.7 Motivation and Contribution

An optimal, energy efficient heat pump system still needs to be developed to face escalating demand on these devices in response to global exigencies of policies to find sustainable, friendly environmental and low-cost energies. In this study, the advancements in heat pump systems are presented and systems parameters are taken into consideration to investigate the performance of a novel hybrid heat pump system.

The system modelling consists of a performance study by mathematical models using Matlab, including input parameters and heat transfer analysis, and a simulation using TRNSYS software.

In the literature, no hybrid heat pump system taking into account the simultaneous direct and indirect expansion with modelling and performance analysis is provided.

The main contribution of the proposed work is that it present a new heat pump system which take advantages from to distinct systems found in literature and take benefits from dual energy sources to harness high available heat. It will make a significant contribution in the research community. Besides, the impact of using different solar thermal collectors and PVT panels areas is discussed and the effect of set-point temperatures of water heating is considered.

The output is that the system functioning in a direct and indirect mode with dual solar-air energy source shows better coefficient of performance, higher seasonal performance factor and explores more solar radiation. The

performance directly relied to solar collector areas and it is economically viable when taking global energy prices.

1.4 Conclusion

This chapter provides a general overview of the materials used in this study. Useful definitions are provided, along with the operating principles of various components and configurations. It begins with a basic heat pump cycle, then discusses how an ASHP heat pump is replaced by a solar-assisted heat pump to improve performance, primarily at night or during unfavourable weather conditions.

We have shown that the heat pump used in the study is double heat sources one, able to absorbs heat from air and water. The heat pump system is photovoltaic/thermal and solar thermal assisted heat pump system. Two categories of SAHP systems are discussed: direct-expansion and indirect-expansion. We have mentioned that the present system is hybrid direct/indirect system. Additionally, the SAHP system arrangement is discussed. Performance indicators are defined and the equations used to determine them are presented.

Next, a literature review is presented summarizing some works relevant to the present study. After clarifying the issue, the motivation for the research is identified, thus presenting the contribution of the thesis work.

Chapter 2

System description and Simulation procedure

2.1 Introduction

This chapter consists of three parts. The first presents the characteristics of the studied building, followed by illustration of climatic conditions of the city under study.
The second part illustrates the schematic of the newly developed system, discusses its functions, and provides a flow-chart of the system operations control.
The third part explains the mathematical and numerical simulation procedure. It discusses the methods, software selection, and materials used in this study. This part divides the procedure into three steps. First, the mathematical modelling of the DX-SAHP using Matlab is explained. Second, the details of the IX-DSHP simulation using TRNSYS are presented, along with the software components (referred to as Types) necessary to build the SAHP system. The third step involves combining these two steps to build the newly developed DX/IX-SAHP system, which can operate in three modes.

2.2 Building characteristics

The building studied in this work is a single-family house of five occupants consisting of three rooms, a living room and a kitchen, see Figure 2.1

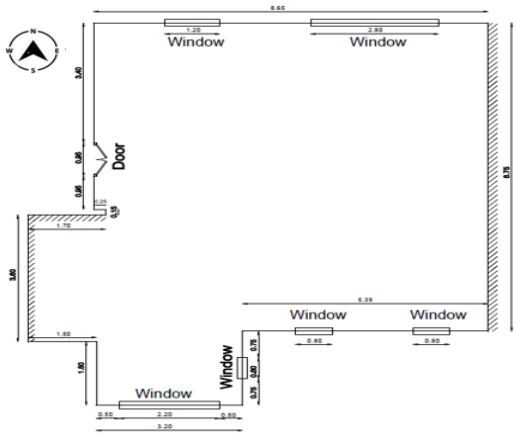

FIGURE 2.1: Building envelope design.

The building is situated in Djelfa. A city located in the highlands region of Algeria with geographic coordinates 34.6874°N and 3.1860°E. This region is known for its cold and arid micro-climate, and is considered as the coldest region of the country, which allows us to perform the simulation in the worse weathering conditions of the country where the demand for space heating and domestic hot water is high in cold season. The meteorological data of the city were obtained from Meteonorm 8 [141]. Figure 2.2 represents the average daily temperature of each month of the year. As shown, the city is characterized by a long cold period (minimal of 6°C) and not very hot period in summer (maximal of 29°C). Figure 2.3 represents monthly global radiation in Djelfa city. As seen, the city has important solar radiation availability. The monthly solar radiation varies between 90 and 230 kW/m². These meteorological conditions are suitable for installing efficient solar systems.

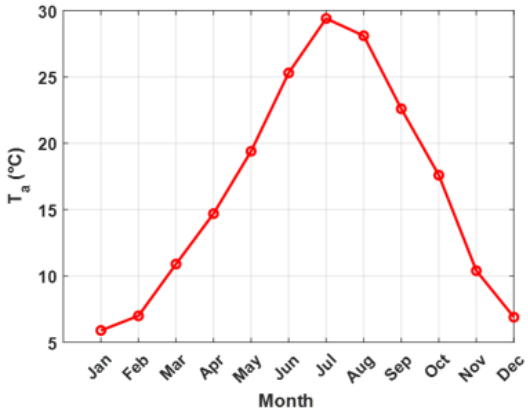

FIGURE 2.2: Average daily temperature for each month in Djelfa city.

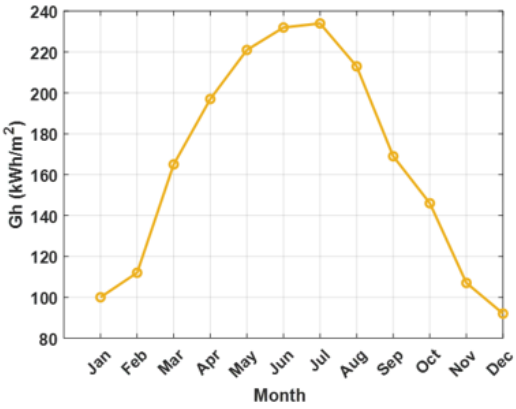

FIGURE 2.3: Monthly global radiation in Djelfa city.

Under TRNSYS, the building is defined as Type 56 multi-zone building. This component models the thermal behaviour of the building having constitution and construction materials characteristics as indicated in Table 2.1.

TABLE 2.1: Building envelop characteristics

Surface	Layout	thickness (cm)	U-value ($W/m^2.K$)
Out-wall	brick	15	0.42
	insulation	8	
	Plaster	1.5	
Ground	Floor	0.5	0.53
	Stone	0.6	
	Silence	0.4	
	Concrete	12	
	Insulation	6	
Roof	Concrete	24	0.23
	Insulation	16	
Windows	Double glazing		1.1

The DHW water load in Figure 2.4 is established based on the hourly daily consumption profile considering a daily hot water consumption of 250 litres. As expected, the highest hot water demand is at the times 07:00 PM, between 07:00 AM and 08:00 AM and at mid-day to respond to occupants needs. For example at 07:00 PM, the DHW consumption is 75 litres.

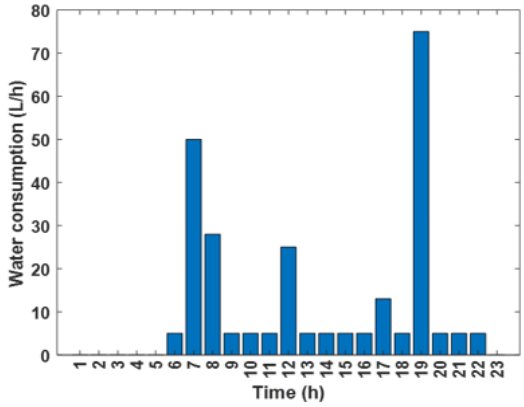

FIGURE 2.4: Hourly-daily water consumption profile.

Figure 2.5 represents the hourly energy demand for space heating and DHW of the building over the heating period. The total thermal energy of heating demand and DHW for the whole period is estimated at 3691 kWh and 747.5 kWh respectively. It is pointed out that the hourly peak loads for heating is around 4.8 kW and the peak load for DHW is near 1.2 kW.

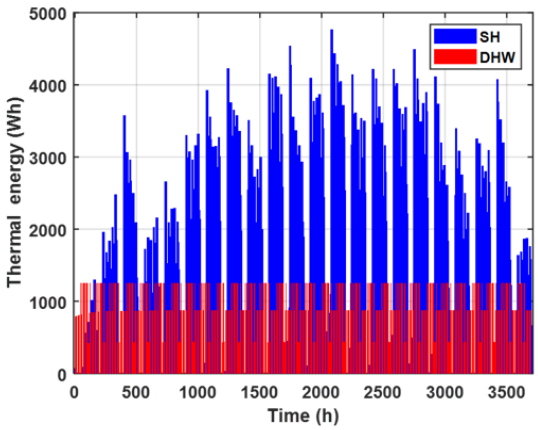

FIGURE 2.5: Energy demand of the building over the heating period.

2.3 System description

In this section, description and schematic illustration of the new system is presented.

The system is designed to supply DHW and space heating for the considered building during all the heating period. Figure 2.6 shows the layout of DX/IX-DSHP system. It consists of PVT solar collector, two storage tanks

(TK1 and TK2) and a dual-source heat pump (DSHP) with a composite evaporator consisting of water evaporator (WE), air evaporator (AE), unglazed solar collector evaporator (SCE), compressor (Comp), condenser (Cond) and expansion valve (EV). The HP condenser is connected to the building and TK2 using a circulating pump P3. The refrigerant selected in this study is R134a for advantages that were discussed earlier in this thesis.

The system can work in three modes, namely DSM, ISM and both D/ISM depending on the control functions. In DSM, the system operates as a direct-expansion dual-source heat pump (DX-DSHP). The refrigerant absorbs heat gained from SCE. The superheated vapour passes through compressor where it becomes at high temperature and high pressure. In the condenser, the refrigerant vapour releases heat to become a saturated liquid. As it continues to flow, the pressure of the liquid refrigerant is decreased at the expansion valve. The cycle is repeated as the refrigerant enters the evaporator-collector. The heat generated by the condenser is initially used to satisfy the energy need of the building. Once the need is satisfied, the thermal energy is directed towards water heating. In absence of solar radiation, AM is activated and AE is used in place of SCE to evaporate the refrigerant by take in heat from ambient air; therefore the system functions as an ASHP. In ISM, the system works as an indirect-expansion dual-source heat pump (IX-DSHP). The thermal energy acquired by PVT collector is initially used to provide TK1, which in turn delivers hot water to the WE heat pump. The refrigerant evaporates by absorbing heat from hot water and the heat produced by the condenser is used to supply space heating or DHW. Once TK1 set-point temperature is attained, the surplus of heat from PVT is transferred to TK2 to produce DHW. In case of insufficient solar energy availability, the system is activated in AM. In D/ISM, the thermal energy produced by direct solar heating is used to satisfy the building heating demand. Simultaneously, the thermal energy produced by PVT is stored in TK1 to supply the WE of the HP; any surplus heat is directed to TK2 for DHW production. In absence of solar radiation and during night hours, the heat stored in TK1 allows the system to work in ISM in response to energy demand of the building.

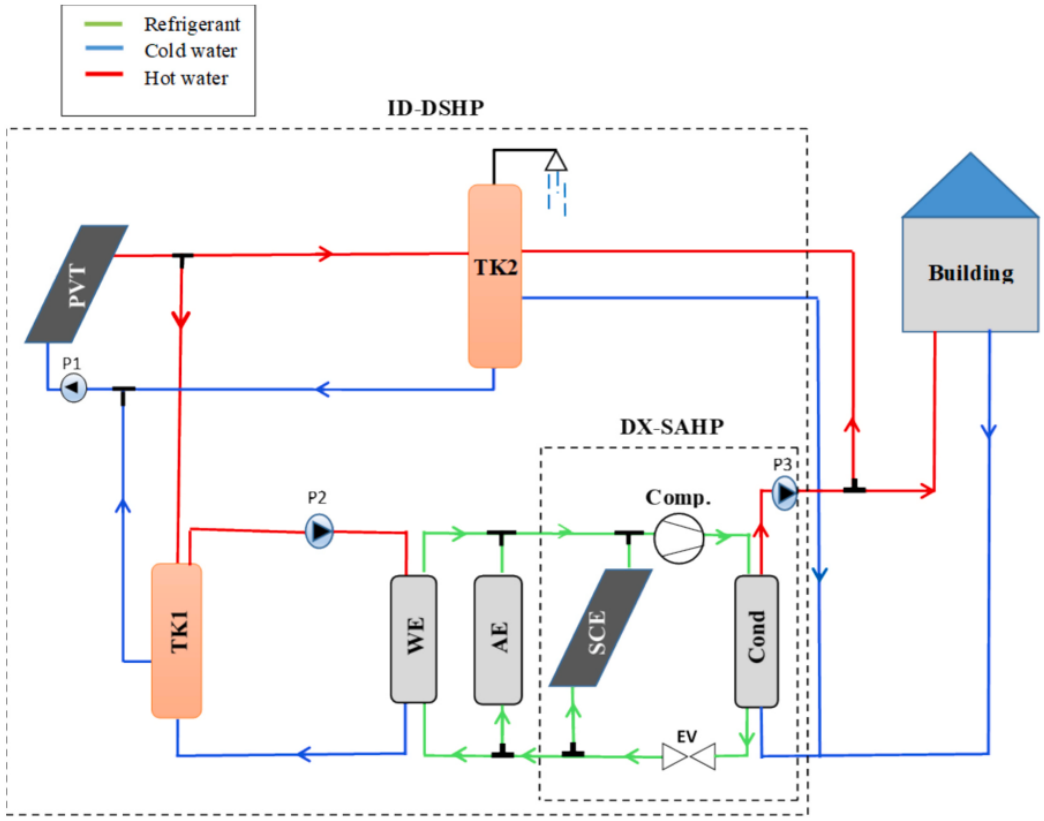

FIGURE 2.6: Schematic representation of the DX/IX-DSHP system.

Figure 2.7 describes the overall operation strategy of the system in D/ISM and its control functions. At available solar radiation, the system is running in DSM to respond to space heating priority whenever the internal temperature of the building is below the set point of 20°C. If the space heating needs are satisfied, the thermal energy is transferred to DHW needs (TK2) unless the water temperature is greater than the set point of 50°C. Otherwise, when DHW temperature exceeds 50°C, the system is turned off. Meanwhile, the PVT collector is requested to supply the first storage tank (TK1) with thermal energy since its temperature is under 40°C. When this set point is attained, the heat provided by the PVT is transferred to TK2 for DHW production (DSH). In absence of solar radiation, if the system working in DSM is unable to produce sufficient heat, the thermal energy previously stored in TK1 is supplied to WE and the system returns to ISM. This tank is designed to supply WSHP under two joint conditions that say when TK1 temperature is greater than 30°C and TK2 temperature is below 50°C. When water temperature in TK1 drops under 30°C and there is a continued demand for heat, the system activates in AM functioning as an ASHP. As heat requirement is satisfied (indoor temperature is above 20°C and TK2 set point temperature is

above 50°C), the ASHP is turned off. It is important to mention that the electricity produced by PVT collector operates the HP compressor along with the circulating pumps.

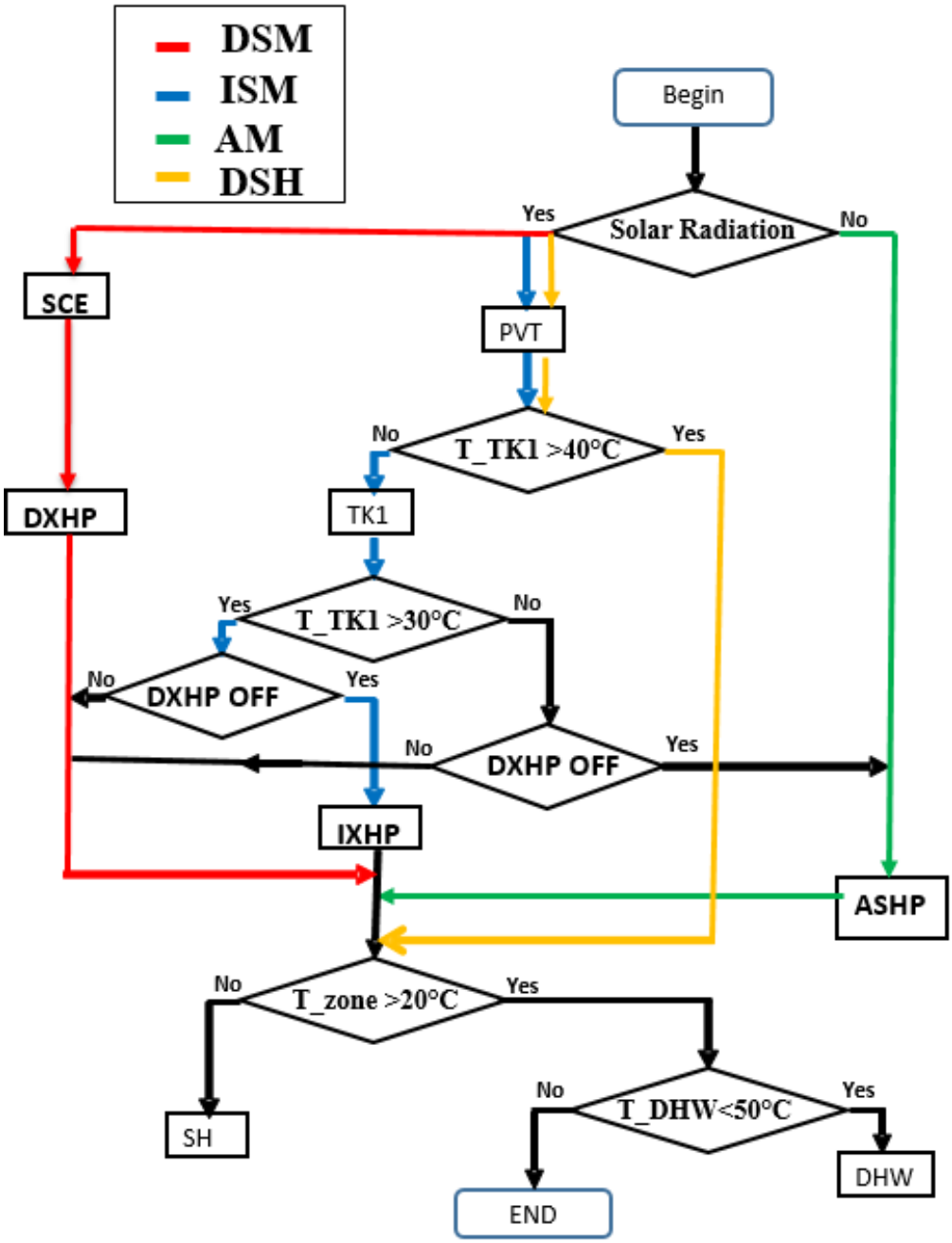

FIGURE 2.7: A flow chart of operation control for the DX/IX-DSHP system.

The heat pump cycle on P-H diagram for different operating modes is shown in Figure 2.8. The composite evaporator (WE, AE and SCE) of the system harnesses heat from different sources to evaporate the refrigerant (liquid-to-vapour state). In absence of solar radiation, the system operates in AM,

taking the ambient air as the heat source by mean of the AE. In high solar radiation availability (DSM), the system extracts heat from solar directly by mean of the SCE and operates with a much higher evaporating temperature. In ISM, the WE of the heat pump extracts heat from hot water maintained at a constant temperature in TK1. Note that the evaporating temperature ability in ISM lies between that of AM and DSM.

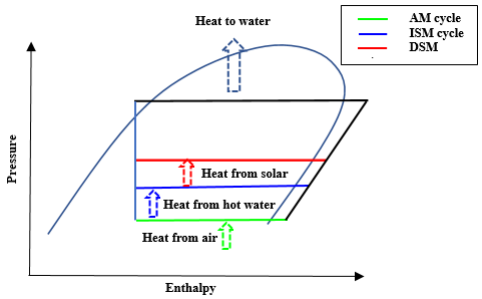

FIGURE 2.8: P-H diagram for different operating modes.

2.4 Modelling and dynamic simulation procedure

The procedure of modelling and simulation consists of three steps. In first step, a mathematical model of a single-source direct-expansion solar assisted heat pump (DX-SAHP) based on lumped and distributed parameters approach of different system components under MATLAB code is developed. In a second step, a model of an indirect-expansion dual-source heat pump (IX-DSHP) is developed under TRNSYS program. In a final step, a combination of the two models was conducted using TRNSYS leading to the final model of the system able to work in three modes.

The detailed procedure of modelling and simulation is discussed in the following paragraphs.

2.4.1 Direct-expansion solar assisted heat pump modelling

The DX-SAHP system is dynamically simulated through a developed mathematical model under MATLAB with 60s time-step. Ambient temperature, network water temperature and wind speed are taken 20°C, 15°C and 3.1m/s respectively. The components models are bare solar collector-evaporator, compressor, condenser and expansion valve. The Specifications of the DX-SAHP system components are listed in Table 2.2.

TABLE 2.2: Specifications of the DX-SAHP system components

Component	Property	Value
Collector-evaporator	Area	4.2 (m^2)
	Thermal conductivity	236 (W/m.K)
	Thickness of collector plate	0.004 (m)
	External diameter of the pipes	0.0094 (m)
	Distance between the pipes	0.04 (m)
	Absorptivity of the plate	0.9 (-)
	Emissivity	0.1 (-)
Compressor	Compressor efficiency	0.75
	Rotational speed	2830 (tr/min)
	Volumetric efficiency	0.91 (%)
	Displacement volume	13.4 (cm^3/rev)
Condenser	Length of serpentine	60 (m)
	Thermal conductivity	398 (W/m.K)
	External diameter of serpentine	0.0095 (m)
	Internal diameter of serpentine	0.0077 (m)
Expansion valve	Orifice cross-sectional area	2 (mm^2)
Storage tank	Capacity	500L

Thermodynamic properties of R134a refrigerant for different temperatures and pressure are taken from REFPROP7 [142]. Values are listed in Appendix.

Mathematical models of the different system components are developed by taking into account some assumptions:

- thermal and physical properties are used at steady-state conditions,
- the small pressure losses in the collector-evaporator and pipes are ignored,
- the refrigerant vapour at the collector-evaporator outlet is considered as a saturated vapour.

Solar collector model

A bare flat plate collector in pure aluminium, known for its good thermal conductivity, high ductility properties and low price [143], without back insulation is used in the DX-SAHP system, which is able to absorb heat from

both solar energy and air ambient and plays the role of a refrigerant evaporator simultaneously. The saturated liquid refrigerant entering the collector-evaporator passes to a liquid-vapour phase inside. At the outlet of the collector-evaporator, a superheat degree of 10°C is considered. The useful heat gain of solar collector/evaporator is evaluated using Equation 2.1 [144] and [112]:

$$Q_{coll} = A_c.F^{'}.[S - U_L.(T_{rm} - T_a] \tag{2.1}$$

Where, A_c, is the solar collector-evaporator area, $F^{'}$ is the collector efficiency factor given as follows [145]:

$$F^{'} = F + (1 - F).(\frac{d}{w}) \tag{2.2}$$

$$F = \frac{tan(U_b)}{U_b} \tag{2.3}$$

$$U_b = \frac{w - d}{2}.\sqrt{\frac{U_L}{k.\delta}} \tag{2.4}$$

S, is a symbol calculated as:

$$S = \theta.I - \epsilon.q_0 \tag{2.5}$$

and,

$$q_0 = \xi.T_a^4 - q_\infty \tag{2.6}$$

Where, θ is the absorptivity of the collector plate, I is the solar radiation intensity on the collector plate, ϵ is the emissivity of the collector plate, q_0 is the difference between the emissive power per unit area from a black body at the ambient air temperature and the emissive power from the sky, ξ is the Stefan–Boltzmann constant with the value of 5.67 × 108 $Wm^{-2}K^4$,q_∞ is the sky radiation, w is the distance between the pipes, d is the external diameter of the pipe and F is the efficiency of fins, U_b is a dimensionless number, k and δ are the thermal conductivity and the thickness of the collector plate respectively. The symbol U_L is expressed as:

$$U_L = \alpha + 4\epsilon.\xi.T_a^3 \tag{2.7}$$

Where, α is the convective heat transfer coefficient, T_a is the ambient temperature and T_{rm} is the average temperature of the refrigerant at the solar collector-evaporator. The refrigerant heat gain at the solar collector level is given by:

$$Q_r = \dot{m}_r(h_{out,SCE} - h_{in,SCE}) \tag{2.8}$$

The mean refrigerant temperature T_{rm} using Equation 2.9:

$$Q_{coll} = A_c.F^{'}.[S - U_L.(T_{rm} - T_a)] = \dot{m}_r(h_{out,SCE} - h_{in,SCE}) \tag{2.9}$$

Where, $\dot{m}_r$ is the refrigerant mass flow rate, $h_{out,SCE}$ and $h_{in,SCE}$ are the outlet and the inlet enthalpy of solar collector evaporator.

Compressor model

For a small-scaled rotary-type and hermetic compressor, the refrigerant mass flow rate $\dot{m}_r$ is given as [146]:

$$\dot{m}_r = \frac{N.\phi.V_d}{60V_{suc}} \tag{2.10}$$

Where, N is the compressor rotational speed, V_{suc} is the specific volume of the refrigerant at the inlet of the compressor, ϕ is the volumetric efficiency of the compressor, and V_d is the displacement volume rate of the compressor. Neglecting the pressure drop at the inlet and outlet of the compressor, the electrical power consumption of the compressor can be determined using Equation 2.11 [147]:

$$W_{com} = \dot{m}_r.\frac{P_{suc}.V_{suc}}{\eta_{com}}.\frac{k}{k-1}.[(\frac{P_{dis}}{P_{suc}})^{\frac{k-1}{k}} - 1] \tag{2.11}$$

Where, P_{suc} and P_{dis} are the suction pressure and discharge pressure of the compressor, η_{com} is the total efficiency of the compressor, and k is the polytropic index of the refrigerant fluid.

Condenser model

Assuming perfect heat transfer between the refrigerant and water, the heat released by the refrigerant across the condenser is equivalent to that absorbed by water. The heat gain in the condenser can be calculated using Equation 2.12 [148]:

$$Q_{cond} = \dot{m}_r.(h_{in,cond} - h_{out,cond}) \tag{2.12}$$

And,

$$Q_{cond} = M_W.C_W.\frac{dT_W}{dt} \tag{2.13}$$

Water temperature with respect-to-time is calculated using Equation 2.14:

$$T_{out,cond} = \frac{Q_{cond}.t}{M_W.C_W} + T_{in,cond} \tag{2.14}$$

Where, M_W is the mass of water , C_W is the specific heat of water, T_W is the water temperature, t is the heating time, $h_{in,cond}$ and $h_{out,cond}$ are the enthalpy at the inlet and the outlet of the condenser respectively and $T_{in,cond}$ is water temperature at the inlet of condenser or the DHW tank temperature.

Expansion valve model

A thermostatic expansion valve is widely used for the SAHP system, which maintains constant superheat at the inlet of the compressor by regulating the mass flow rate of refrigerant [44], [54], [115] and [117] . The throttling process within the expansion valve is assumed to be isenthalpic; therefore, the thermodynamic equation of a thermostatic expansion valve is expressed as in Equation 2.15:

$$h_4 = h_3 \tag{2.15}$$

where h_4 and h_3 in (J/kg) represent the specific enthalpies of the circulating fluid at the inlet and outlet of the thermal expansion valve, respectively [112] and [149] .

The flow-chart of the DX-SAHP model is outlined in Figure 2.9. Mathematical equations are solved using a developed MATLAB program, taking into account the interactions between various system components models. The calculations sequence is as follows:

- read the program's data: meteorological and structural parameters,
- assume the evaporation and condensation pressures,
- calculate the compressor work and mass flow rate,
- calculate the solar collector evaporator heat gain and the average refrigerant temperature,
- compare the refrigerant temperatures (T_{rm}) and evaporation temperature (T_{evap}),
- if the absolute value between T_{rm} and T_{evap} is greater than the degree of super-heating (ΔT), correct the evaporation pressure,
- Otherwise, calculate the condenser heat gain and the tank water temperature,
- If water temperature in the tank is below the target temperature, increase the time step until the required temperature is reached.

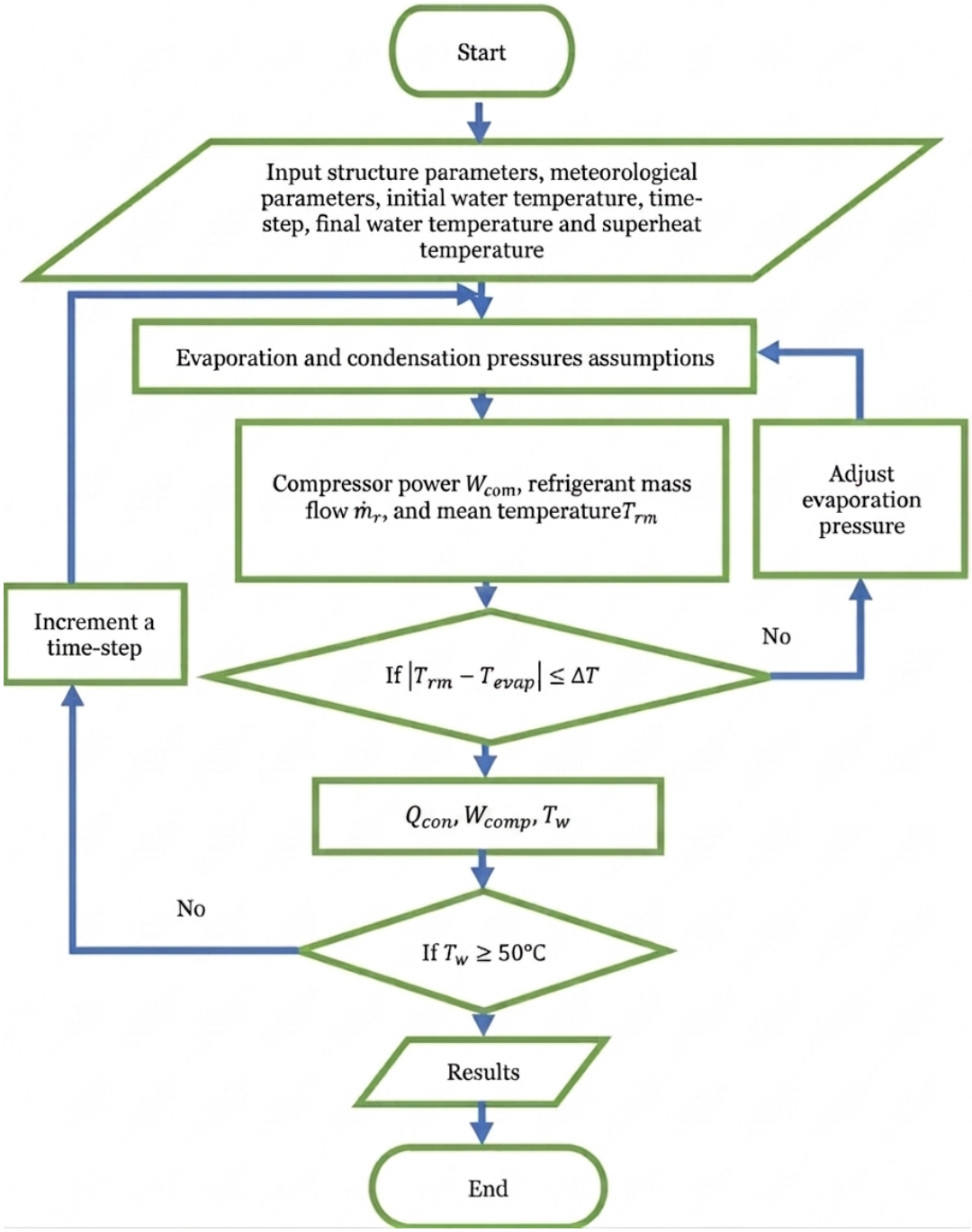

FIGURE 2.9: Mathematical modelling flow chart of DX-SAHP system.

2.4.2 Indirect-expansion solar-air dual source heat pump modelling

The simulation of the IX-DSHP system was performed using TRNSYS. TRNSYS is a transient system simulation program with a modular structure that was designed to solve complex energy systems problems by breaking the

problem down into a series of smaller components known as Types [24]. It is a well-recognized tool simulation program internationally [122] offering a wide library of validated component models. The high flexibility of TRNSYS allows users to customize existing components, interacted them with other software like Matlab and compile own components [150]. Dynamic modelling approaches enable modelling of the physical characteristics of heat pumps; hence, the simulated results are in agreement with the measured data [151].

Figure 2.10 illustrates the TRNSYS model of indirect-dual source heat pump system assisted by PVT panels.

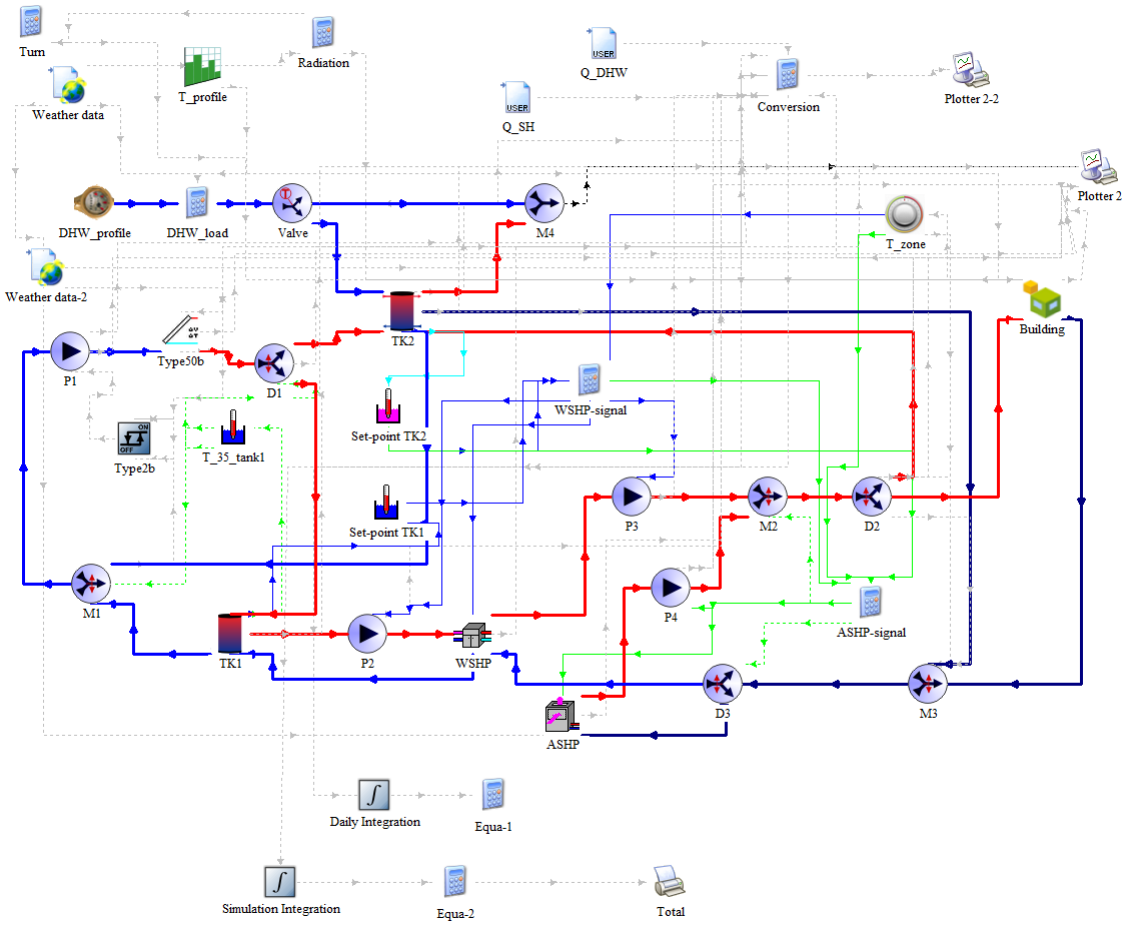

FIGURE 2.10: The TRNSYS modelling of IX-DSHP system.

An ASHP (Type 941) and a WSHP (Type 927) are used to simulate the operation of DSHP, as the duality is not available in TRNSYS library. The other components are PVT panels (Type 50), two storage tanks, one for supplying WSHP (Type 158) and the other for DHW (Type 534). Each of these components are modelled under TRNSYS as detailed below.

PVT collector

The PVT model is a combined of photovoltaic and thermal solar collector by adding a PV module to the standard flat-plate collector. Table 2.3 summarizes PVT collector (Type 50) characteristics.

TABLE 2.3: PVT collector Type 50 characteristics

Characteristic/Property	Value	Unit
Collector area	-	m^2
Collector fin efficiency factor	0.96	
Fluid thermal capacitance	4.19	kJ/kg.°K
Collector plate absorptance	0.92	
Transmittance absorbtance product	0.9	
Number of glass covers	1	
Collector plate emittance	0.09	
Collector slope	45	degrees
Temperature coefficient of PV cell efficiency	0.0032	1/K
Temperature for cell reference efficiency	25	°C

The PVT collector model used was established based on the mathematical model presented by Fudholi et al. [152] and Xia et al. [153]. The useful heat gain, the electricity generation of the PVT collector and the outlet water temperature from the PVT collector can be calculated using Equation 2.16, Equation 2.17 and Equation 2.18 respectively.

$$Q_{PVT} = \eta_{th}.A_{PVT}.G_t \tag{2.16}$$

$$E_{PVT} = G_t.\eta_{PV}.A_{PVT}.(\tau.\alpha)_{PV} \tag{2.17}$$

$$T_{out,PVT} = \frac{Q_{PVT}}{\dot{m}_{PVT}.C_P} + T_{in,PVT} \tag{2.18}$$

Instantaneous thermal efficiency and electrical efficiency of the PVT collector are computed using Equation 2.19 and Equation 2.20, respectively.

$$\eta_{th} = a_1.F_{R,r}.(\tau\alpha)_{PV} - a_2.U_{L,r}.F_{R,r}.(\frac{T_{in} - T_{amb}}{G_t}) \tag{2.19}$$

$$\eta_{PV} = \eta_r.(1 - a_3.\phi.(T_c - T_r)) \tag{2.20}$$

Where, η is the efficiency, A_{pvt} is the area of the PVT collector, G_t is the incident solar radiation on the PVT collector, $(\tau\alpha)_{PV}$ is the product of the transmittance and absorptance of the PV cell, T is the temperature, $\dot{m}_{PVT}$ is the circulating water flow rate through the PVT collector, C_P is the specific heat

of the circulating water, a_1 and a_3 are the model parameters, $F_{R,r}$ is the heat removal efficiency factor, $U_{L,r}$ is the overall loss coefficient, ϕ is the temperature coefficient and the subscripts *th*, *pv*, *in*, *amb*, *c*,*r* and *out* are thermal, photovoltaic, inlet, ambient, cell, reference and outlet respectively.

Air-to-water heat pump

The air-to-water heat pump is a heating device of type 941 in TRNSYS library. The heating capacity and heating power of the heat pump were specified as 8kW and 1.7 kW respectively. The component allows entering source water temperature and entering air temperature to the HP. The amount of thermal energy provided by the heat pump is defined as:

$$Q_{ASHP} = Q_{HP} - P_{comp} \tag{2.21}$$

Where Q_{ASHP} is the heating power of the heat pump and P_{comp} is the compressor power. The state of the air exiting the evaporator is determined as follows:

$$h_{cond,out} = h_{cond,in} + \frac{Q_{HP}}{\dot{m}_{air}} \tag{2.22}$$

The COP of the heat pump is calculated using Equation 2.23:

$$COP = \frac{Q_{HP}}{P_{comp}} \tag{2.23}$$

Water-to-water heat pump

The water-to-water heat pump used in simulation is a normalized one of Type 927 in TRNSYS library. The heating capacity and heating power of the heat pump were specified as 8kW and 2.5 kW respectively. The component allows entering water temperature from the source and entering load water temperature and returns COP as in Equation 2.24, $T_{source,out}$ as in Equation 2.25 and $T_{load,out}$ as in Equation 2.26:

$$COP = \frac{Cap_{heating}}{\dot{P}_{heating}} \tag{2.24}$$

$$T_{source,out} = T_{source,in} - \frac{\dot{Q}_{absorb}}{\dot{m}_{source}.C_{P,source}} \tag{2.25}$$

$$T_{load,out} = T_{load,in} - \frac{Cap_{heating}}{\dot{m}_{load}.C_{P,load}} \tag{2.26}$$

Where, $Cap_{heating}$ is HP heating capacity, $\dot{P}_{heating}$ is HP power consumption. The amount of energy absorbed from the source fluid stream in heating is

given by Equation 2.27:

$$\dot{Q_{absorb}} = Cap_{heating} - \dot{P}_{heating} \tag{2.27}$$

Thermal storage tanks

Tank 1 is a heat storage tank specified of Type 158 in TRNSYS library. Tank 2 is used for direct DHW production and space heating specified of Type 534 in TRNSYS library. It is a cylindrical tank with immersed heat exchanger type. Both tanks are of $1m^3$ volume storage with vertical configuration where thermal losses are assumed to be from the top, bottom and edges. For both tanks, the problem breaks down into the solution of the differential equation in Equation 2.28:

$$\frac{dT_{tank}}{dt} = \frac{Q_{in,tank} - Q_{out,tank}}{C_{tank}} \tag{2.28}$$

Validation of the models

Validation of the DX-SAHP model

To verify the developed DX-SAHP system model, the simulation results were compared with the experimental results of Ji et al. [114] taking similar conditions.

TABLE 2.4: Specifications of the DX-SAHP system components

Component	Experimental work	Present model
Collector-evaporator		
Type	bare-plate unglazed	bare-plate unglazed
Area	4m²	4.2m²
Material	Aluminium	Aluminium
Compressor		
Efficiency	0.75	0.75
Indoor temperature	20°C	20°C
Water temperature	15°C	15°C
Storage tank		
Capacity	500L	500L

The simulation results are in good agreement with the experimental results. Indeed, with the increase in solar radiation from 100 to 500 W/m², the COP increases from 2.01 to 2.40 in the present model and increased from 2.06 to 2.36 in the experimental work.

Validation of the IX-DSHP model

As discussed above in paragraph 2.4.2, TRNsys is a well-recognized tool simulation program internationally offering a wide library of validated component models. Furthermore, the present model of IX-DSHP developed in this study is compared to other similar studies of PVT dual sloar-air source SAHP working in indirect-expansion mode. The coefficient of performance obtained in the currecnt study is 2.63 which is seen lies in the same range of COPs obtained in numerical and/or experimental other studies as shown in Table 2.5.

TABLE 2.5: Comparative studies on IX-DSHP

Author	**Study**	**Application**	**COP**	**Data type**
Aste et al. [136]	numerical	DHW, SH/SC	month. av. 3 to 4.8	1-year simulation
Simonetti et al. [137]	num. and exp.	water heating	2.0 to 5.5	parametric simulations
Besagni et al. [138]	experimental	DHW, SH/SC	month. av. 2.47 to 3.75	1-year experiment
Wang et al. [154]	experimental	water heating	2.49 to 3.54	1-month experiment
Qu et al. [155]	experimental	water heating	2.63 to 5.05	1-day simulation

2.4.3 Coupling Mathematical model and TRNSYS model

After being developed, the two models of the DX-SAHP system and the IX-DSHP system are coupled under one TRNSYS environment. The final model of the new system abbreviated as DX/IX-DSHP system is shown in Figure 2.11.

The heat released by refrigerant at condenser level of the DXHP and temperature of returned water from TK2 are used to calculate the outlet temperature of water at each time step.

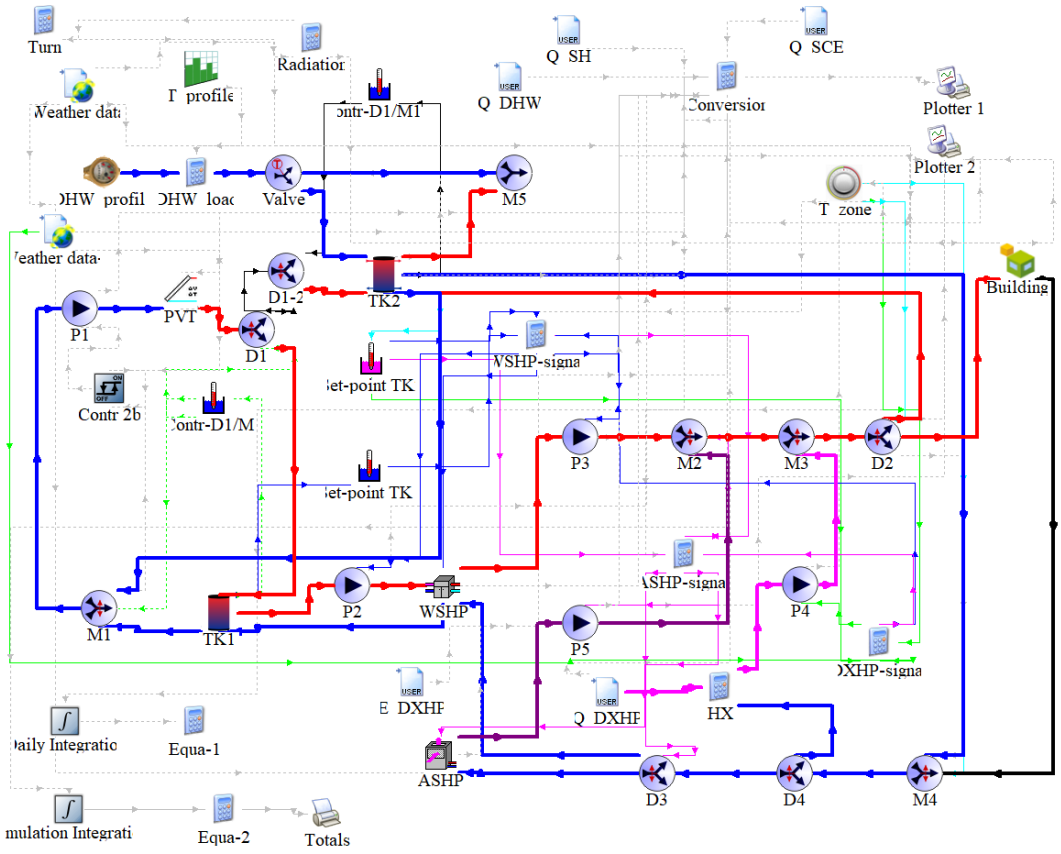

FIGURE 2.11: The TRNSYS modelling of DX/IX-DSHP system.

2.5 Conclusion

This chapter highlights essentially the procedure of numerical modelling using Matlab software and dynamic simulation with TRNSYS transient system simulation program.

It starts by the description of the building under study accompanied with climatic conditions of the city of Djelfa. The hourly needs of the occupants for DHW for a day is shown and then the energy demand for space heating and DHW production is discussed with corresponding curves.

In a next stage, the schematic representation of the DX/IX-SAHP system is shown jointly with the control strategies chart.

To simply explain the procedure of modelling and simulation, it is divided into three succeeded steps. Firstly, the Matlab model for the DXHP system, secondly, the TRNSYS model for the IX-SAHP system and finally, the coupled TRNSYS-Matlab model for the whole DX/IX-SAHP system.

Chapter 3

Results and discussions

3.1 Introduction

This chapter is dedicated to point out and discuss simulation results of the presented system in a bid to show its consistency to operate continuously at different weather conditions for all the heating period. Simulation of the coupled TRNSYS-Matlab model was carried out in the different modes. For each time step, weather data, DHW and building load profiles are required as model inputs for each iteration.
Preliminary simulations were carried out in order to design the system for changing operating modes and variable PVT areas with the aim to satisfy the building demand. It was observed that the DSM requires a larger TK2 storage volume to meet the demand while in the other modes; the storage volume of TK2 is directly linked to the PVT area. The larger the area of the PVT, the smaller the storage volume of TK2 is needed. Therefore, in the simulations, the system is configured using a PVT area of 8 m² and TK1 and TK2 volumes of $0.3m^3$ and $1.5m^3$ respectively.

3.2 Daily results

In order to highlight the system ability to operate in different modes, hourly electrical consumption and thermal energy supplied by the system are explored in a typical sunny day.

In AM, Figure 3.1, the system acts as a conventional ASHP, taking heat from ambient air, ensuring the total thermal energy required to maintain the building within thermal comfort and DHW provision. The inconvenient in this mode is that an ASHP is known by its high electricity consumption

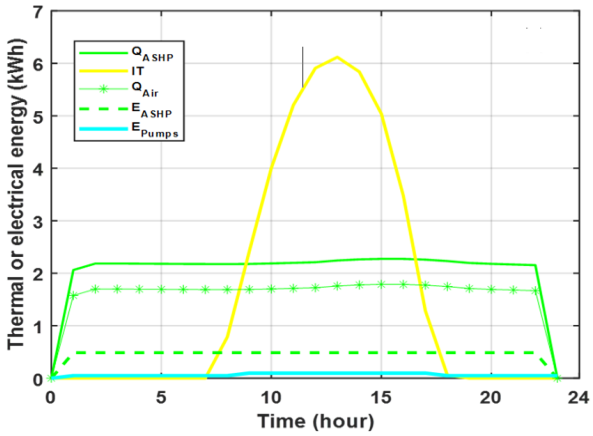

FIGURE 3.1: A typical day thermal energy supplied and electrical energy consumed in AM.

In DSM, Figure 3.2, the DXHP is on at around 07:00 AM because it can absorb heat directly from low solar radiation and ambient air, but it turns off near 07:00 PM as the solar radiation is not available and there is no heat storage in this mode. Therefore, the ASHP is activated to ensure the required thermal energy. It is worth noting that the electrical energy consumption in DSM mode is reduced compared to ISM.

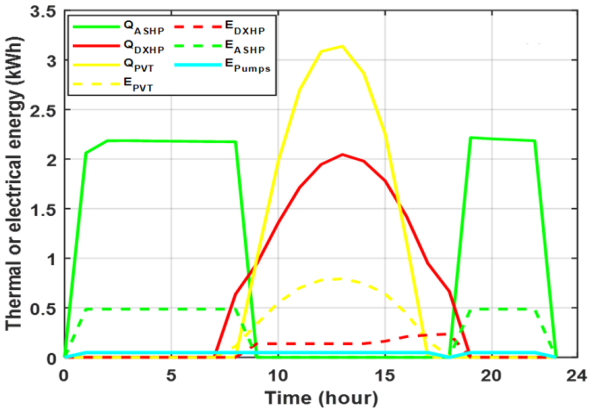

FIGURE 3.2: A typical day thermal energy supplied and electrical energy consumed in DSM.

In ISM, as seen in Figure 3.3, the heat is supplied by the ASHP at night and early day hours. When the thermal energy in the storage tank is sufficient, the WSHP turns on from around 09:00 AM to 09:00 PM. Afterwards, ASHP turns on, ensuring heat supply in the remaining hours of the day.

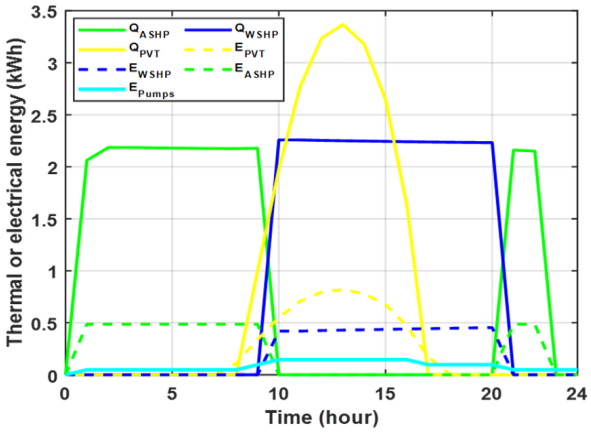

FIGURE 3.3: A typical day thermal energy supplied and electrical energy consumed in ISM.

The D/ISM combines the advantages of the two other modes. It has the thermal storage possibility, the direct solar heating and the ability to harness low solar radiation, as seen in Figure 3.4. The ASHP supplies heat in early day hours only whereas in the rest of the day heat is provided by solar thermal energy, which results in an important reduction in electricity consumption.

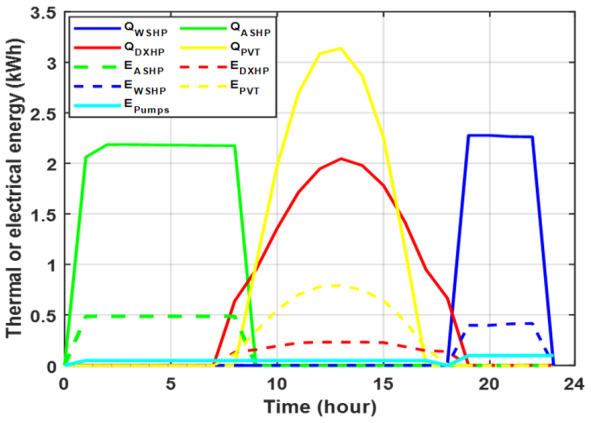

FIGURE 3.4: A typical day thermal energy supplied and electrical energy consumed in D/ISM.

3.3 The whole heating period results

3.3.1 System design

It is worth to remember that the system is designed with a SCE of 2m² area, a PVT area of 8 m². As well, in order to ensure the required thermal energy for the building, an ASHP of 8kW and a WSHP of 8kW are considered.

3.3.2 Temperature profiles with supplied and consumed energies

Figure 3.5 highlights temperature profiles with supplied and consumed energies by the ASHP and pumps across the heating period. It is clear that both set-points of 20°C (T_{Zone} in the label of the curve) for space heating and 45°C for DHW (T_{DHW}) are guaranteed throughout heating period by the ASHP alone, without any contribution of solar radiation.

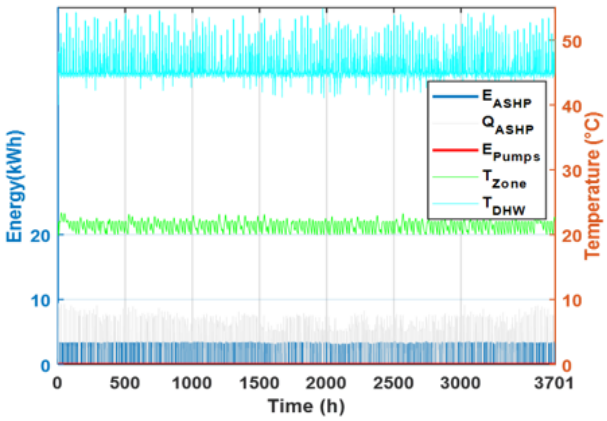

FIGURE 3.5: Temperature profiles with supplied and consumed energies by ASHP and pumps.

3.3.3 Thermal energy supplied by the system

This section depicts the thermal energy supplied in the different modes. In case of DSM, Figure 3.6, it is observed in the histograms that much amount of thermal energy is provided by the ASHP. The daily heat production of the ASHP attains a maximum of 100kWh. The low heat production with DSM is explained by the small area of the unglazed solar collector.

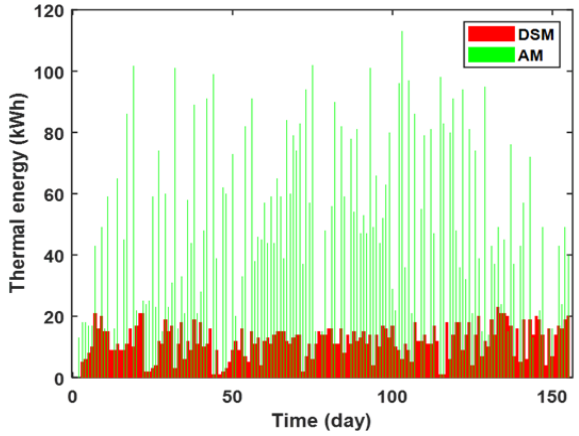

FIGURE 3.6: Thermal energy supplied by the system in DSM.

In ISM, as shown in Figure 3.7, an important part of required thermal energy is provided by the WSHP with a peak of 80 kWh. This is because of larger area of the PVT collector and the use of thermal storage tank, which allows the system to exploit more solar energy. Any surplus of heat produced by PVT collectors is supplied directly for DHW production. Consequently, the contribution of ASHP is less important.

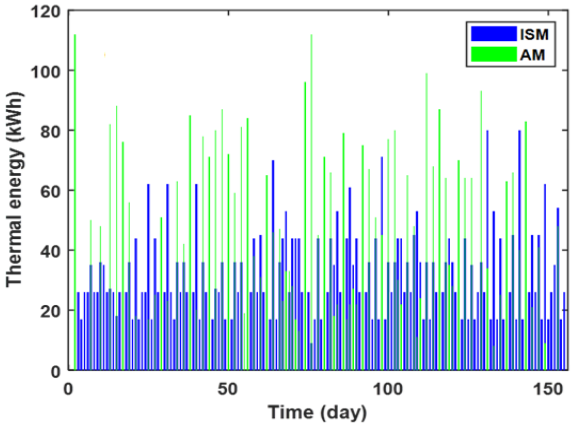

FIGURE 3.7: Thermal energy supplied by the system in ISM.

In D/ISM, as seen in Figure 3.8, heat supplied by ASHP is the lowest compared to other modes, which confirms the high ability of the system in this mode to exploit solar energy since heat is supplied in direct and indirect modes. It is important to notice that although the system produces less thermal energy than other modes, it meets the building energy demand thanks to the simultaneous working modes.

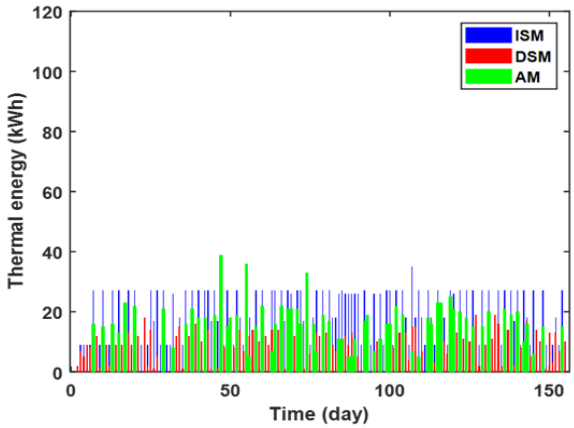

FIGURE 3.8: Thermal energy supplied by the system in D/ISM.

3.3.4 Electrical energy

The histograms in Figure 3.9, Figure 3.10 and Figure 3.11 represent the electrical energy consumed by the system in different modes during the heating period.
The highest power consumption is registered is DSM as a great part of heat required is provided by the ASHP, as seen in Figure 3.9. The electrical consumption attains 40 kWh.

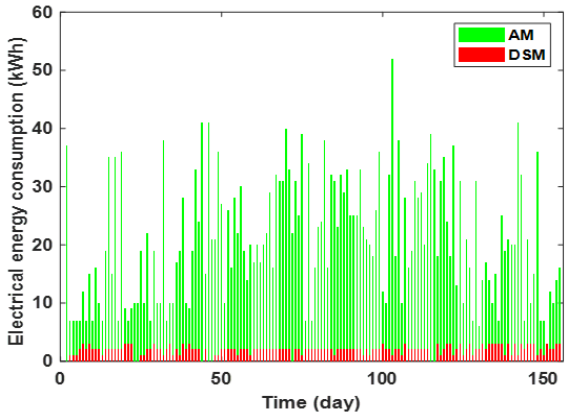

FIGURE 3.9: Electrical energy consumption in DSM.

The ISM is characterized by the simultaneous electrical consumption of the ASHP and the WSHP due to their both contribution in thermal energy production as seen in Figure 3.9. The electrical consumption of ASHP in ISM is less than that consumed in case of DSM, even it exceeds 30 kWh. This is owing to high working time of WSHP, and it is additionally explained by the great contribution of PVT and solar collectors in heat production which tends to increase heat pump evaporating temperature, lowering thus its electricity consumption.

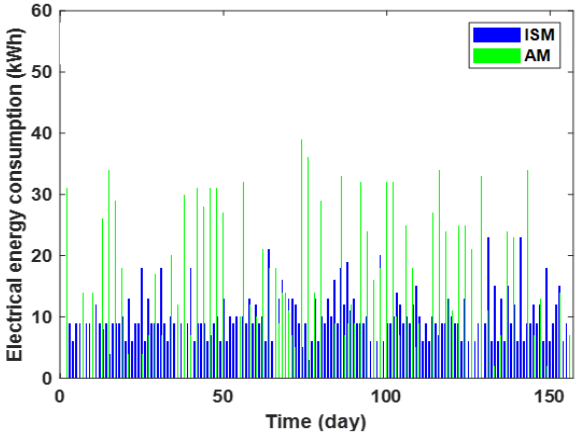

FIGURE 3.10: Electrical energy consumption in ISM.

The lowest electrical energy consumption is observed in D/ISM because the heat generated by PVT and unglazed solar collectors significantly contribute in increasing the evaporation temperature of the heat pump, thereby reducing its heat consumption, as shown in Figure 3.11. The consumption of electrical energy is high by WSHP, medium by ASHP and low by DXHP.

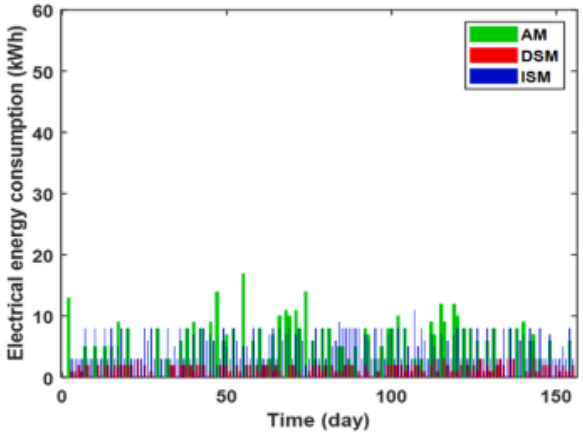

FIGURE 3.11: Electrical energy consumption in D/ISM.

3.3.5 Performance indicators

Coefficient of performance (COP)

Figure 3.12, Figure 3.13 and Figure 3.14 show daily changes in COP of the system in three modes across the heating period. Figure 3.12 shows that the COP in DSM is higher if compared to AM. It locally exceeds 7.0, while the maximum COP value in the AM mode is below 4.0. This is because the SEC directly absorbs heat, resulting in a higher evaporation temperature of the refrigerant, which reduces power consumption.

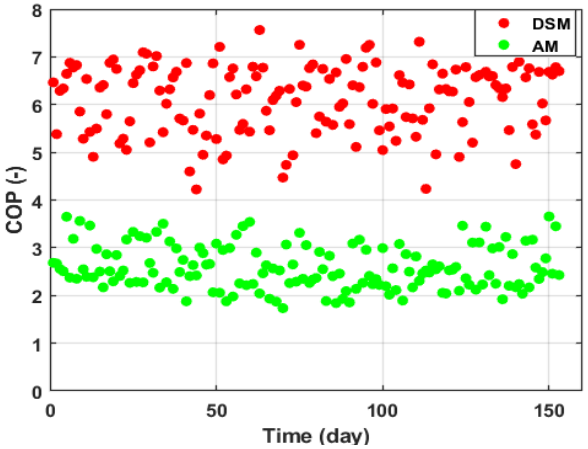

FIGURE 3.12: Coefficients of performance of the system in DSM.

In Figure 3.13, it can be seen that the COP in ISM is almost better than the COP in AM exceeding 4.0, which justifies the contribution of heat produced by PVT collector in reducing the electrical energy consumption of WSHP.

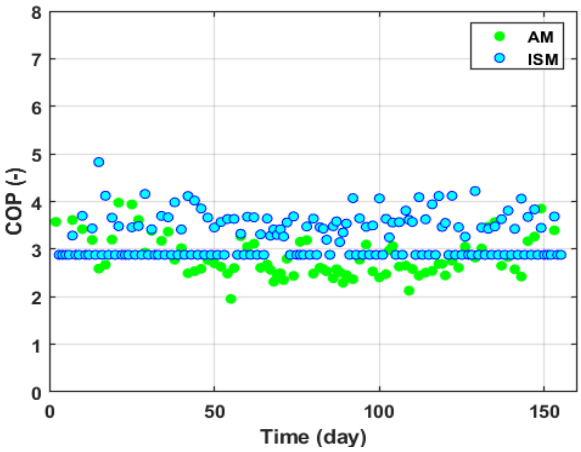

FIGURE 3.13: Coefficients of performance of the system in ISM.

As expected, the COP in D/ISM is the highest as illustrated in Figure 3.14 evidenced by low electrical energy consumption compared to DSM and ISM.

The COP of the new system still high exceeding 6.0 in case of DSM. The COP of ISM is around 3.0 and the COP of AM is between 2.0 and 3.0.

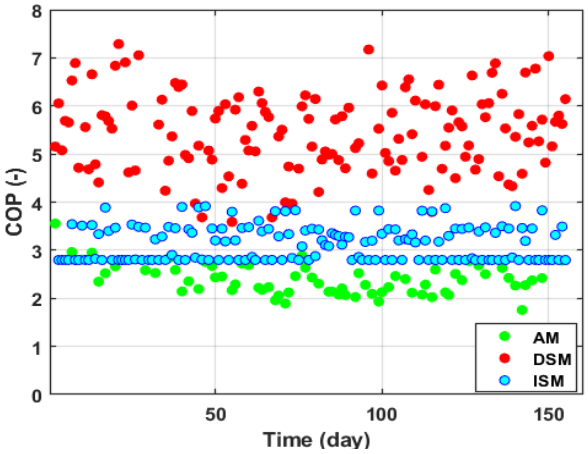

FIGURE 3.14: Coefficients of performance of the system in D/ISM.

Seasonal performance factor (SPF)

In relation with seasonal performance factor, the D/ISM of the system presents a notable improvement in comparison to two other modes.

Although the high COP, the worse results in SPF were recorded with DSM (around 2.0) as shown in Figure 3.15. This is mainly due to high electrical energy consumption of the heat pump in AM in one hand and the absence PVT electricity production in other hand.

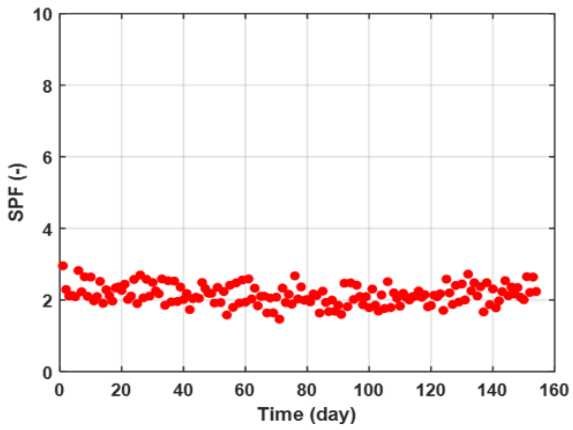

FIGURE 3.15: Seasonal performance factor of the system in DSM.

The SPF in ISM mode turns around 5.0, as shown in Figure 3.16. This improved SPF is achieved thanks to PVT electrical energy production.

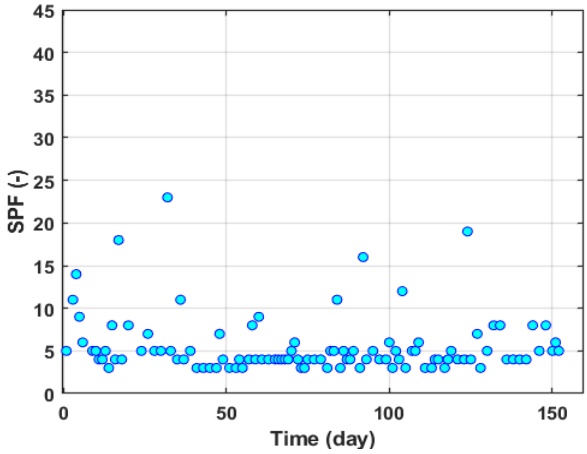

FIGURE 3.16: Seasonal performance factor of the system in ISM.

As shown in Figure 3.17, the SPF of the system running in D/ISM is high in most days ranging between 5.0 and 40. This is due to low electrical energy consumption in DSM and ISM modes and the contribution of PVT in electrical energy production. Concretely, this means that in winter months of the city of Djelfa, the around-season performance, based on the mean outdoor temperatures varies between 5.0 and 40 and considering the totality of system components consumption like pumps and auxiliary devices.

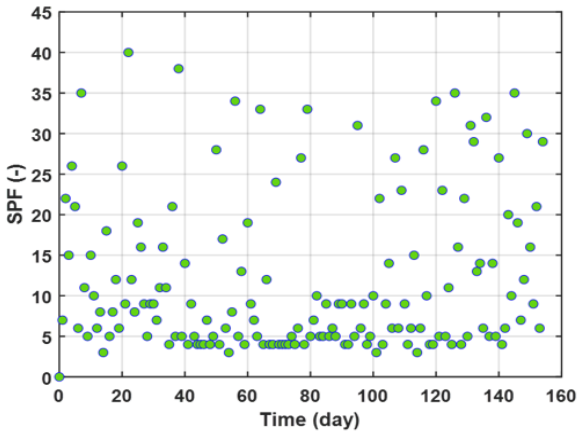

FIGURE 3.17: Seasonal performance factor of the system in D/ISM.

Solar fraction (SF)

In addition to the contribution of the new system in improving the SPF, following results depict analogous behaviour regarding solar fraction. That say, the D/ISM discloses significant improvement in term of SF.
In a comparison between the three modes, Figure 3.18 shows that the SF in DSM does not surpass 50% which practically means that the solar system covers less than fifty percent of thermal energy needs, even much more less in particular days.

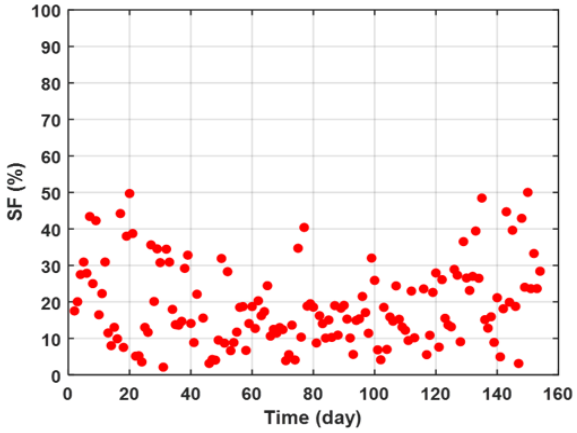

FIGURE 3.18: Solar fraction of the system in DSM.

Figure 3.19 shows that the SF in ISM ranges from 10% to 100% depending on heating period days.

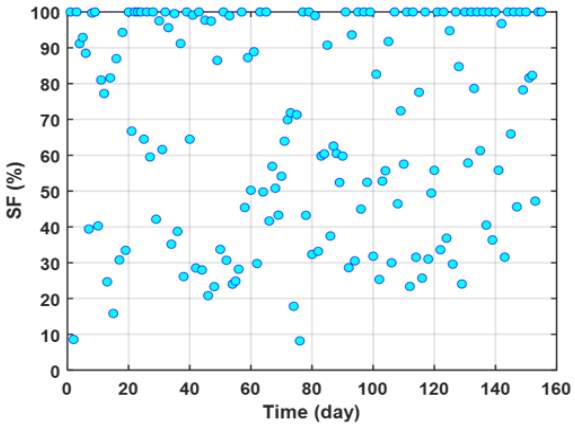

FIGURE 3.19: Solar fraction of the system in ISM.

The SF of the system in D/ISM is significantly improved since solar energy provides the majority of the required electrical and thermal energy. Figure 3.20 outlines that the SF remains all the time higher than 50% during the whole heating demand period and it occasionally rises to 100%. Tangibly, this is interpretable by that the solar system (solar thermal and PVT collectors) contribute efficiently in thermal energy needed by the heat pumps and the building and in electrical energy needed to run the heat pumps. Attaining 100% means that the system covers the totality of required energy and it is totally independent on auxiliary energy and public electricity grid. The system at least covers, by renewable energy, fifty percent of both building heating and components running needs, which is a high achievement in heat pump technology.

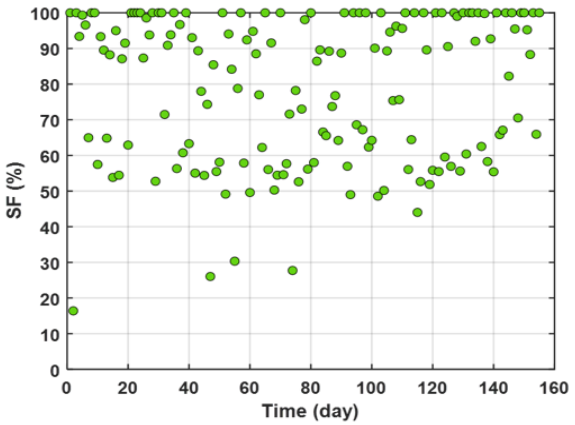

FIGURE 3.20: Solar fraction of the system in D/ISM.

3.4 Total results

3.4.1 Heat supply and electricity consumption and production

Table 3.1 summarizes the total energy and performance results of the system running in different modes throughout the heating period. The effect of AM is introduced as well for comparative reasons.
The total heat supply represents the sum of heat produced by heat pumps and direct solar heating. It is 5176.98 kWh, 5019.25 kWh and 5041.11 kWh in DSM, ISM and D/ISM respectively. The similarity of these findings depicts in same time that the design of the novel system works well whatever be the mode and that the heat demand of the application (DWH and SH) are in this range.
The corresponding electrical consumptions are 2242.63 kWh, 1625.43 kWh and 1374.53 kWh. It is apparent that in D/ISM the system consumes the lowest electrical energy. This is because in addition to the electrical energy produced by PVT, the direct solar produces thermal energy by PVT and SCE and it is stored in the tanks with an amount of 2639.23 kWh.
In DSM, the SCE is the component generating thermal energy as the system operates like a DX-SAHP system. The generation of thermal energy (Q_{SCE}) reaches 1175. 48 kWh. In ISM, PVT panels generate thermal energy of is 1762. 36 kWh (Q_{PVT}). A portion of this thermal energy is used for directly heating domestic water (Q_{DSH}) with 977. 03 kWh. The thermal energy supplied in D/ISM is shared between the SCE and PVT panels, providing 780. 06 kWh and 1859. 17 kWh, respectively where direct solar heating achieves a total of 1313 kWh.
As well as thermal energy, PVT panels produce electrical energy. They generate 875 kWH of electrical energy (E_{PVT}) in ISM. When the system operates in D/ISM, the generation of electrical energy is 817 kWh.

From the total results above, the system in D/ISM achieves better yields, which are explained by best performance indicators. The COP in D/ISM reaches 2.89, which is the highest, followed by that of ISM (2.63) and then DSM (2.37). The SPF of the system working in D/ISM is also the highest reaching 9.19 followed by that of ISM (6.23) and DSM (3.76). The SF in D/ISM is 63% followed by ISM and then DSM at 51% and 29% for each respectively. When comparing the air mode to the other modes, it is clear that all solar running modes have significantly better system performance than the former.

TABLE 3.1: Total results

Energy (kWh) or Performance		AM	DSM	ISM	D/ISM
Heat supply	ASHP	5091	4218.57	2848.91	2245.97
	DXHP	-	958.41	-	605.62
	WSHP	-	-	1193.31	876.52
	DSH	-	-	977.03	1313
	Total	5091	5176.98	5019.25	5041.11
Electricity consumption	ASHP	2080	1942.58	1197.63	933.11
	DXHP	-	201.29	-	126.53
	WSHP	-	-	336.43	229.26
	Pumps	99.1	98.76	91.37	85.63
	Total	2179.1	2242.63	1625.43	1374.53
Solar heat production	PVT to TK1	-	-	785.33	546.17
	PVT to TK2	-	-	977.03	1313
	SCE	-	1175.48	-	780.06
	Total	-	1175.48	1762.36	2639.23
PVT electricity production				875	817
Heat absorbed by ASHP		3800	3715.81	2611.82	2069.02
COP (-)	ASHP	2.11	2.17	2.38	2.41
	DXHP	-	4.76	-	4.79
	WSHP	-	-	3.55	3.82
	System	2.11	2.41	2.63	2.89
SPF (-)		2.01	3.76	6.23	9.19
SF (%)		-	29	51	63

To more demonstrate the distinct functions of the two types of solar panels, SCE and PVT, in the new system, the histograms presented in Figure 3.21 depict the contribution of each of them in three modes related to the provision of thermal and electrical energy.

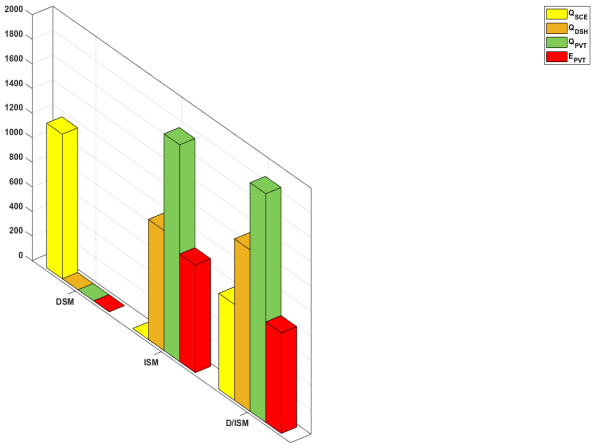

FIGURE 3.21: Illustration of SCE and PVT contribution in different modes.

3.4.2 Comparison between ISM and D/ISM in term of COP

Following the order of performance seen in the last section, where results grades D/ISM as the most efficient one followed by ISM and then DSM. It is now to confirm furthermore that the D/ISM surpasses ISM largely. Figure 3.22, Figure 3.23 and Figure 3.24 outlines additional performance indicators comparison when the system operates in ISM or in D/ISM taking into consideration the total heat collection area . The total HCA is represented by a line segment connecting the two modes. Noting that the system in D/ISM has an extra-heat collection area of 2m² SCE. The total heat collection area means simply the sum of PVT panels area and SCE area. The SCE area is unique equals 2m² but PVT panels area is incremented from 2m² to 20m². For instance, when the PVT area is 4m², the total heat collection area becomes 6m² in D/ISM (4m² PVT area plus 2m² SCE area) .

As shown in Figure 3.22, for the same HCA the COP in D/ISM is always better than in ISM. For example, when the HCA is 4m², the COP is 2.63 in D/ISM and 2.39 in ISM. It is observed that difference between COPs of the two modes decreases with the increase in HCA area. For example, for 4m² PVT area the difference in COP is 0.24 and becomes 0.11 for 18m².

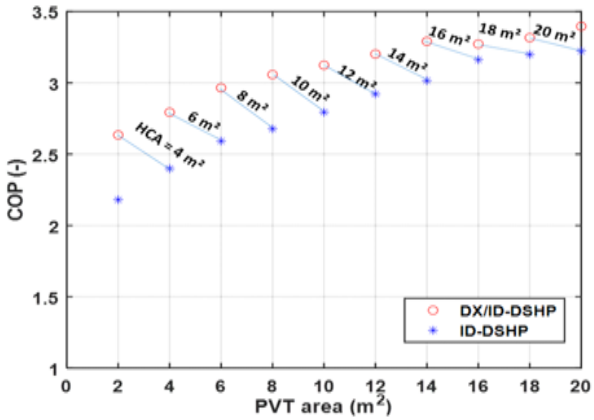

FIGURE 3.22: Comparison between ISM and D/ISM in term of COP.

Regarding SPF and SF comparison between D/ISM and ISM when considering total heat collection area, as illustrated in Figure 3.23 and Figure 3.24, it is apparent that both indicators are higher in D/ISM compared to ISM as the HCA is between 2 and 8m². However, beyond this range, no significant difference in SPF nor in SF is observed between the two modes. This is justified by that the electrical energy consumption is entirely satisfied for higher areas in both modes which tends to reduce the differences between them. Consequently, a conclusion that can be drawn here is that the system operating in D/ISM is more advantageous for lower PVT areas.

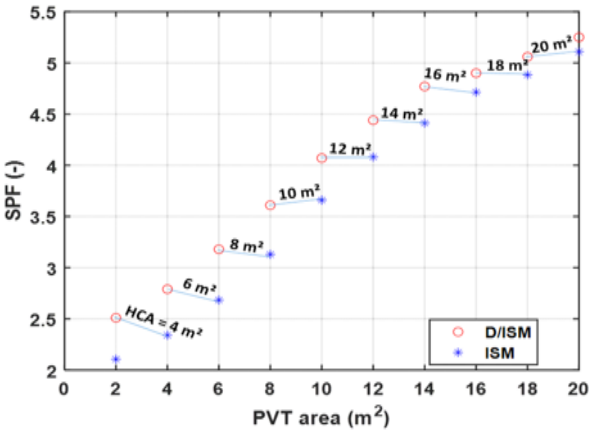

FIGURE 3.23: Comparison between ISM and D/ISM in term of SPF.

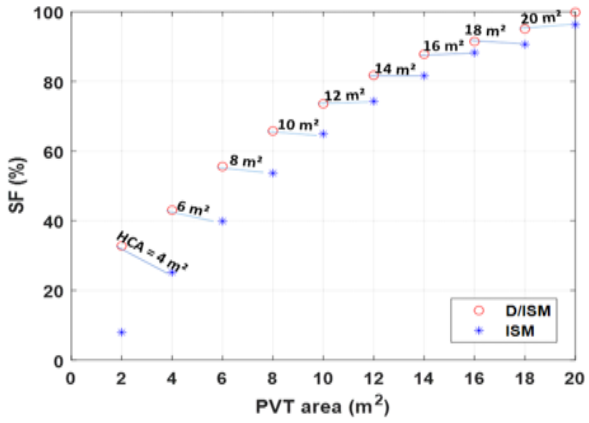

FIGURE 3.24: Comparison between ISM and D/ISM in term of SF.

3.5 Parametric study

Having presented and discussed daily, heating season period and total results of the investigated new system showing its performance when operating in composite D/ISM compared to single modes, the rest of the study will look into the parameters design optimisation for usable purposes.
The investigated parameters are PVT area, tank 1 (TK1) set-point temperature, tank 2 (TK2) set-point temperature and SCE area. As depicted in the forthcoming curves and in attempt to simplify data reading the curves are increasingly coloured for a more inclusive readership. In each figure, the light yellow colour zone corresponds to maximum values, while the dark blue corresponds to minimum values.

3.5.1 Influence of tank 1 set-point temperature and PVT area

To study the influence of TK1 set-point temperature and PVT area, TK2 temperature and SCE area were set at 50°C and 2m² respectively. PVT area was changed from 2m² to 20m² and TK1 temperature was changed from 35°C to 50°C. The COP slightly increases with the increase in TK1 set temperature at higher PVT area as seen in Figure 3.25. For example, with a PVT area of 2m², the COP goes from 2.54 to 2.59 when increasing the temperature from 30°C to 50°C. Whereas, with 20m² area, the COP goes from 2.92 to 3.07 for the same interval of temperature. This finding is explained by the fact that TK1 set temperature enhances the heat storage capacity of TK1, which in turn improves the evaporating temperature in ISM improving thus the COP. In term of PVT area influence, it is observed that the increase in COP is important

when PVT area changes from 2 to 4 m² due to the rise of solar heat collection. Beyond this PVT area range, the effect becomes less important since the excess of heat production is supplied to TK2.

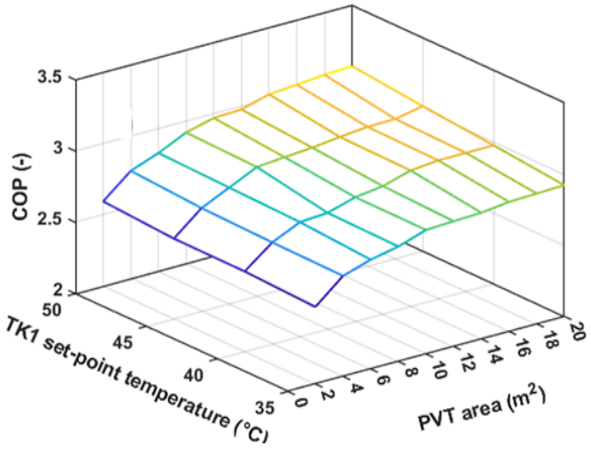

FIGURE 3.25: Influence of TK1 set-point temperature and PVT area on COP.

As illustrated in Figure 3.26, the increase in TK1 set-point temperature has no big influence on SPF for different PVT areas since the electrical energy consumption reduction in ISM is not significant. Whereas, the effect of PVT area is remarkable. The higher the PVT area, the higher is the SPF. Rapid increase in SPF recorded up to 14m² area. A maximum SPF of 5.09 is obtained with 20m² PVT area and 35°C Tk1 temperature. After 14m², the electricity production by PVT collector becomes higher than the electricity required by the system (HPs compressor and circulating pumps); therefore, no more enhancement in SPF is possible.

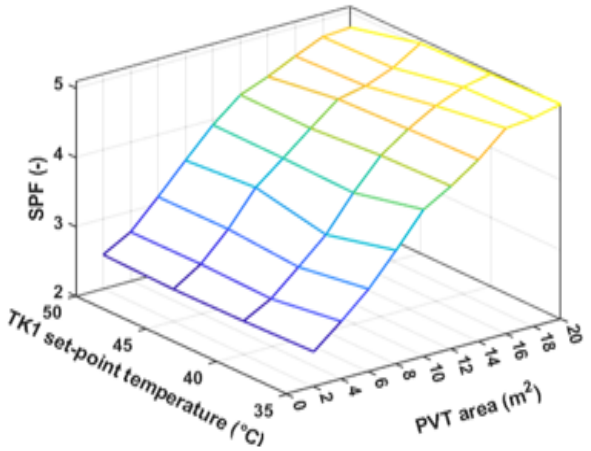

FIGURE 3.26: Influence of TK1 set-point temperature and PVT area on SPF.

As seen in Figure 3.27, there is no significant impact of TK1 set-point temperature variation on SF values. However, the improvement in SF can be

seen when the PVT area rises. For different set-point temperatures, the SF augments from 29.47% for 2m² to 94.26% for 20m² PVT areas. The reason is that the augmentation in PVT area leads to a clear improvement in SF owing to the higher electricity production by PVT collector, which tends to reduce auxiliary electricity consumption.

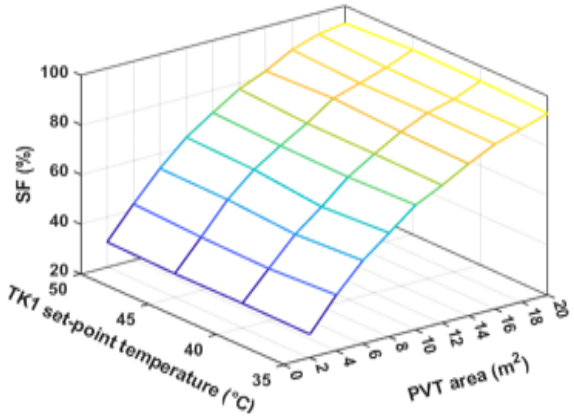

FIGURE 3.27: Influence of TK1 set-point temperature and PVT area on SF.

3.5.2 Influence of tank 2 set-point temperature and PVT area

Now, to study the influence of TK2 set-point temperature versus PVT area on performance, TK1 temperature is set at 40°C and SCE area at 2 m². The PVT area was changed from 2m² to 20m² and the TK2 temperature was changed from 45°C to 60°C. In general, it is observed that the performances of the system are less sensitive to changes in TK2 set-point temperature compared to changes in TK1 set-point temperature. This is interpreted as the most thermal energy produced by PVT collector, stored in TK1, is to be used in ISM and only a small amount is supplied to TK2 regardless its set-point temperature. Regarding PVT area effect, it is found that for all set-point temperatures, the COP little increases with the increase in PVT area, as seen in Figure 3.28.

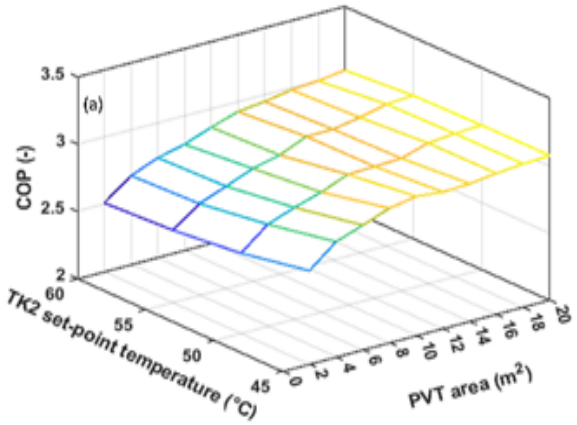

FIGURE 3.28: Influence of TK2 set-point temperature and PVT area on COP.

The impact of PVT area elevation is clearly observed in SPF and SF, as shown in Figure 3.29 and Figure 3.30. A rapid increase in SPF is observed until 12m², followed by slower alteration thereafter. A maximum value of SPF (4.80) is reached. Similarly, in Figure 3.30 there is a rapid increase in SF until 14m², followed by slowly change. A SF of 93.28% is achieved with a PVT area of 20m² at TK2 set temperature of 45°C.

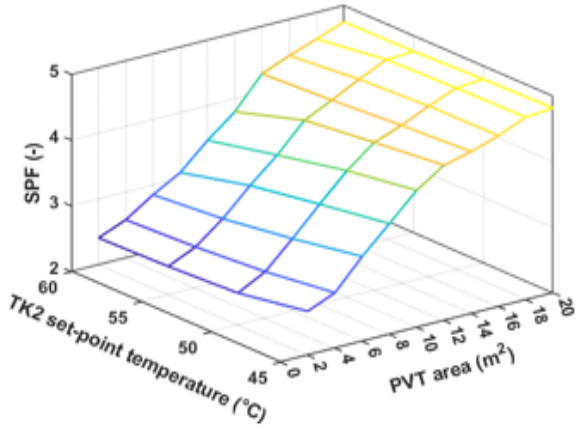

FIGURE 3.29: Influence of TK2 set-point temperature and PVT area on SPF.

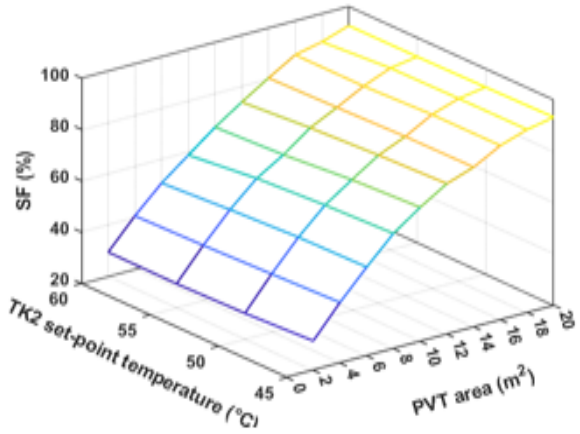

FIGURE 3.30: Influence of TK2 set-point temperature and PVT area on SF.

3.5.3 Influence of SCE area and PVT area

The effect of SCE versus PVT areas is investigated under the considerations of TK1 and TK2 set-point temperatures of 40°C and 50°C respectively. Here we take three different possible areas of SCE 2m², 4m² and 6m² to study the impact of possible increasing in that areas. PVT areas are varied from 2m² to 20m² by a step of 2m². Figure 3.31, Figure 3.32 and Figure 3.33 point out the effect of SCE for different PVT areas on system performance. As seen in Figure 3.31, the COP rises rapidly between 2 and 4 m² PVT area and becomes almost constant after this range. This is because the extra heat collection is supplied directly to the DHW tank. The COP appears more sensible to SCE area change. It changes from 2.62 to 2.94 as SCE area varies from 2 to 6m². This can be explained by the fact that while the system is running in direct mode, it absorbs more solar thermal energy as the SCE area increases on one hand and raises refrigerant evaporation temperature on the other, resulting in reduced electrical energy consumption.

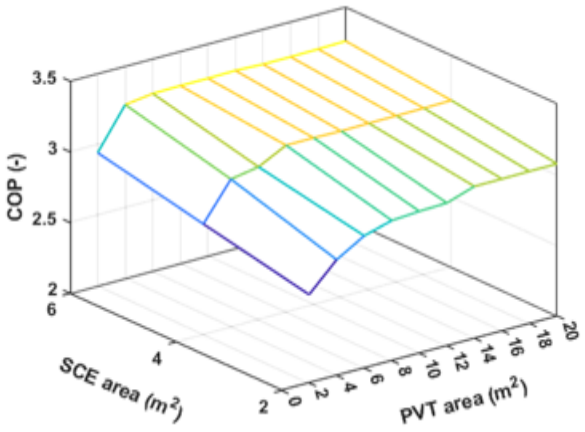

FIGURE 3.31: Influence of SCE area and PVT area on COP.

However, the SPF and SF appear more sensitive to PVT area increase rather than to SCE area change due to extra-production of electricity in addition to thermal energy by the former. The SPF ranges from 2.51 to 5.34 with indication that the important change is with lower PVT areas as the electrical energy demand of the system is significant and becomes low for higher PVT areas, as seen in Figure 3.32.

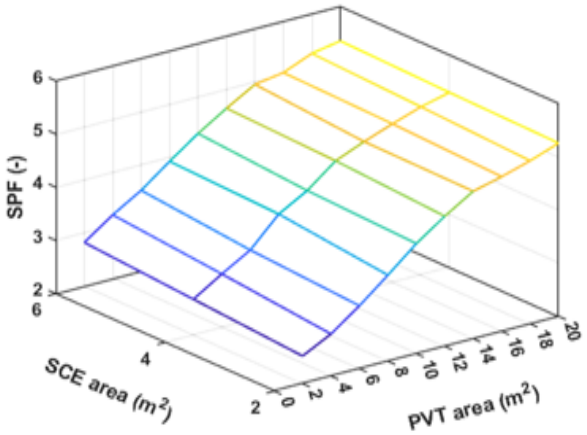

FIGURE 3.32: Influence of SCE area and PVT area on SPF.

The SF attains 96.57% with 20m² PVT area as illustrated in Figure 3.33 which is a high achievement in SF value demonstrating the high contribution of the solar system and the independence in term of auxiliary electricity.

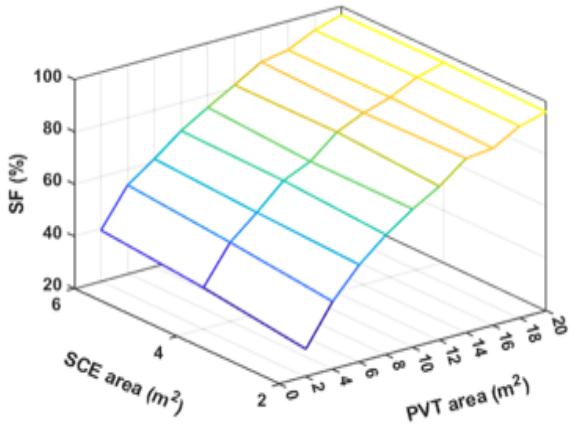

FIGURE 3.33: Influence of SCE area and PVT area on SF.

3.6 Economic analysis

The complexity of solar heat pump systems is expressed with the type and number of components used, and the cost of systems are compared taking into account the payback period (PBP) [53].

To study the economic viability of the studied solar system in different modes, the initial investment cost (IC) including system components cost, installation cost, and operating cost (OC) are firstly determined based on the system components market and previous studies in the field. Then, the cost saving (CS) caused by electrical energy saving is estimated. Finally, payback period of the system is calculated using Equation 3.1 [156] and [131]:

$$PBP = \frac{IC}{CS} \tag{3.1}$$

Where, investment cost and cost saving are obtained as in Equation 3.2 and Equation 3.3:

$$IC = IC_{SS} - IC_{EH} \tag{3.2}$$

$$CS = OC_{EH} - OC_{SS} \tag{3.3}$$

Which yields to the final expression of PBP as in Equation 3.4:

$$PBP = \frac{IC_{SS} - IC_{EH}}{PEC_{EH}.C_{ELEC} - PEC_{SS}.C_{ELEC}} \tag{3.4}$$

Where, PEC is the primary energy consumed by electrical heater (EH) and solar system (SS).

The energy cost of electricity (C_{ELEC}) in Algeria is taken 0.05 €/kWh based on the quarterly bill of electricity delivered by the National Society of Electricity and Gas (SONELGAZ). It is important to notice that this cost is significantly lower than globally applicable cost of electricity. The PVT cost is taken 285 €/m² [157] and the bare SCE manufacture cost is taken 104€/m² [111]. Note that the economic analysis is based on PVT area of 8m² and SCE area of 2 m². The storage tank cost is estimated at 342.2 € per 100L [131]. The ASHP and DSHP of 8kW costs are estimated at 134.61 € and 160 € respectively for each 1kW [158]. The cost of a circulating fluid pump is estimated at 11.8€, noting that the system comprises three pumps.
Thereby, the total system costs are 3169.08€, 5444.2€ and 5652.2€ in DSM, ISM and D/ISM, respectively. In D/ISM, the system has an extra cost, this is due to SCE implementation with PVT panels.

The total results from the economic analysis are shown in Table 3.2. In general, the system can be criticized in point of view cost, which appears not economically viable in all studied modes due to higher system investment costs on one hand but mainly to the lower cost of energy in Algeria on the

other hand. However, in term of payback period comparison between the three working modes, the D/ISM has shown the lowest PBP (37 years) followed by ISM (38 years) and then DSM (45 years). Indeed, the PBP values can be considerably reduced when electricity energy prices differ from that of Algeria. For instance, taking electricity cost of 0.26€ per kWh which is similar to a city in UK [139], the PBP becomes 9, 8 and 7 years in DSM, ISM and D/ISM accordingly denoted PBP1 in Table 3.2.

TABLE 3.2: Economic analysis (*prices in (€)*)

		EH	DSM	ISM	D/ISM
Heat supply (kWh)		5091	5332.90	4903.99	5352.50
PEC (kWh)		3684	2023.43	615.52	554.50
PES (kWh)		0	1660.57	3068.49	3129.50
Initial cost	SCE	0	208	0	208
	PVT	0	0	2280	2280
	Tank	1368.8	1368.8	1368.8	1368.8
	EH/GB	70.8	0	0	0
	HP	0	1284.88	1280	1488
	Pumps	0	35.4	35.4	35.4
	Installation	0	480	480	480
	Total	1439.6	3169.08	5444.2	5652.2
Investment cost		0	1729.48	4004.6	4212.6
Operating cost		184.2	101.17	30.78	27.73
Cost saving		0	83.03	153.42	156.47
PBP		-	45	38	37
PBP1		-	9	8	7

Moreover, the influence of PVT area and SCE area on the PBP in ISM and D/ISM is studied. Three SCE areas of 2, 4 and 6m² are investigated. It is found that the PBP decreases as PVT area increases from 2 to 10 m² but increases with higher areas as shown in Figure 3.34. The best PBP of 33 years in D/ISM is obtained with area of 10m². Whereas, it appears that the increase in SCE area augments the PBP because the operating cost saving becomes less than the SCE cost. The best PBP is achieved with 2m² SCE area.

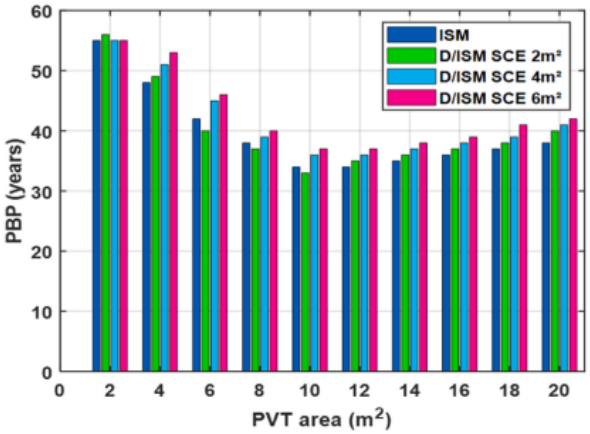

FIGURE 3.34: PBP comparison between ISM and D/ISM.

3.7 Conclusion

In this chapter, the results of the study are detailed and discussed. They can be resumed in five items as follows:

- A typical day from the heating period is selected to show the new system ability to work in AM, DSM, ISM and in D/ISM. All the curves prove that the system operates correctly.

- In winter months, the results confirm that new system guarantees the space heating set-temperature of 20°C and the DHW set-temperature of 45°C the whole period. Beside, they point out that the lowest electricity consumption is attributed to the D/ISM. The COP can reach 7.0, the SPF is between 5 and 40 and the SF is greater that 50% attaining 100%.

- The total results indicate that the new system supplies 5041.11 kWh of heating energy and consumes the lowest total electrical energy of 933.11kWh. The highest solar heat production as well as the performance indicators goes to the D/ISM. Its total heat provision is 2639.23kWh. The COP, SPF and SF of the system are 2.89, 9.19 and 63% respectively.

- The parametric study outlines that the PVT area increase enhances COP, SF and SPF. Excepting that its impact on COP declines as PVT area is greater than 8m².
  TK1 temperature increase improves COP but TK2 temperature increase

reduces it. The effect of both tanks temperature is not significant on SF and SPF.
Finally, the parametric study results reveal that the effect of SCE area is important as the PVT area is 2m².

- The economic analysis shows that, with actual electricity prices in Algeria, the system is not economically viable. However, when the study is extended to global mean energy cost, the system working in D/ISM still preferable since the PBP is 7. Compared to the two other modes, it is the lowest, ISM (8) and DSM (9).

General Conclusion

This study aims to advance the goal of meeting recommendations of countries and international organizations, including Algeria, to ensure energy security while addressing climate and environmental priorities by examining the performance of residential heat pump systems that operate on a dual energy source, solar and air, to provide space heating and domestic hot water in winter.

The novelty introduced is the investigation of a solar-assisted heat pump system that operates in three different modes. It can operate in direct-expansion mode, in indirect-expansion mode, or direct/indirect mode simultaneously. The heat pump is dual solar-air source connected to photovoltaic/thermal and solar thermal collectors.

The method consists of using a coupled TRNSYS-Matlab model to be simulated on a building located in Djelfa as a cold climate region representative. Daily, heating season-round and total performances of the considered system in the selected modes have been studied to point out D/ISM advantages.

- Results confirm that the system guarantees provision in DHW and SH across heating period for all considered working modes. The findings reveal that combined DX/IX-DSHP system performs better than separated DX-DSHP and IX-DSHP systems.
- Daily results show that in DSM the system achieves high COPs exceeding 7.0. In ISM, the system achieves high SPF (exceeding 10) and high SF (100%). In D/ISM, the best results are evidenced by the profit from different modes. High performance indicators are obtained with continuous heat supply. The maximum daily COP, SF and SPF are 7.28, 100% and 40 respectively.

- The total performance results revealed that the system is more efficient in D/ISM. The thermal energy stored is evaluated at 2639.23 kWh. The total heat supply by the system is 5176.98 kWh, 5019.25 kWh and 5041.11 kWh and the corresponding electrical consumptions is 2242.63 kWh, 1625.43 kWh and 1374.53 kWh depending on the system works in DSM, ISM and D/ISM respectively. The COP is 2.41, 2.63 and 2.89 respectively in DSM, ISM and D/ISM, respectively. Significant impact is observed regarding SPF and SF in D/ISM. The SPF is 9.19 and the SF is 63%, which are clear improvements over ISM (6.23) and (51%) respectively.

- A further comparison between ISM and D/ISM, in term of total heat collection area effect, reveals that high improvement in the COP can be obtained in D/ISM with all areas. The SPF and SF in D/ISM are also much better with PVT areas less than 10m² compared to ISM. The gap between the two modes in SPF and SF is gradually reduced with increasing PVT areas between 10m² and 20m².

- The parametric study discloses that in all modes the SPF and SF improve significantly with the increase in PVT area. An increase in area from 2m² to 20m², at 50°C TK1 temperature, leads to the SPF increase from 2.48 to 4.78 and the SF increase from 30% to 92.8%.
  Compared to SPF and SF, the improvement in COP with increasing PVT area is less pronounced mainly when it surpasses 8 m². As the PVT area varies from 8 to 20m², the COP rises from 2.89 to 3.0 at TK1 temperature 50°C and rises from 3.0 to 3.06 at TK2 temperature 45°C.
  Regarding the two tanks temperature effect, it was found that the COP increases with the increase in TK1 temperature but decreases when the TK2 temperature increases. With 8m² PVT area, the COP increases from 2.80 to 2.89 as TK1 temperature increases from 35°C to 50°C and decreases from 3.0 to 2.78 as the TK2 temperature rises from 45°C to 60°C. The impact of TK1 and TK2 temperature on SPF and SF is not significant. With PVT area 8m², as the TK1 temperature increases from 35°C to 50°C, the SPF changes from 3.64 to 3.52 and the SF changes from 61.8% to 63.6%. When TK2 temperature increases from 45°C to 60°C, the SPF changes from 3.68 to 3.08 and the SF changes from 64.8% to 58.7%.
  The SCE area slightly increases the COP and its effect on SPF and SF is significant only with low PVT area (2m²). For PVT area 8m², the COP increases from 2.99 to 3.23 when the SCE changes from 2m² to 6m². For

PVT area 2m², as the SCE augments from 2m² to 6m², the SPF varies from 2.51 to 2.82 and the SF varies from 30.6% to 39.4%. For PVT area 20m², as the SCE augments from 2m² to 6m², the SPF varies from 5.25 to 5.34 and the SF varies from 96.0% to 96.5%.

- The economic analysis shows that the studied system is not economically viable in Algeria due to actual high solar energy components investment costs and low primary energy prices. The payback period is 45, 38 and 37 years for DSM, ISM and D/ISM, respectively. However, taking worldwide electricity prices, the PBP will be considerably reduced. When taking an electricity cost of 0.26€ per kWh, which is the mean applicable in many countries, the PBP becomes 9, 8 and 7 years in DSM, ISM and D/ISM respectively.
  In term of PVT and SCE area influence, the PBP decreases as PVT area increases from 2 to 10m², regardless of the SCE area (2, 4 or 6m²). However, it increases beyond this range. The best PBP is achieved with 10m² PVT area and 2m² SCE area.

Future work

Future research should extend this work by implementing an alternative type to the bare solar collector evaporator, which allows an exploration of its effect on heat pump system performance.

Appendix

Physical and thermodynamic properties

1. Physical properties of R134a refrigerant

TABLE A.1: Physical properties of R134a refrigerant [40],[159]

Property	Value
Molar mass (kg/kmol)	102.03
Boiling temperature at 1 atm (°C)	-26.2
Freezing point (°C)	-101
Critical temperature (°C)	101.15
Critical pressure (bar)	40.64
Critical density (kg/m^3)	508
Latent heat of vaporization (kJ/kg)	215.5
Saturated vapour specific volume at 20°C	0.035

2. Thermodynamic properties of R134a refrigerant at point1

TABLE A.2: Thermodynamic Properties of R134a from REFPROP

T_{evap} (°C)	P_{evap} (bar)	ρ (kg/m^3)	V (m^3/kg)	H (kJ/kg)	E (kJ/kg·K)	C_p (kJ/kg·K)	k (mW/m·K)	μ (μPa·s)
-24.263	1.1	5.6814	0.17601	383.91	1.7454	0.8005	9.4631	9.8449
-22.31	1.2	6.1677	0.16214	385.12	1.7435	0.80743	9.6247	9.9158
-20.481	1.3	6.6522	0.15033	386.26	1.7418	0.81404	9.7765	9.9821
-18.76	1.4	7.1353	0.14015	387.32	1.7402	0.82037	9.9197	10.044
-17.132	1.5	7.6172	0.13128	388.32	1.7388	0.82646	10.055	10.103
-15.588	1.6	8.0979	0.12349	389.27	1.7376	0.83232	10.185	10.159
-14.117	1.7	8.5776	0.11658	390.17	1.7364	0.838	10.308	10.212

Continued on next page...

Table A.2 – Continued from previous page

T_{evap}	P_{evap}	ρ	V	H	E	C_p	k	μ
-12.712	1.8	9.0566	0.11042	391.02	1.7353	0.8435	10.426	10.263
-11.367	1.9	9.5348	0.10488	391.84	1.7343	0.84884	10.54	10.312
-10.076	2.0	10.012	0.099877	393.37	1.7317	0.86406	10.856	10.447
-8.8344	2.1	10.489	0.095334	394.09	1.731	0.8689	10.955	10.489
-7.6377	2.2	10.966	0.091191	394.78	1.7303	0.87363	11.05	10.53
-6.4824	2.3	11.442	0.087395	395.44	1.7296	0.87828	11.143	10.569
-5.3653	2.4	11.918	0.083906	396.08	1.729	0.88283	11.234	10.608
-4.2837	2.5	12.394	0.080685	396.7	1.7283	0.88731	11.322	10.645
-3.235	2.6	12.869	0.077704	397.3	1.7278	0.8917	11.407	10.681
-2.217	2.7	13.345	0.074937	397.89	1.7272	0.89603	11.491	10.716
-1.2277	2.8	13.82	0.07236	398.45	1.7267	0.90029	11.573	10.751
-0.26521	2.9	14.295	0.069955	399.0	1.7262	0.90449	11.653	10.785
0.67206	3.0	14.77	0.067704	399.53	1.7257	0.90863	11.731	10.817
1.5856	3.1	15.245	0.065594	400.04	1.7253	0.91271	11.807	10.85
2.4768	3.2	15.721	0.063611	400.54	1.7249	0.91675	11.882	10.881
3.3469	3.3	16.196	0.061744	401.03	1.7244	0.92073	11.956	10.912
4.1969	3.4	16.671	0.059983	401.51	1.724	0.92467	12.028	10.942
5.0281	3.5	17.147	0.058319	401.97	1.7237	0.92856	12.099	10.972
5.8412	3.6	17.623	0.056744	402.42	1.7233	0.93242	12.169	11.001
6.6372	3.7	18.099	0.055252	402.87	1.7229	0.93623	12.238	11.03
7.417	3.8	18.575	0.053835	403.3	1.7226	0.94001	12.305	11.058
8.1812	3.9	19.052	0.052488	403.72	1.7223	0.94375	12.372	11.086
8.9306	4.0	19.529	0.051207	404.13	1.7219	0.94746	12.437	11.114
9.6658	4.1	20.006	0.049985	404.53	1.7216	0.95114	12.502	11.141
10.388	4.2	20.483	0.04882	404.93	1.7213	0.95478	12.565	11.167
11.096	4.3	20.961	0.047707	405.31	1.721	0.9584	12.628	11.193
11.792	4.4	21.439	0.046643	405.69	1.7207	0.962	12.69	11.219
12.477	4.5	21.918	0.045625	406.06	1.7205	0.96556	12.751	11.245
13.15	4.6	22.397	0.044649	406.43	1.7202	0.96911	12.812	11.27
13.811	4.7	22.876	0.043713	406.78	1.7199	0.97263	12.871	11.295
14.463	4.8	23.356	0.042815	407.13	1.7197	0.97612	12.93	11.32
15.104	4.9	23.837	0.041952	407.47	1.7194	0.9796	12.988	11.344
15.735	5.0	24.317	0.041123	407.81	1.7192	0.98306	13.046	11.368
16.356	5.1	24.799	0.040325	408.14	1.719	0.9865	13.103	11.392
16.969	5.2	25.28	0.039556	408.46	1.7187	0.98992	13.159	11.415
17.572	5.3	25.763	0.038816	408.78	1.7185	0.99332	13.215	11.438
18.167	5.4	26.246	0.038102	409.09	1.7183	0.99671	13.271	11.462
18.754	5.5	26.729	0.037413	409.4	1.7181	1.0001	13.325	11.484
19.332	5.6	27.213	0.036747	409.7	1.7179	1.0034	13.38	11.507
19.903	5.7	27.698	0.036104	409.99	1.7177	1.0068	13.433	11.529

Continued on next page...

Table A.2 – Continued from previous page

T_{evap}	P_{evap}	ρ	V	H	E	C_p	k	μ
20.467	5.8	28.183	0.035483	410.28	1.7175	1.0101	13.487	11.552
21.023	5.9	28.668	0.034882	410.57	1.7173	1.0134	13.54	11.574
21.572	6.0	29.155	0.0343	410.85	1.7171	1.0168	13.592	11.596
22.114	6.1	29.642	0.033736	411.13	1.7169	1.0201	13.644	11.617
22.649	6.2	30.129	0.03319	411.4	1.7167	1.0233	13.696	11.639
23.178	6.3	30.617	0.032661	411.67	1.7165	1.0266	13.747	11.66
23.701	6.4	31.106	0.032148	411.94	1.7163	1.0299	13.798	11.682
24.217	6.5	31.596	0.03165	412.2	1.7161	1.0331	13.848	11.703
24.728	6.6	32.086	0.031166	412.45	1.716	1.0364	13.898	11.724
25.232	6.7	32.577	0.030697	412.7	1.7158	1.0396	13.948	11.744
25.731	6.8	33.068	0.03024	412.95	1.7156	1.0429	13.997	11.765
26.225	6.9	33.561	0.029797	413.2	1.7155	1.0461	14.046	11.786
26.713	7.0	34.054	0.029365	413.44	1.7153	1.0494	14.095	11.806
27.196	7.1	34.547	0.028946	413.68	1.7151	1.0526	14.144	11.826
27.674	7.2	35.042	0.028537	413.91	1.715	1.0558	14.192	11.846
28.147	7.3	35.537	0.02814	414.14	1.7148	1.059	14.24	11.866
28.615	7.4	36.033	0.027752	414.37	1.7147	1.0622	14.288	11.886
29.078	7.5	36.53	0.027375	414.59	1.7145	1.0654	14.335	11.906
29.537	7.6	37.027	0.027007	414.81	1.7143	1.0686	14.382	11.926
29.991	7.7	37.526	0.026649	415.03	1.7142	1.0718	14.429	11.946
30.441	7.8	38.025	0.026299	415.25	1.714	1.075	14.476	11.965
30.886	7.9	38.524	0.025958	415.46	1.7139	1.0782	14.523	11.985
31.327	8.0	39.025	0.025625	415.67	1.7137	1.0814	14.569	12.004
31.765	8.1	39.527	0.025299	415.88	1.7136	1.0846	14.615	12.024
32.198	8.2	40.029	0.024982	416.08	1.7135	1.0878	14.661	12.043
32.627	8.3	40.532	0.024672	416.28	1.7133	1.091	14.707	12.062
33.052	8.4	41.036	0.024369	416.48	1.7132	1.0942	14.752	12.081
33.473	8.5	41.541	0.024073	416.67	1.713	1.0974	14.798	12.1
33.891	8.6	42.047	0.023783	416.87	1.7129	1.1006	14.843	12.119
34.305	8.7	42.553	0.0235	417.06	1.7127	1.1038	14.888	12.138
34.715	8.8	43.061	0.023223	417.25	1.7126	1.107	14.933	12.157
35.123	8.9	43.569	0.022952	417.43	1.7125	1.1102	14.977	12.176
35.526	9.0	44.078	0.022687	417.61	1.7123	1.1134	15.022	12.194
35.926	9.1	44.589	0.022427	417.79	1.7122	1.1166	15.066	12.213
36.323	9.2	45.1	0.022173	417.97	1.7121	1.1198	15.111	12.232
36.717	9.3	45.612	0.021924	418.15	1.7119	1.123	15.155	12.25
37.108	9.4	46.125	0.02168	418.32	1.7118	1.1262	15.199	12.269
37.495	9.5	46.638	0.021442	418.5	1.7117	1.1295	15.243	12.287
37.879	9.6	47.153	0.021207	418.67	1.7115	1.1327	15.287	12.306
38.261	9.7	47.669	0.020978	418.83	1.7114	1.1359	15.33	12.324

Bibliography

[1] X. Cao, X. Dai, J. Liu, Building energy-consumption status worldwide and the state-of-the-art technologies for zero-energy buildings during the past decade, *Energy and Buildings*, 128 **(2016)**198–213.

[2] US Energy information Administration2016, International Energy Outlook **(2023)**. https://www.eia.gov/outlooks/ieo/data.php.

[3] European Commission **(2019)**, going climate-neutral by 2050. P20. https://climate.ec.europa.eu/eu-action/climate-strategies-targets/2050-long-term-strategy.

[4] T. Fleiter, R. Elsland, M. Rehfeldt, J. Steibach, U. Reiter, G. Catenazzi, M. Jakob, C. Rutten, R. Harmsen, F. Dittman, et al., Heat Roadmap Europe: EU Profile of Heating and Cooling Demand in 2015, *Heat Roadmap EU*, **(2017)**. https://dspace.library.uu.nl/server/api/core/bitstreams/1dd8ab14-3127-427d-8446-a4415a1dab44/content

[5] A. Soleimani, P. Davidsson, R. Malekian, R. Spalazzese, Modeling hybrid energy systems integrating heat pumps and district heating: A systematic review, *Energy and Buildings*, 329 **(2025)** 115253. https://doi.org/10.1016/j.enbuild.2024.115253

[6] Y. Wang, Z. Ye, Y. Song, X. Yin, F. Cao, Energy, exergy, economic and environmental analysis of refrigerant charge in air source transcritical carbon dioxide heat pump water heater, *Energ. Convers. Manage.*, 223 **(2020)**, 113209. https://doi.org/10.1016/j.enconman.2020.113209

[7] MEM (Ministère de l'énergie et des mines). Agence Nationale pour la Promotion et Rationalisation de l'Utilisation de l'énergie (APRUE), Consommation Energétique Finale de l'Algérie, **(2017)**, www.aprue.org.dz.

[8] T. Hasni, R. Malek, N. Zouioueche, l'Algérie 100% énergies renouvelables, étude **(2021)**,Friedrich Elbert Stiftung. https://algeria.fes.de

[9] H. Jouhara, N. Khordehgah, S. Almahmoud, B. Delpech, A. Chauhan, S. A. Tassou, Waste heat recovery technologies and applications, *Thermal Science and Engineering Progress*, 6 **(2018)** 268-289.

[10] K. Chua, S. Chou, W. Yang, Advances in heat pump systems: A review, *Appl. Energy*, 87 **(2010)** 3611–3624.

[11] Y. Baradey, M. Hawlader, A.F. Ismail, M. Hrairi, Waste heat recovery in heat pump systems: solution to reduce global warming, *IUM Eng. J.* 16 (2) **(2015)**. DOI:10.31436/iiumej.v16i2.602

[12] R. Conte, M. Tancon, M. Mozafarivanani, E. Zanetti, M. Azzolin, D. Del Col, Investigation on a direct expansion multisource carbon dioxide heat pump to maximize the use of renewable energy sources, *Applied Thermal Engineering*, 274 **(2025)** 126533. https://doi.org/10.1016/j.applthermaleng.2025.126533

[13] P. Carroll, M. Chesserb, P. Lyons, Air Source Heat Pumps field studies:A systematic literature review, *Renewable and Sustainable Energy Reviews*, 134 **(2020)** 110275. DOI:10.1016/j.rser.2020.110275

[14] W. Lyu, Z. Wang, X. Li, Z. Xu, Z. Pu, W. Zhao, A simplified model for correcting the heating capacity of air source heat pumps in high-altitude plateau areas, *Energy*, 305 **(2024)** 132173. https://doi.org/10.1016/j.energy.2024.132173

[15] Y. Ren, Comprehensive Evaluation of Three Major Heat Pump Technologies: Air-Source, Ground-Source, and Water-Source Heat Pump, Proceedings of the 3rd International Conference on Functional Materials and Civil Engineering, *Applied and Computational Engineering*, DOI: 10.54254/2755-2721/143/ **(2025)** 23349. DOI:10.54254/2755-2721/2025.23349

[16] A. Badiei, Y. G. Akhlaghi, X. Zhao, S. Shittu, X. Xiao, J. Li, Y. Fan, G. Li, A chronological review of advances in solar assisted heat pump technology in 21st century, *Renewable and Sustainable Energy Reviews*, 132 **(2020)** 110132. https://doi.org/10.1016/j.rser.2020.110132

[17] S.Bhadra and A. Mwesigye, Influence of control strategy on the energetic performance of an air source heat pump coupled with a solar air collector for domestic hot water in a cold climate, *Renewable Energy*, 244 **(2025)** 122682. https://doi.org/10.1016/j.renene.2025.122682

[18] I. Staffell, D. Brett, N. Brandonc, A. Hawkes, A review of domestic heat pumps, *Energy Environmental Science*, 5 **(2012)** 9291. DOI:10.1039/C2EE22653G

[19] A. Gaur, D. Z. Fitiwi, J. Curtis, Heat pumps and our low-carbon future: A comprehensive review, *Energy Research Social Science*, 71 **(2021)** 101764. https://doi.org/10.1016/j.erss.2020.101764

[20] Z. Wang, M. B. Luther, M. Amirkhani, C. Liu, P. Horan, State of the Art on Heat Pumps for Residential Buildings, *Buildings* **(2021)**, 11, 350. https://doi.org/10.3390/buildings11080350.

[21] B. Wang, X. Kong, X. Yan, Y. Shang, Y. Li, Influence of subcooling on performance of direct-expansion solar assisted heat pump, *International Journal of Refrigeration*, 122 **(2021)** 201-209.

[22] B. Xiao, L. He, S. Zhang, T. Kong, B. Hu, R.Z. Wang, Comparison and analysis on air-to-air and air-to-water heat pump heating systems, *Renewable Energy* 146 **(2020)** 1888-1896.

[23] Z. Liu, Y. Liu, D. Zhang, B. Cai, C. Zheng, Fault diagnosis for a solar assisted heat pump system under incomplete data and expert knowledge, *Energy*, 87 **(2015)** 41-48.

[24] I. Sarbu and C. Sebarchievici, Solar-assisted heat pump systems, *Nova Science Publishers, Inc.* **(2016)**. DOI: 10.1016/B978-0-12-811662-3.00009-8.

[25] Y. Chen, H. Hua, J. Xu, J. Wang, P.D. Lund, Y. Han, T. Cheng, Energy, environmental-based cost, and solar share comparisons of a solar driven cooling and heating system with different types of building, *Applied Thermal Engineering*, 211 **(2022)** 118435. https://doi.org/10.1016/j.applthermaleng.2022.118435

[26] A. Hepbasli and Y. Kalinci, A review of heat pump water heating systems, *Renewable and Sustainable Energy Reviews*, 13 **(2009)** 1211–1229.

[27] C. Zheng, K. Kang, Yu. Xie, X. Yang, L. Lan, H. Song, H. Han, S. Bai, Dynamic adsorption behavior of 1.1.1.2-tetrafluoroethane (R134a) on activated carbon beds under different humidity and moisture levels, *Separation and Purification Technology*, 329 **(2024)** 124851. https://doi.org/10.1016/j.seppur.2023.124851

[28] Z. Zhang, G. He, Q. Ning, Z. Wang, W. Yang, J. Hua, S. Zhou, Evaluation of flammability characteristics of mixed refrigerants R134a/R1270, R134a/R170, and R170/R1270, *International Journal of Refrigeration*, 156 **(2023)** 1-11. https://doi.org/10.1016/j.ijrefrig.2023.09.013

[29] P. Poredoš, U. Tomc, N. Petelin, B. Vidrih, U. Flisar, A. Kitanovski, Numerical and experimental investigation of the energy and exergy performance of solar thermal, photovoltaic and photovoltaic-thermal modules based on roll-bond heat exchangers, *Energy Conversion and Management*, 210 **(2020)** 112674. https://doi.org/10.1016/j.enconman.2020.112674

[30] Sabrina N. Rabelo, Tiago de F. Paulino, Willian M. Duarte, Samer Sawalha, Luiz Machado, Experimental Analysis of the Influence of Water Mass Flow Rate on the Performance of a CO2 Direct-Expansion Solar Assisted Heat Pump, *International Journal of Chemical and Molecular Engineering*, 12 **(2018)**, DOI: 10.5281/zenodo.1317384.

[31] https://moircooling.com/product/mini-rotary-compressor-ts1901y4/

[32] D. Gross, . Fatigue design and safety factor for scroll compressor wraps. 8th International Conference on Compressors and Their Systems, **(2013)** 285–300. doi:10.1533/9781782421702.5.285

[33] U.S. Environmental Protection Agency, Report for Oil and Natural Gas Sector Compressors Review Panel **(2014)**. https://www.ourenergypolicy.org/wp-content/uploads/2014/04/epa-compressors.pdf

[34] M. Stewart, Compressor fundamentals: Surface Production Operations, **(2019)** 457–525. doi:10.1016/b978-0-12-809895-0.00007-7

[35] V. T. Nguyen, A. Danlos, F. Ravelet, M. Deligant, M. Solis, S. Khelladi, F. Bakir, Numerical Analysis of a Novel Twin-Impeller Centrifugal Compressor, *Computation*, 12 **(2021)** 143; https://doi.org/10.3390/computation9120143.

[36] I. Sarbu, and C. Sebarchievici, Types of Compressors and Heat Pumps. Ground-Source Heat Pumps, **(2016)** 47–70. doi:10.1016/b978-0-12-804220-5.00004-7

[37] E. Broerman, T. Manthey, J. Wennemar, J. Hollingsworth, Screw Compressors. Compression Machinery for Oil and Gas, **(2019)** 253–307. doi:10.1016/b978-0-12-814683-5.00006-7

[38] R. K. Mobley, Compressors. Fluid Power Dynamics, **(2000)** 203–231. doi:10.1016/b978-075067174-3/50065-2

[39] A. Gużda, N. Szmolke, Compressors in Heat Pumps, *Machine Dynamics Research* , 39 **(2015)** 71-83.

[40] T.El Samad, A. Żabnieńska-Góra, H. Jouhara, A. I. Sayma, A review of compressors for high temperature heat pumps, *Thermal Science and Engineering Progress*, 51 **(2024)** 102603. https://doi.org/10.1016/j.tsep.2024.102603

[41] J. Zhang, R.Z. Wang, J.Y. Wu, System optimization and experimental research on air source heat pump water heater, *Applied Thermal Engineering*, 27 **(2007)** 1029–1035.

[42] B.D. Sloane, R.C. Krise, D.D. Kent, Energy Utilization Systems, Inc., Demonstration of a heat pump water heater, *A subcontracted report, ORNL/Sub-7321/3*, **(1979)**. https://digital.library.unt.edu/ark:/67531/metadc1198131/m2/1/high-resd/6723359.pdf

[43] Reis, R. V. D. M. Analise experimental comparativa entre uma bomba de calor e uma resistenica eletricamodo dispositivo de apoio de energia para um aquecedor solar de agua, *(Tese de Doutorado)*, **2012**. http://hdl.handle.net/1843/BUOS-8YHPE2.

[44] P. Omojaro and C. Breitkopf, Direct expansion solar assisted heat pumps: A review of applications and recent research, *Renewable and Sustainable Energy Reviews*, 22 **(2013)** 33–45.

[45] https://www.linquip.com/blog/types-of-expansion-valves-guide/

[46] https://chinasolenoidvalve.en.made-in-china.com

[47] https://hvac-eng.com/fr/r

[48] J. Chen, K. Chen, W. Zhang, J. M. Su, B. Zhao, M. Hu, G. Pei, Numerical study of a solar district heating system with photovoltaic-thermal collectors and pit thermal energy storage, *Energy* 317 **(2025)** 134705. https://doi.org/10.1016/j.energy.2025.134705

[49] S. A. Kalogirou, Solar thermal collectors and applications, *Progress in Energy and Combustion Science*, 30 **(2004)** 231-295.

[50] L. Evangelisti, R. De Lieto Vollaro, F. Asdrubali, Latest advances on solar thermal collectors: A comprehensive review, *Renewable and Sustainable Energy Reviews*, 114 **(2019)** 109318. https://doi.org/10.1016/j.rser.2019.109318

[51] J. Allan, Z. Dehouche, S. Stankovic, and L. Mauricette, Performance testing of thermal and photovoltaic thermal solar collectors, *Energy Science Engineering*, 3 **(2015)** 310–326.

[52] F. Rubbi, L. Das, K. Habib,N. Aslfattahi, R. Saidur, M. T. Rahman, State-of-the-art review on water-based nanofluids for low temperature solar thermal collector application, *Solar Energy Materials and Solar Cells*, 230 **(2021)** 111220. https://doi.org/10.1016/j.solmat.2021.111220

[53] K. Sezen and A. Gungor, Comparison of solar assisted heat pump systems for heating residences: A review, *Solar Energy*, 249 **(2023)** 424-445.

[54] M. S. Buker, S. B. Riffat, Solar assisted heat pump systems for low temperature water heating applications: A systematic review, *Renewable and Sustainable Energy Reviews*, 55 **(2016)** 399–413.

[55] S. Eichera, C. Hildbranda, J. Bonya, M. Buneaa, J-C. Hadornb, S. Citherlet, Solar assisted heat pump for domestic hot water production, *Energy Procedia*, 30 **(2012)** 571 – 579.

[56] S. Chinnasamy, A. Arunachalam, Experimental investigation on direct expansion solar-air source heat pump for water heating application, *Renewable Energy*, 202 **(2023)** 222–233.

[57] B. Parida, S. Iniyan, and R. Goic, "A review of solar photovoltaic technologies, *Renewable and Sustainable Energy Reviews*, 15 **(2011)** 1625–1636.

[58] A. Sharma, A comprehensive study of solar power in India and World, *Renewable and Sustainable Energy Reviews*, 15 **(2011)** 1767–1776.

[59] M. Rommel, D. Zenhäusern,A. Baggenstos, O. Türk, S. Brunold, Application of unglazed PVT collectors for domestic hot water preheating in a development and testing system, *Energy Procedia*, 48 **(2014)** 638–644.

[60] H. A. Zondag, D. W. de Vries, W. G. J. van Helden, R. J. C. van Zolingen, and A. A. van Steenhoven, The yield of different combined PV-thermal collector designs, *Solar Energy*, 74 **(2003)** 253–269.

[61] A. Makki, S. Omer, and H. Sabir, Advancements in hybrid photovoltaic systems for enhanced solar cells performance, *Renewable and Sustainable Energy Reviews*, 41 **(2015)** 658-684.

[62] T. T. Chow, A review on photovoltaic/thermal hybrid solar technology, *Applied Energy*, 87 **(2010)** 365–379.

[63] W. Liu, J. Yao, T.Jia, Y. Zhao, Y. Dai, J. Zhu, V.Novakovic, The performance optimization of DX-PVT heat pump system for residential heating, *Renewable Energy*, 206 **(2023)**1106–1119.

[64] M. Noro and R. Lazzarin, PVT and ETC coupling for annual heating and cooling by absorption heat pumps. *Sustainability*, 12 **(2020)** 7042. DOI:10.3390/su12177042

[65] Z. Song, J. Ji, J. Cai, Z. Li, B. Yu, The performance comparison of the direct-expansion solar assisted heat pumps with three different PV evaporators, *Energy Conversion Management*, 213 **(2020)** 112781. https://doi.org/10.1016/j.enconman.2020.112781

[66] H. Namdar, E. R. Schio, G. Semprini, P. Valdiserri, Photovoltaic-thermal solar-assisted heat pump systems for building applications: A technical review on direct expansion systems, *Energy Buildings*, 334 **(2025)** 115516. https://doi.org/10.1016/j.enbuild.2025.115516.

[67] Y. Lin, Z. Bu, W. Yang, H. Zhang, V. Francis; C.-Q. Li, A Review on the Research and Development of Solar-Assisted Heat Pump for Buildings in China, *Buildings*, 12 **(2022)** 1435. DOI: 10.3390/buildings12091435

[68] M. Missoum, L. Loukarfi, Investigation of a Solar Poly generation System for a Multi-Story Residential Building-Dynamic Simulation and Performance Analysis, *Int. Journal of Renewable Energy Development*, 10 **(2021)** 445-458.

[69] F. Aguilar, D. Crespí-Llorens, P.V. Quiles, Environmental benefits and economic feasibility of a photovoltaic assisted heat pump water heater, *Solar Energy*, 193 **(2019)**, 20-30.

[70] W. Youssef, Y.T. Ge, S.A. Tassou, Effects of latent heat storage and controls on stability and performance of a solar assisted heat pump system for domestic hot water production,*Solar Energy*, 150 **(2017)** 394-407.

[71] W. Huang, J. Ji, M. Modjinou, J. Qin, Effects of Ambient Parameters on the Performance of a Direct-Expansion Solar-Assisted Heat Pump with Bare Plate Evaporators for Space Heating, *International Journal of Photoenergy*, **(2017)** 3082740. https://doi.org/10.1155/2017/3082740.

[72] O. Kara, K. Ulgen, A. Hepbasli, Exergetic assessment of direct-expansion solar-assisted heat pump systems: Review and modeling, *Renewable and Sustainable Energy Reviews*, 12 **(2008)**, 1383–1401.

[73] D. Zhang, Q.B. Wu, J.P. Li, X.Q. Kong, Effects of refrigerant charge and structural parameters on the performance of a direct-expansion solar-assisted heat pump system, *Applied Thermal Engineering*, 73 **(2014)** 522-528.

[74] P. D. Malali, S. K. Chaturvedi, T. M. Abdel-Salam, An approximate method for prediction of thermal performance of direct expansion-solar assisted heat pump (DX-SAHP) systems for water heating applications, *Energy Conversion and Management*, 127 **(2016)** 416-423.

[75] B. J. Kim, S.-Y. Jo, J.-W. Jeong, Energy performance enhancement in air-source heat pump with a direct evaporative cooler-applied condenser, *Case Studies in Thermal Engineering*, 35 **(2022)** 102137. https://doi.org/10.1016/j.csite.2022.102137

[76] L. Croci, L. Molinaroli, P. Quaglia, Dual source solar assisted heat pump model development, validation and comparison to conventional systems, *Energy procedia*, 140 **(2017)** 408-422.

[77] D.A. Chwieduk, Active solar space heating, *Advances in Solar Heating and Cooling*, **(2016)** 151-202. http://dx.doi.org/10.1016/B978-0-08-100301-5.00008-4

[78] C. Huan, S. Li, F. Wang, L. Liu, Y. Zhao, Z. Wang, P. Tao, Performance Analysis of a Combined Solar-Assisted Heat Pump Heating System in Xian China, *Energies*, 12 **(2019)** 2515; doi:10.3390/en12132515.

[79] J. Ruschenburg, S. Herkel, H-M. Henning, A statistical analysis on market-available solar thermal heat pump systems, *Solar Energy*, 95 **(2013)** 79–89.

[80] M.Y. Haller, D. Carbonell, I. Mojic, C. Winteler, E. Bertram, M. Bunea, W. Lerch, F. Ochs, Solar and Heat Pump Systems – Summary of Simulation Results of the IEA SHC Task 44/HPP Annex 38,*11th IEA Heat Pump Conference*, Montréal, Canada **(2014)**. http://www.iea-hpc2014.org/

[81] C. Fraga, P. Hollmuller, F. Mermoud, B. Lachal, Solar assisted heat pump system for multifamily buildings: Towards a seasonal performance factor of 5? Numerical sensitivity analysis based on a monitored case study, *Solar Energy*, 146 **(2017)** 543–564.

[82] H. Cassard, P. Denholm, S. Ong, Technical and economic performance of residential solar water heating in the United States, *Renewable and Sustainable Energy Reviews*, 15 **(2011)** 3789-3800.

[83] Study on a direct-expansion solar-assisted heat pump water heating system, *International Journal of Energy Research*, 27 **(2003)** 531-548.

[84] Y.H. Kuang, R.Z. Wang, Performance of a multi-functional direct-expansion solar assisted heat pump system, *Solar Energy*, 80 **(2006)** 795-803.

[85] G. Xu, S. Deng, X. Zhang, L. Yang, Y. Zhang, Simulation of a photovoltaic/thermal heat pump system having a modified collector/evaporator, *Solar Energy*, 83 **(2009)** 1967–1976.

[86] B.J. Huang, J.H. Wu, H.Y. Hsu, J.H. Wang, Development of hybrid solar-assisted cooling/heating system, *Energy Conversion and Management* 51 **(2010)** 1643-1650.

[87] L. Paradeshi, M. Srinivas, S. Jayaraj, Experimental Studies on Direct Expansion Solar Assisted Heat Pump: An Energy Point View, *Journal of Advanced Engineering Research*, 3 **(2016)** 141-148.

[88] F.B. G. Chata, S.K. Chaturvedi, A. Almogbel. Analysis of a direct expansion solar assisted heat pump using different refrigerants, *Energy Conversion and Management*, 46 **(2005)** 2614–2624.

[89] W. M. Duarte, T. F. Paulinoc, J. J.G. Pabond, S. Sawalhae, L. Machado, Refrigerants selection for a direct expansion solar assisted heat pump for domestic hot water, *Solar Energy*, 184 **(2019)** 527-538.

[90] G. Leonzio, P. S. Fennell, N. Shah, Air-source heat pumps for water heating at a high temperature: State of the art, *sustainable energy technologies and assessments*, 54 **(2022)** 102866. https://doi.org/10.1016/j.seta.2022.102866

[91] W. Wu, B. Wang, T. You, W. Shi, X. Li, Configurations of solar air source absorption heat pump and comparisons with conventional solar heating, *Applied Thermal Engineering* 141 **(2018)** 630-641.

[92] R. S. Kamel, A. S. Fung, Modeling, simulation and feasibility analysis of residential BIPV/T+ASHP system in cold climate-Canada, *Energy and Buildings*, 82 **(2014)** 758-770.

[93] Z. Liu, Y. Wang, Z. Xie, H. Yu, W. Ma, The related problems and development situation of air source heat pump in the cold and serve cold climate areas, *Procedia Engineering*, 205 **(2017)** 368–372. 10.1016/j.proeng.2017.10.385.

[94] P. Mehrfeld, Evaluation of heat pump systems under dynamic operating conditions, Doctorate thesis, Faculty of Mechanical Engineering of the Rhine-Westphalia, Technical University of Aachen, Germany, 2022. DOI: 10.18154/RWTH-2022-06640

[95] A. Heinz and R. Rieberer, Energetic and economic analysis of a PV-assisted air-to-water heat pump system for renovated residential buildings with high-temperature heat emission system, *Applied Energy*, 293 **(2021)** 116953. https://doi.org/10.1016/j.apenergy.2021.116953

[96] C. Karmann, S. Schiavon, F. Bauman, Thermal comfort in buildings using radiant vs. all-air systems: A critical literature review, *Building and Environment*, 111 **(2017)** 123-131.

[97] X. Wang, L. Xia, C. Bales, X. Zhang, B. Copertaro, S. Pan, J. Wu, A systematic review of recent air source heat pump (ASHP) systems assisted by solar thermal, photovoltaic and photovoltaic/thermal sources, *Renewable Energy*, 146 **(2020)** 2472-2487.

[98] G. Wang, Z. Quan, Y. Zhao, C. Sun, Y. Deng, J. Tong, Experimental study on a novel PV/T air dual-heat-source composite heat pump hot water system, *Energy and Buildings*, 108 **(2015)** 175-184. http://dx.doi.org/10.1016/j.enbuild.2015.08.016.

[99] Y. Jung, J. Oh, U. Han, H. Lee, A comprehensive review of thermal potential and heat utilization for water source heat pump systems, *Energy and Buildings*, 266 **(2022)** 112124. https://doi.org/10.1016/j.enbuild.2022.112124

[100] Maria Pinamonti, Ian Beausoleil-Morrison, Alessandro Prada, Paolo Baggio, Water-to-water heat pump integration in a solar seasonal storage system for space heating and domestic hot water production of a single-family house in a cold climate, *Solar Energy*, 213 **(2021)** 300–311.

[101] G. Wang, Y. Zhao, Z. Quan, J. Tong, Application of a multi-function solar-heat pump system in residential buildings, *Applied Thermal Engineering*, 11244 (2017). https://doi.org/10.1016/j.applthermaleng.2017.10.046.

[102] P. Jadwiszczak1 and E. Niemierka, Water pipe network as a heat source for heat pump integrated into a district heating, *E3S Web of Conferences 22*, 00210 **(2017)**. DOI: 10.1051/e3sconf/20172200210.

[103] G. H. Shia, L. Ayeb, D. Lia, X. J. Duc, Recent advances in direct expansion solar assisted heat pump systems: A Review, *Renewable and Sustainable Energy Reviews*, 106 **(2019)** 349–366.

[104] M. Masiukiewicz, Mariusz Tanczuk , S. Anweiler, G. Streckiene, S. Boldyryev, Long-term climate-based sizing and economic assessment of air-water heat pumps for residential heating, *Applied Thermal Engineering*, 258 **(2025)** 124627, https://doi.org/10.1016/j.applthermaleng.2024.124627.

[105] Y. Cao, L. W. W. Mihardjo, T. Parikhanic, Thermal performance, parametric analysis, and multi-objective optimization of a direct-expansion solar-assisted heat pump water heater using NSGA-IIand decision makings, *Applied Thermal Engineering*, 181 **(2020)** 115892. https://doi.org/10.1016/j.applthermaleng.2020.115892

[106] T. Xian, J. Wu, X. Zhang, Study on the operating characteristics of a solar heat pump water heater based on data fusion, *Solar Energy*, 212 **(2020)** 113–124.

[107] S. Zhang, S. Liu, J. Wang, Y. Li, Z. Yu, Analysis of a solar-assisted heat pump system with hybrid energy storage for space heating, *Applied Thermal Engineering*, 231 **(2023)** 120884, https://doi.org/10.1016/j.applthermaleng.2023.120884.

[108] H. Fares, N. Le Pierrès, D. Chèze, E. Wurtz, Assessing the energy performance of solar photovoltaic, thermal and hybrid PVT panels in a building context: A systematic study of the criteria definitions and studies parameters, *Solar Energy*, 286 **(2025)** 113126. https://doi.org/10.1016/j.solener.2024.113126

[109] L. A. Tagliafico, F. Scarpa, F. Valsuani, Direct expansion solar assisted heat pumps - A clean steady state approach for overall performance analysis, *Applied Thermal Engineering*, 66 **(2014)** 216-226.

[110] J. Cai, Z. Li, J. Ji, F. Zhou, Performance analysis of a novel air source hybrid solar assisted heat pump, *Renewable Energy*, 139 **(2019)** 1133–1145.

[111] J. Cai, F. Zhang, J. Ji, Comparative analysis of solar-air dual source heat pump system with different heat source configurations, *Renewable Energy*, 150 **(2020)** 191-203.

[112] X. Kong, Y. Li, L. Lin, Y. Yang, Modeling evaluation of a direct-expansion solar assisted heat pump water heater using R410A, *Int. J. Refrig.* , 76 **(2017)** 136–146.

[113] Z. Zheng, Y. Jin, J. Zhou, Y. Yang, F. Xu, H. Liu, A novel dynamic operation method for solar assisted air source heat pump systems: Optimization control and performance analysis, *Energy*, 316 **(2025)** 134535, https://doi.org/10.1016/j.energy.2025.134535.

[114] W. Ji, J. Cai,, J., Ji, W. Huang, Experimental study of a direct expansion solar-assisted heat pump (DX-SAHP) with finned-tube evaporator and comparison with conventional DX-SAHP, *Energy Buildings*, 207 **(2020)** 109632. https://doi.org/10.1016/j.enbuild.2019.109632

[115] M. Hawlader, S. Chou, M. Ullah, The performance of a solar assisted heat pump water heating system, *Applied Thermal Engineering*, 21 **(2001)** 1049–1065.

[116] J. Chyng, C. Lee, B. Huang, Performance analysis of a solar-assisted heat pump water heater, *Solar Energy*, 74 **(2003)** 33–44.

[117] A. Moreno-Rodríguez, A. González-Gil, M. Izquierdo, N. Garcia-Hernando, Theoretical model and experimental validation of a direct-expansion solar assisted heat pump for domestic hot water applications, *Energy*, 45 **(2012)** 704–715.

[118] X. Kong, K. Jiang, S. Dong, Y. Li, J. Li, Control strategy and experimental analysis of a direct-expansion solar-assisted heat pump water heater with R134a, *Energy*, 145 **(2018)** 17–24.

[119] X. Kong, P. Sun, S. Dong, K. Jiang, Y. Li, Experimental performance analysis of a direct-expansion solar-assisted heat pump water heater with R134a in summer, *International Journal of Refrigeration*, 91 **2018** 12–19.

[120] M. Herrando, K. Wang, G. Huang, T. Otanicar, O. B. Mousa et al., A review of solar hybrid photovoltaic-thermal (PV-T) collectors and systems, *Progress in Energy and Combustion Science*, 97 **(2023)** 101072. https://doi.org/10.1016/j.pecs.2023.101072

[121] Z. Li, X. Huang, Simulation analysis on operation performance of a hybrid heat pump system integrating photovoltaic/thermal and air source, *Applied Thermal Engineering*, 200 **(2022)** 117693. https://doi.org/10.1016/j.applthermaleng.2021.117693.

[122] S. Ma, S. Lu, D. Ma, C. Li, C. Liu, L. Wu, M. Chen, C. Xu, H. Ma, Investigation on the thermal performance and economy of a solar assisted air source heat pump domestic hot water system, *Applied Thermal Engineering*, 232 **(2023)** 121007. https://doi.org/10.1016/j.applthermaleng.2023.121007

[123] J. Li, S. Wei, Y. Dong, X. Liu, V. Novakovic; Technical and economic performance study on winter heating system of air source heat pump assisted solar evacuated tube water heater, *Applied Thermal Engineering*, 221 **(2023)** 119851. https://doi.org/10.1016/j.applthermaleng.2022.119851

[124] J. Chu and C. A. Cruickshank, Assisted Heat Pump Systems: A Review of Existing Studies and Their Applicability to the Canadian Residential Sector, *Journal of solar energy engineering*, 136 **(2014)** 041013. DOI:10.1115/ES2013-18177

[125] G. Panaras, E. Mathioulakis, V. Belessiotis, Investigation of the performance of a combined solar thermal heat pump hot water system, *Solar Energy*, 93 **(2013)** 169–182.

[126] G. Panaras, E. Mathioulakis, V. Belessiotis, A method for the dynamic testing and evaluation of the performance of combined solar thermal heat pump hot water systems, *Applied Energy*, 114 **(2014)** 124–134.

[127] Y. Yerdesh, Z. Abdulina, A. Aliuly, Y. Belyayev, M. Mohanraj , A. Kaltayev, Numerical simulation on solar collector and cascade heat pump combi water heating systems in Kazakhstan climates, *Renewable Energy*, 145 **(2020)** 1222-1234.

[128] C. Tzivanidis, E. Bellos, G. Mitsopoulos, K. A. Antonopoulos, A. Delis, Energetic and financial evaluation of a solar assisted heat pump heating system with other usual heating systems in Athens, *Applied Thermal Engineering*, 106 **(2016)** 87–97.

[129] R. M. Lazzarin, Dual source heat pump systems: Operation and performance, *Energy and Buildings*, 52 **(2012)** 77–85.

[130] C. Huan, S. Li, F. Wang, L. Liu, Y. Zhao, Z. Wang,P. Tao, Performance Analysis of a Combined Solar-Assisted Heat Pump Heating System in Xi'an, China, *Energies*, 12 **2019** 2515. doi:10.3390/en12132515).

[131] L. W. Yang, Y. Li, T. Yang, H. S. Wang, Low temperature heating operation performance of a domestic heating system based on indirect expansion solar assisted air source heat pump, *Solar Energy*, 244 **(2022)** 134–154.

[132] Y. Wang, Z. Quan, Y. Zhao, .L. Wang, Z. Liu, Performance and optimization of a novel solar-air source heat pump building energy supply system with energy storage, *Applied Energy*, 324 **(2022)** 119706. https://doi.org/10.1016/j.apenergy.2022.119706

[133] J. Ji, J. Cai, W. Huang, Y. Feng, Experimental study on the performance of solar-assisted multifunctional heat pump based on enthalpy difference lab with solar simulator. *Renewable Energy*, 75 **(2015)** 381-388.

[134] E. Bellos, C. Tzivanidis, K. Moschos, K. A. Antonopoulos, Energetic and financial evaluation of solar assisted heat pump space heating systems, *Energy Conversion and Management*, 120 **(2016)** 306–319.

[135] N. Shao, L. Ma, J. Zhang, Experimental investigation on the performance of direct-expansion roof-PV/T heat pump system, *Energy*, 195 **(2020)** 116959. https://doi.org/10.1016/j.energy.2020.116959

[136] N. Aste, C.D. Pero, F. Leonforte, R.S. Adhikari, Energy and economic assessment of a hybrid solar assisted heat pump system, *International Conference on Clean Electrical Power (ICCEP)*, **(2015)**110–114. https://doi:10.1109/ICCEP.2015.7177609.

[137] R. Simonetti, L. Molinaroli, G. Manzolini, Experimental and analytical study of an innovative integrated dual-source evaporator for solar-assisted heat pumps, *Solar Energy*, 194 **(2019)** 939–951.

[138] G. Besagni, L. Croci, R. Nesa, L. Molinaroli, Field study of a novel solar-assisted dual-source multifunctional heat pump, *Renewable Energy*, 132 **(2019)** 1185–1215.

[139] F. Leonforte , A. Miglioli, C. Del Pero, N. Aste, N. Cristiani, L. Croci, G. Besagni, Design and performance monitoring of a novel photovoltaic-thermal solar-assisted heat pump system for residential applications, *Applied Thermal Engineering*, 210 **(2022)**, 118304. https://doi.org/10.1016/j.applthermaleng.2022.118304

[140] N. Dai, X. Xu, S. Li, Z. Zhang, Simulation of Hybrid Photovoltaic Solar Assisted Loop Heat Pipe/Heat Pump System, *Appl. Sci.*, 7 **(2017)** 197. doi:10.3390/app7020197.

[141] Meteonorm 8: Meteonorm Software Worldwide Europe irradiation data. Intersolar Europe, **(2022)**. https://meteonorm.com/en/news.

[142] E.W. Lemmon, M.L. Huber, M.O. McLinden, NIST Reference Fluid Thermodynamic and Transport Properties – *REFPROP* NIS, **(2013)** .

[143] G-H. Shi, L. Ayeb, D. Lia, X-J. Du, Recent advances in direct expansion solar assisted heat pump systems: A review, *Renewable and Sustainable Energy Reviews*, 109 **(2019)** 349-366.

[144] J. A. Duffie, A. William, A. W. Beckman, Solar Engineering of Thermal Processes. 4th Ed. Published by John Wiley Sons **(2013)**. https://doi.org/10.1002/9781118671603.

[145] S. Ito, N. Miura, K. Wang, Performance of a heat pump using direct expansion solar collectors, *Sol. Energy*, 65 **(1999)** 189-196.

[146] X. Kong, X. Yan, Z. Yue, P. Zhang, Y. Li, Influence of refrigerant charge and condenser area on direct-expansion solar-assisted heat pump system for radiant floor heating, *Solar Energy*, 247 **(2022)** 499-509.

[147] Y.Z., Wu, Miniature Refrigeration Equipment Design Guidelines, Machinery Industry Press, Beijing, **(2004)** 66–214.

[148] X. Sun, Y. Dai, V. Novakovic, J. Wua, R. Wang, Performance comparison of direct expansion solar-assisted heat pump and conventional air source heat pump for domestic hot water, *Energy Procedia*, 70 **(2015)** 394 – 401.

[149] X.Q. Kong a,*, D. Zhang b, Y. Li a, Q.M. Yang, Thermal performance analysis of a direct-expansion solar-assisted heat pump water heater, *Energy*, 36 **(2011)** 6830-6838.

[150] F. Bava and S. Furbo, Development and validation of a detailed TRNSYS-Matlab model for large solar collector fields for district heating applications, *Energy*, 135 **(2017)** 698-708, https://doi.org/10.1016/j.energy.2017.06.146.

[151] L. Fu, G. Ding, C. Zhang, Dynamic simulation of air-to-water dual-mode heat pump with screw compressor, *Applied Thermal Engineering*, 23 **(2003)** 1629–1645.

[152] A. Fudholi, K. Sopian, M.H. Yazdi, M.H. Ruslan, A. Ibrahim, H.A. Kazem, Performance analysis of photovoltaic thermal (PVT) water collectors, *Energy Conversion Manageement*, 78 **(2014)** 641–51.

[153] L. Xia, Z. Ma, G. Kokogiannakis, S. Wang, X. Gong, A model-based optimal control strategy for ground source heat pump systems with integrated solar photovoltaic thermal collectors, *Applied Energy*, 228 **(2018)** 1399–1412.

[154] G. Wang, Z. Quan, Y. Zhao, C. Sun, Y. Deng, J. Tong, Experimental study on a novel PV/T air dual-heat-source composite heat pump hot water system, *Energy and Buildings* 108 **(2015)** 175–184.

[155] M. Qu, J. Chen, L Nie, F. Li, Q. Yu, T. Wang, Experimental study on the operating characteristics of a novel photovoltaic/thermal integrated dual-source heat pump water heating system, *Applied Thermal Engineering*, V. 94 **(2016)** 819-826. https://doi.org/10.1016/j.applthermaleng.2015.10.126

[156] S. Poppi, N. Sommerfeldt, C. Bales, H. Madani, P. Lundqvist, Techno-economic review of solar heat pump systems for residential heating applications, *Renewable and Sustainable Energy Reviews*, 81 **(2018)** 22–32.

[157] S. Abdul-Ganiyu, D. A. Quansah, E. W. Ramde, R. Seidu, M. S. Adaramola, Techno-economic analysis of solar photovoltaic (PV) and solar photovoltaic thermal (PVT) systems using exergy analysis, *Sustainable Energy Technologies and Assessments*, 47 **(2021)** 101520. https://doi.org/10.1016/j.seta.2021.101520

[158] X. Li, W. Lyu, S. Ran, B. Wang, W. Wu, Z. Yang, S. Jiang, M. Cui, P. Song, T. You, W. Shi, Combination principle of hybrid sources and three typical types of hybrid source heat pumps for year-round efficient operation, *Energy*, 193 **(2020)** 116772. https://doi.org/10.1016/j.energy.2019.116772

[159] H. Z. Abou-Ziyan, M. F. Ahmed, M. N. Metwally and H. M. Abd E1-Hameed, Solar-assisted R22 and R134a heat pump systems for low-temperature applications, *Applied Thermal Engineering*, Vol. 17, No. 5 **(1997)** 455-469.